On the semiclassical limit of the defocusing Davey-Stewartson II equation

Olga Assainova

Université de Bourgogne, U.F.R Sciences et Techniques
Institut de Mathématiques de Bourgogne
Ecole doctorale Carnot-Pasteur

THÈSE

pour l'obtention du grade de

Docteur de l'Université de Bourgogne

en Mathématiques

présentée et soutenue publiquement par

Olga Assainova

le 30 novembre 2018

Sur la limite semi-classique de l'équation Davey-Stewartson II défocalisant

Directeur de thèse : **Christian Klein**

Jury composé de

Jörg Frauendiener	University Of Otago	Rapporteur
Georgi Grahovski	University of Essex	Rapporteur
Jean-Claude Saut	Université Paris-Sud 11	Président de jury
Mariana Haragus	Université de Franche-Comté	Examinatrice
Christian Klein	Université de Bourgogne	Directeur

Acknowledgements

First of all I would like to thank my thesis advisor for making me go through these three years, Professor Christian Klein who was pushing me and motivating me. Thanks to him I got an opportunity to meet incredible collaborators.

My sincere thanks to Professor Peter Miller from the University of Michigan. Without him we would not have been able to obtain most of the results presented here.

I would also like to acknowledge Professor Kenneth McLaughlin, I highly appreciate the time of intensive collaboration at the Research Institute in Oberwolfach.

I also wish to express my gratitude to the referees, Professor Jörg Frauendiener and Professor Georgi Grahovski, it is a great honour for me that you agreed to read the manuscript and to provide your comments.

I am particularly grateful to Professor Jean-Claude Saut and professor Mariana Haragus who kindly accepted the proposition to be the part of the thesis committee.

I am forever thankful to Nikola Stoilov and Maxim Pavlov. Without their help and support I would not have started my thesis at all. Nikola is one of the persons whom I can ask for an advice or for help as a colleague, and also as a friend. No doubt, I can count my master project as the very beginning of my thesis and this was done by careful guidance accompanied with enormous help and support of Maxim Valentinovich.

Also I am very grateful to Professor Johannes Sjöstrand for enriching meetings and discussions.

I am profoundly grateful to the whole staff of the IMB, l'Ecole Doctorale Carnot-Pasteur and all PhD students. It was a great pleasure to be part of this incredible team.

My sincere thanks also go to Hans-Rudolf Jauslin, José-Luis Jaramillo, Anissa Bellaassali, Magali Crochot, Caroline Gérin, Francis Léger, Emeline Iltis, Connie Wu, Evgeny Ferapontov, Karima Khusnutdinova.

Heartfelt thanks go to my family, nothing has been possible without them and without their endless support.

Finally, thank you, Jérémy.

Résumé

La méthode de diffusion inverse est la plus efficace dans la théorie des systèmes intégrables. Introduite dans les années soixantes, d'importants résultats ont été obtenus pour les problèmes de dimension 1+1 et notamment sur l'interaction de solitons. Depuis quelques années, l'intérêt est porté sur des problèmes de dimensions supérieures comme les équations de Davey-Sterwartson, une généralisation de l'équation intégrable de Schrödinger cubique non linéaire en dimension 1+1. Des études numériques en limite semi-classique de l'équation de Davey-Stewartson II (DSII) défocalisant, font apparaître des points communs avec le cas réduit unidimensionnel, par exemple sur l'existence *d'ondes de choc dispersives* : des conditions initiales lisses mènent à une région d'oscillations rapides et modulées dans le voisinage des chocs des solutions des équations non dispersives dotées des mêmes conditions initiales.

Cette thèse donne les premières étapes pour l'étude analytique de ce problème basée sur la méthode de la transformée de diffusion inverse. Les deux types de méthodes, directe et inverse, pour l'équation de DSII permettent de réécrire le problème sous la forme des équations D-bar. On considère la transformée spectrale directe pour l'équation DSII avec des conditions initiales lisses en limite semi-classique. La transformée spectrale directe mène à un système de Dirac elliptique singulièrement perturbé en deux dimensions. On introduit une méthode de type BKW pour ce problème et on montre qu'il est bien défini pour des paramètres spectraux $k \in \mathbb{C}$ dont les modules sont suffisamment grands en controllant la solution d'une équation eikonale non linéaire. Aussi cette méthode donne des résultats numériques précis pour de tels k en limite semi-classique. Ces résultats reposent sur la solution numérique du système de Dirac singulièrement perturbé et la solution numérique du problème eikonal.

On résout le problème eikonal de manière explicite pout tout k dans le cas d'un potentiel particulier. Ces calculs donnent une explication sur le fait que l'on ne puisse pas ap-

pliquer la méthode BKW pour des valeurs de $|k|$ plus petites. On présente une nouvelle méthode numérique pour calculer la solution du problème eikonal avec des valeurs de $|k|$ suffisamment grandes. Les calculs numériques de la transformée spectrale directe offrent une manière d'analyser le système de Dirac singulièrement perturbé pour des valeurs de $|k|$ si petites qu'il n'y a pas de solution globale au problème eikonal. On donne une analyse semi-classique rigoureuse sur la solution pour des potentiels radiaux en $k = 0$, ce qui donne une expression asymptotique du coefficient de réflexion pour $k = 0$ et suggère une structure annulaire pour la solution, ce qui peut être utilisé quand $|k| \neq 0$ est petit. L'étude numérique suggère aussi que pour certains potentiels, le coefficient de réflexion converge simplement, quand $\epsilon \downarrow 0$, vers une fonction limite définie pour des valeurs de k pour lesquelles le problème eikonal n'a pas de solution globale. On propose que les singularités de la fonction eikonale jouent un rôle aussi similaire que les points tournants de la théorie unidimensionelle.

Abstract

Inverse scattering is the most powerful tool in theory of integrable systems. Starting in the late sixties resounding great progress was made in $(1+1)$ dimensional problems with many break-through results as on soliton interactions. Naturally the attention in recent years turns towards higher dimensional problems as the Davey-Stewartson equations, an integrable generalisation of the $(1+1)$-dimensional cubic nonlinear Schrödinger equation. The defocusing Davey-Stewartson II equation, in its semi-classical limit has been shown in numerical experiments to exhibit behaviour that qualitatively resembles that of its one-dimensional reduction, namely the generation of a *dispersive shock wave*: smooth initial data develop a zone rapid modulated oscillations in the vicinity of shocks of solutions for the corresponding dispersionless equations for the same initial data. The present thesis provides a first step to study this problem analytically using the inverse scattering transform method. Both the direct and inverse scattering transform for DSII can be expressed as D-bar equations. We consider the direct spectral transform for the defocusing Davey-Stewartson II equation for smooth initial data in the semi-classical limit. The direct spectral transform involves a singularly perturbed elliptic Dirac system in two dimensions. We introduce a WKB-type method for this problem and prove that it is well defined for sufficiently large modulus of the spectral parameter $k \in \mathbb{C}$ by controlling the solution of an associated nonlinear eikonal problem. Further, we give numerical evidence that the method is accurate for such k in the semiclassical limit. Producing this evidence requires both the numerical solution of the singularly perturbed Dirac system and the numerical solution of the eikonal problem. We present a new method for the numerical solution of the eikonal problem valid for sufficiently large $|k|$. For a particular potential we are able to solve the eikonal problem in a closed form for all k, a calculation that yields some insight into the failure of the WKB method for smaller values of $|k|$. The numerical calculations of the direct spectral transform indicate how to study the

singularly perturbed Dirac system for values of $|k|$ so small that there is no global solution of the eikonal problem. We provide a rigorous semiclassical analysis of the solution for real radial potentials at $k = 0$, which yields an asymptotic formula for the reflection coefficient at $k = 0$ and suggests an annular structure for the solution that may be exploited when $|k| \neq 0$ is small. The numerics also suggest that for some potentials the reflection coefficient converges point-wise as $\epsilon \downarrow 0$ to a limiting function that is supported in the domain of k-values on which the eikonal problem does not have a global solution. We suggest that singularities of the eikonal function play a role similar to that of turning points in the one-dimensional theory.

Contents

Chapter 1

Introduction

In this chapter we introduce the motivation for the present work and briefly outline the results that were obtained.

1.1 Nonlinear Schrödinger equations

This work is concerned with *nonlinear Schroödinger equations* (NLS) which appear in applications in hydrodynamics, nonlinear optics, plasma physics, ... whenever the modulation of plane waves is considered. They can be cast into the form

$$i\psi_t + \Delta\psi + f(|\psi|)\psi = 0; \tag{1.1}$$

here and in the following partial derives are denoted by the variable appearing as an index, $\psi : \mathbb{R} \times \mathbb{R}^d \mapsto \mathbb{C}$, where $d \in \mathbb{N}$ gives the spatial dimension and where Δ is the d-dimensional Laplace operator; the function f is a smooth, not necessary local function of $|\psi|^2$. In $(1+1)$ dimensions, the important case of a $f = |\psi|^2$, i.e., the cubic NLS equation is of particular importance. It has been a break-through results by Zakharov and Shabat [43] that the cubic NLS equation is completely integrable which means in practical terms that powerful solution generation techniques exist to solve the equation.

Whereas the $1+1$ dimensional case has been intensely studied, there are only scattered results in higher dimensions. In $(2+1)$ dimensions, the Davey-Stewartson (DS) equation, here written in a general form

$$i\epsilon q_t + \tfrac{1}{2} q_{xx} + \tfrac{1}{2}\alpha q_{yy} = -|q|^2 q - \varphi q,$$

$$\varphi_{xx} + \beta\varphi_{yy} = -2\left(|q|^2\right)_{xx},$$

where $\alpha = \pm 1$ and $\beta = \pm 1$ (see below) is also completely integrable. This equation was introduced by Davey and Stewartson [1] as a model describing the evolution of three-dimensional water wave packet in a weakly non-linear regime. The rigorous derivation of the DS equation in the modulational scaling regime was presented by Craig, Schanz and Sulem in [2] as an approximation to the gravity-capillary wave problem in (2+1) dimensions.

In $(1+1)$ dimensional integrable PDEs inverse scattering in general involves the solution of so-called Riemann-Hilbert problems (RHPs), i.e., the construction of functions which are holomorphic except for a prescribed singular behaviour at a set of contours, for instance jump discontinuities. In $(2+1)$ dimensions D-bar problems appear in the context of integrable PDEs where the anti-holomorphic derivative of a function is prescribed. Such problems have been much less studied in the context of integrable PDEs than RHPs, and no asymptotic techniques have been developed as *nonlinear steepest descent* for RHPs. This thesis provides a first step towards asymptotic analysis for D-bar problems. D-bar problems prominently appear in *Calderón's problem*, a method for reconstructing a unknown potential for a Helmholtz type equation, supported on a compact domain, from the Dirichlet-to Neumann map on the boundary on said domain. There are extensive results on the applicability of the method for various applications, for example im medical imaging and mineral prospecting, as well as rich analytic results on smoothness and other conditions of the Dirichlet to Neumann map, allowing full reconstruction of the unknown potential. See details and references in [4]

As mentioned above the DS equations can be thought of as a 2+1 dimensional integrable generalisation of the non-linear Schrödinger equation including a non-locality. We can distinguish 4 types of the DS equation which exhibit qualitatively different behaviours, depending on the choice of α and β: elliptic-elliptic, hyperbolic-elliptic, elliptic-hyperbolic and hyperbolic-hyperbolic. DS is integrable, admits a Lax pair allowing an Inverse Scattering transformation. Thus it can be expected that results that have been obtained for the 1+1 NLS can be potentially extended on the 2+1 dimensional case. In particular, following the results of WKB approximation in the semi-classical limit limit $\epsilon \to 0$ for the 1+1 defocussing NLS, we aim to develop a semi-classical theory for the defocussing DSII, posed as an initial-value problem,

$$\begin{aligned} i\epsilon q_t + 2\epsilon^2 \left(\bar{\partial}^2 + \partial^2\right) q + (g + \bar{g})\, q &= 0 \\ \bar{\partial} g + \partial \left(|q|^2\right) &= 0, \end{aligned}$$

where the initial data are of the form

$$q(x,y,0) = A(x,y,0)e^{iS(x,y,0)/\epsilon} \tag{1.2}$$

with real A and S. In this work we also provide numerical analysis of this problem.

A central problem of this work is the direct problem associated to the Inverse Scattering method for the defocusing DSII

$$\begin{aligned} \epsilon\bar{\partial}\mu_1 &= \frac{1}{2}e^{\frac{kz-kz}{\epsilon}}q\bar{\mu}_1 \\ \epsilon\bar{\partial}\mu_2 &= \frac{1}{2}e^{\frac{kz-kz}{\epsilon}}q\bar{\mu}_2 \end{aligned} \tag{1.3}$$

alled the D-bar problem for defocusing DSII, where we assume a potential q in WKB form:

$$q(x,y) = A(x,y)e^{iS(x,y)/\epsilon}. \tag{1.4}$$

The asymptotic condition is $\mu_1 \to 1$ and $\mu_2 \to 0$ as $|z| \to \infty$. The *reflection coefficient* $R = R^\epsilon(k;t)$ is defined in terms of μ_2 as follows:

$$\overline{\mu_2(z;k,t)} = \tfrac{1}{2}R^\epsilon(k;t)z^{-1} + O(|z|^{-2}), \quad |z| \to \infty. \tag{1.5}$$

The ultimate goal of our work is to find an asymptotic formula for the reflection coefficient $R_0^\epsilon(k)$ associated with suitably general real-valued amplitude and phase functions A and S. Such a formula should contain sufficient information about the latter functions to allow their reconstruction via the inverse problem [1], also considered in the semiclassical limit $\epsilon \downarrow 0$. For the two-dimensional problem(1.3)–(1.4), *there exist no known potentials other than* $q \equiv 0$ *for which the direct spectral problem can be solved and the reflection coefficient* $R_0^\epsilon(k)$ *recovered for all* $k \in \mathbb{C}$ *and a set of* $\epsilon > 0$ *with accumulation point* $\epsilon = 0$.

1.2 Main results

In this section we will present the main analytical and numerical results in this context, all justification and detailed analysis can be found in the later chapters. In the absence of any exact solutions, a natural approach to the two-dimensional generalization (1.3)–(1.4) of this problem is to mimic the WKB ansatz that produces such useful and explicit formulae. As will

1. An important observation is that, even though the direct and inverse problems are formally similar, they may be quite different in character in the semiclassical limit, if it happens that the reflection coefficient depends on ϵ in a more subtle way than does the initial data $q^\epsilon(x,y,0) = A(x,y)\mathrm{e}^{\mathrm{i}S(x,y)/\epsilon}$.

be shown in Chapter 8.2, this leads one to consider a certain complex-valued *eikonal function* $f(x,y;k)$ that is an analogue of the WKB exponent E trivially computed for the Zakharov-Shabat system [43] as the antiderivative of an eigenvalue of the coefficient matrix in the system obtained from the Zakharov-Shabat system [43] by a simple gauge transformation to remove the oscillatory factors $\mathrm{e}^{\pm \mathrm{i}S(x)/\epsilon}$. In the two-dimensional setting, this function satisfies the *eikonal equation*:

$$\left[2\bar{\partial}f + \mathrm{i}\bar{\partial}S\right]\left[2\partial f - \mathrm{i}\partial S\right] = A^2, \tag{1.6}$$

a nonlinear partial differential equation in the (x,y)-plane. If A, S, and $E := f - \mathrm{Re}(kz)$ are independent of y, with $k = -\mathrm{i}\lambda$ and $\lambda \in \mathbb{R}$ this equation reduces to the far simpler (solvable by quadrature) one-dimensional eikonal equation. For formal validity of the WKB ansatz near $|z| = \infty$ we insist that f is subject to the asymptotic condition

$$\lim_{|z|\to\infty}\left(f + \frac{\mathrm{i}}{2}S - kz\right) = 0, \quad z = x + \mathrm{i}y. \tag{1.7}$$

We refer to the problem of finding a function $f = f(x,y;k)$ that satisfies (1.6)–(1.7) as the *eikonal problem*. An important point is that unlike the direct scattering problem (1.3)–(1.4), the eikonal problem is independent of the parameter $\epsilon > 0$, so although it is nonlinear it is not a singularly perturbed problem at all. This may be viewed as a distinctive advantage [2] of the WKB approach to the direct scattering problem. In Chapter 5 we prove the following result. Here $\mathrm{W}(\mathbb{R}^2)$ is the Wiener algebra of functions with Lebesgue integrable Fourier transforms, equipped with the norm $\|\cdot\|_{\mathrm{W}}$ defined in (5.7).

Theorem 1.2.1. *Suppose that $u = A^2 \in L^p(\mathbb{R}^2) \cap \mathrm{W}(\mathbb{R}^2)$ for some $p \in [1,2)$, that $S \in C^1(\mathbb{R}^2)$, and that $v = \partial S \in \mathrm{W}(\mathbb{R}^2)$. Then for every $B > \|v\|_{\mathrm{W}}$, if k satisfies the inequality*

$$|k| > B + \max\left\{\frac{1}{4}\frac{\|u\|_{\mathrm{W}}}{B - \|v\|_{\mathrm{W}}}, \frac{1}{2}\sqrt{\|u\|_{\mathrm{W}}}\right\}, \tag{1.8}$$

there is a unique global classical ($C^1(\mathbb{R}^2)$) solution $f(x,y;k)$ of the eikonal problem (1.6)–(1.7) *that satisfies the estimate*

$$\left\|\partial f - k - \frac{1}{2}\mathrm{i}\partial S\right\|_{\mathrm{W}} \leq B. \tag{1.9}$$

In particular, (1.8) *and* (1.9) *imply that* $\mathrm{i}\partial S - 2\partial f$ *is bounded away from zero on* $\mathbb{R}^2$.

One interpretation of Theorem 1.2.1 is that the eikonal problem (1.6)–(1.7) is of nonlinear

2. Note, however, that unlike the one-dimensional reduction of the eikonal problem which is explicitly solvable by quadratures and square roots, to our knowledge there is no analogous elementary integration procedure for the two-dimensional eikonal problem (1.6)–(1.7).

elliptic type for sufficiently large $|k|$. The leading term of the WKB approximation explained in Section 8.2 is proportional to a complex-valued function $a_0 = a_0(x, y; k)$ that is required to solve the following linear equation in which the eikonal function f appears as a coefficient:

$$\mathcal{L}a_0 := (2\bar{\partial}f + \mathrm{i}\bar{\partial}S)\partial(Aa_0) + A\bar{\partial}((2\partial f - \mathrm{i}\partial S)a_0) = 0. \tag{1.10}$$

Theorem 1.2.2. *Under the same conditions on $u = A^2$, S, $v = \partial S$, and k as in Theorem 1.2.1, there is a unique solution a_0 of* (1.10) *for which $a_0^2 - 1 = m \in \mathrm{W}(\mathbb{R}^2)$.*

These two results provide conditions on k sufficient to guarantee the *formal* validity of the WKB expansion in the whole (x, y)-plane. As will be shown in Section 8.2, global validity of the WKB expansion for a given $k \in \mathbb{C}$ implies that the reflection coefficient $R_0^\epsilon(k)$ tends to zero with ϵ. This situation is therefore completely analogous to the fact that in the one-dimensional analogue of this problem, if $|\lambda|$ is sufficiently large there are no turning points and hence a globally defined (purely imaginary) WKB exponent function $E(x; \lambda)$ exists and leads to negligible reflection. *Theorems 1.2.1 and 1.2.2 would therefore provide a two-dimensional analogue of the fact that in the one-dimensional setting the reflection coefficient is asymptotically supported on the finite interval $[\lambda^-, \lambda^+]$.*

In Chapter 8 we give convincing numerical evidence that in the situation covered by Theorems 1.2.1 and 1.2.2 (and more generally, that the eikonal problem (1.6)–(1.7) has a global classical solution) the leading term of the WKB expansion indeed gives the expected order of relative accuracy as $\epsilon \downarrow 0$. Unfortunately, a proof of accuracy of the method, even in the favourable situation of global existence of the eikonal function, eludes us. Nonetheless the numerical results suggest the following conjecture:

Conjecture 1.2.3. *Suppose (for instance) that A and $S - S_\infty$ are Schwartz-class functions for some constant $S_\infty \in \mathbb{R}$, and that $k \in \mathbb{C} \setminus \{0\}$ is such that there exists a global classical solution $f(x, y; k)$ of the eikonal problem* (1.6)–(1.7)*. Then the solution $\boldsymbol{\psi}^\epsilon(z; k)$ of the direct scattering problem* (1.3)–(1.4) *at $t = 0$, well defined for all $\epsilon > 0$, satisfies*

$$\begin{aligned} &\mathrm{e}^{-f(x,y;k)/\epsilon}\mathrm{e}^{-\mathrm{i}S(x,y)\sigma_3/(2\epsilon)}\boldsymbol{\psi}^\epsilon(x + \mathrm{i}y; k) \\ &\qquad = \frac{a_0(x, y; k)}{2k}\begin{bmatrix} 2\partial f(x, y; k) - \mathrm{i}\partial S(x, y) \\ A(x, y) \end{bmatrix} + o(1), \quad \epsilon \downarrow 0 \end{aligned} \tag{1.11}$$

with the convergence measured in a suitable norm and the $o(1)$ symbol on the right-hand side can be uniquely continued to a full asymptotic power series in positive integer powers of ϵ.

Some of the issues that would need to be addressed to give a proper proof of Conjecture 1.2.3 are mentioned in Section 4.1.1. The accuracy of the WKB approximation predicted

by Conjecture 1.2.3 is illustrated in Figure 1.1, in which the solution of the Dirac problem (1.3)–(1.4) for a Gaussian potential $A(x,y)e^{iS(x,y)/\epsilon} = e^{-(x^2+y^2)}$ at $k = 1$ and $\epsilon = 1/16$ is plotted in the upper row (for numerical reasons we plot the modulus of the components multiplied by $e^{-kz/\epsilon}$ in order to have functions bounded at infinity), while plots for the corresponding WKB approximation indicated in the conjecture are shown in the lower row. The qualitative accuracy of the approximation is obvious from these plots, however a more systematic numerical study of these questions is presented in Chapter 8.

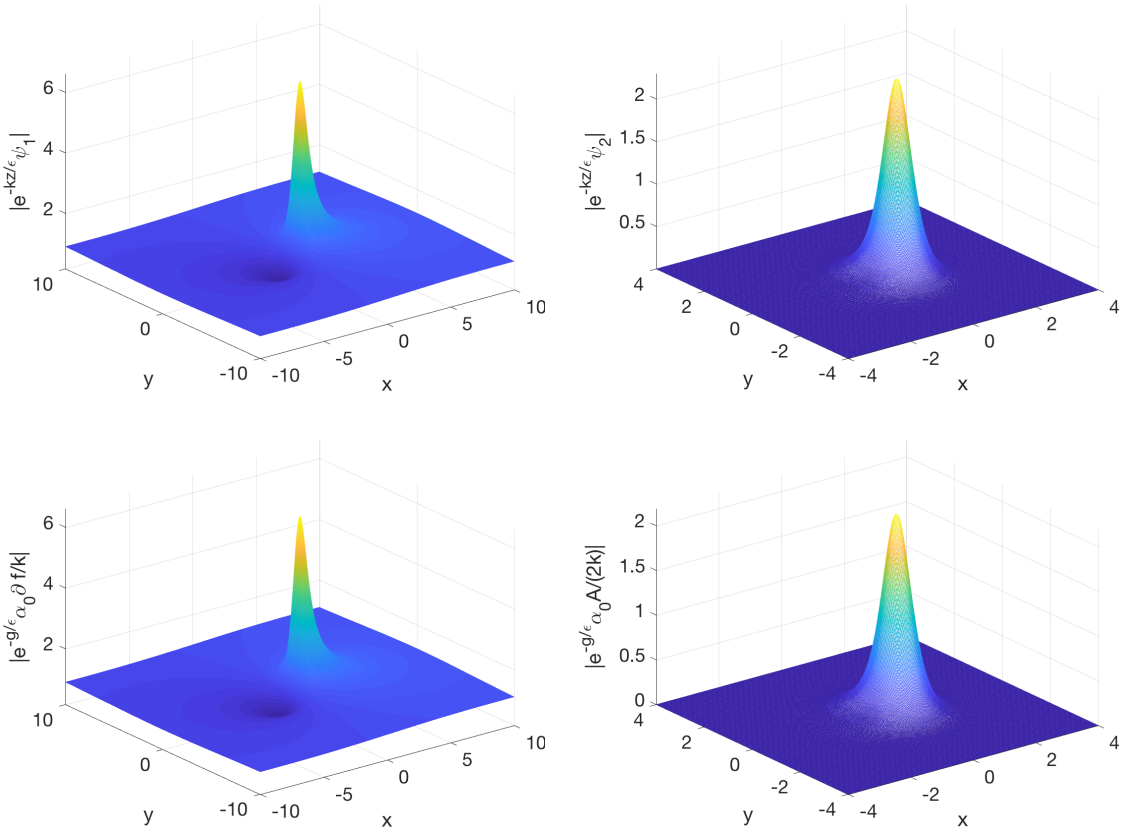

Figure 1.1 – Comparison between the solution to the Dirac system (1.3)–(1.4) with Gaussian potential $e^{-(x^2+y^2)}$ for $k = 1$ and $\epsilon = 1/16$ with the WKB approximation. First row: the modulus of $e^{-kz/\epsilon}\psi_1$ (left) and of $e^{-kz/\epsilon}\psi_2$ (right). Second row: the corresponding WKB approximations of Conjecture 1.2.3.

A corollary of the existence of the full asymptotic expansion anticipated by Conjecture 1.2.3 is the following stronger control on the reflection coefficient.

Corollary 1.2.4. *Under the same conditions on A, S, and k as in Conjecture 1.2.3, the reflection*

coefficient satisfies $R_0^\epsilon(k) = O(\epsilon^p)$ *as* $\epsilon \downarrow 0$ *for all* p.

The proof is simply based on the a priori existence of the reflection coefficient and is given in Section 4.1.

If $|k|$ becomes too small, we can no longer guarantee the existence of a global solution to the eikonal problem (1.6)–(1.7). As long as $k \neq 0$ it is, however, possible to find a solution in a k-dependent neighbourhood of $z = \infty$:

Theorem 1.2.5. *Suppose that* $u = A^2 \in L^p(\mathbb{R}^2) \cap \mathrm{W}(\mathbb{R}^2)$ *for some* $p \in [1, 2)$, *that* $S \in C^1(\mathbb{R}^2)$, $S - S_\infty \in \mathrm{W}(\mathbb{R}^2)$ *for some constant* $S_\infty \in \mathbb{R}$, *and* $v = \partial S \in \mathrm{W}(\mathbb{R}^2)$, *and let* $k \neq 0$ *be a given complex value. Then there exists* $\rho > 0$ *such that there is a classical solution* $f(x, y; k)$ *of* (1.6)–(1.7) *defined for* $|z| \geq \rho$. *There is also a corresponding classical solution* $\alpha_0(x, y; k)$ *of* (1.10) *in the same domain* $|z| \geq \rho$ *satisfying* $\alpha_0 \to 1$ *as* $|z| \to \infty$.

The proof is given in Chapter 5.1.1. This result leads to the question of what goes wrong with the eikonal problem if, given $k \neq 0$ with $|k|$ sufficiently small, one tries to continue the solution inwards from $z = \infty$. Here we cannot say much yet; however we can present a potentially illustrative example. Namely, if $A(x, y) = (1 + x^2 + y^2)^{-1}$ (a Lorentzian potential) and $S(x, y) \equiv 0$, we show in Section 5.1.2 that for $|k| > \frac{1}{2}$, the eikonal problem (1.6)–(1.7) has the explicit global solution

$$f(x, y; k) = kz + \frac{1}{2}\arcsin(W) + \frac{(1 - W^2)^{1/2} - 1}{2W}, \quad W := \frac{\overline{z}}{k(1 + z\overline{z})}, \tag{1.12}$$

and the equation (1.10) has the explicit solution

$$\alpha_0(x, y; k) = \sqrt{2}\left(\left(1 - W^2\right)^{1/2}\left(1 + \left(1 - W^2\right)^{1/2}\right)\right)^{-1/2} \tag{1.13}$$

for which $\alpha_0(x, y; k) \to 1$ as $|z| \to \infty$. Note that α_0 is well-defined and smooth as long as $|k| > 1/2$, i.e., exactly the same condition under which $f(x, y; k)$ is smooth.

With these explicit formulae at hand, we can begin to address the question of what happens to $f(x, y; k)$ when $|k| < 1/2$, a necessary condition for the reflection coefficient to be non-negligible in the limit $\epsilon \to 0$. It is easy to see that the whole complex z-plane is mapped onto the closed disk $D_{1/(2|k|)}$ in the W-plane of radius $(2|k|)^{-1}$ centered at $W = 0$. Each point in the interior of $D_{1/(2|k|)}$ has exactly two preimages in the z-plane along the ray satisfying $\arg(z) + \arg(k) + \arg(W) = 0$, one with $|z| < 1$ and one with $|z| > 1$, while the map is one-to-one from the unit circle in the z-plane onto the boundary of $D_{1/(2|k|)}$. When $|k| < 1/2$, the disk $D_{1/(2|k|)}$ necessarily intersects both branch cuts emanating from $W = \pm 1$. Pulling the parts of the branch cuts in $D_{1/(2|k|)}$ back to the z-plane, one sees that $f(x, y; k)$ is well-defined

and smooth with the exception of two cuts, each of which connects the two preimages in the z-plane of the branch points $W = \pm 1$, joining them through the point on the unit circle in the z-plane corresponding to where the branch cut in the W-plane meets the boundary of $D_{1/(2|k|)}$. Assuming $|k| < 1/2$, the two preimages of $W = \pm 1$ are

$$z = \pm \frac{1}{2k} \left[1 + \sigma \sqrt{1 - 4|k|^2} \right], \quad \sigma^2 = 1. \tag{1.14}$$

This calculation is interesting because it shows that at branch points of f, which may be compared with turning points in the one-dimensional problem, the amplitude function α_0 given by (1.13) exhibits $-1/4$ power singularities, exactly as in the one-dimensional problem (see [29, Section 7.2] and [31, Appendix B.2]). *This suggests that the branch points might play the role in the two-dimensional problem that turning points play in the one-dimensional problem.* The branch points and cuts for $f(x, y; k)$ are shown in the z-plane for two values of k in Figure 1.2.

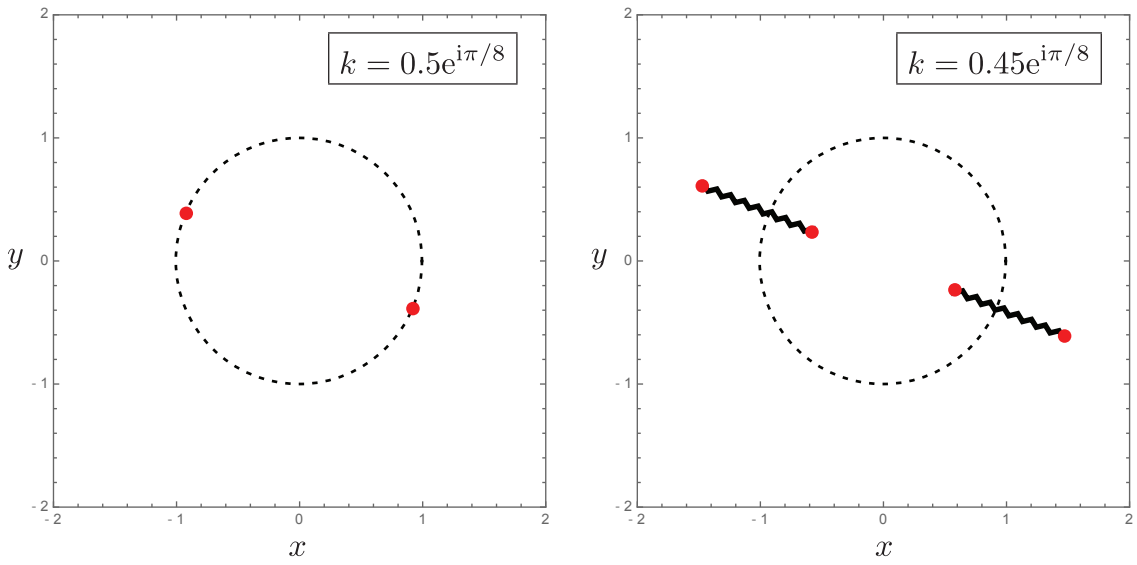

Figure 1.2 – The branch points (red) and cuts (wavy lines) in the z-plane for the continuation below $|k| = \frac{1}{2}$ of the solution (1.12) of the eikonal problem (1.6)–(1.7) for the Lorentzian potential $A(x, y) = (1 + x^2 + y^2)^{-1}$ with $S(x, y) \equiv 0$. Left: $k = \frac{1}{2}e^{i\pi/8}$. Right: $k = 0.45e^{i\pi/8}$. For reference, the unit circle is shown with a dashed line.

In the one-dimensional problem, the reflection coefficient fails to converge to zero with ϵ as soon as turning points appear in the problem, and one might therefore be led to believe

that in the two-dimensional problem something similar occurs when $|k|$ decreases within a finite radius (e.g., $|k| = 1/2$ for $A(x,y) = (1+x^2+y^2)^{-1}$ and $S(x,y) \equiv 0$) at which point singularities first appear in the solution of the eikonal problem. *Numerical reconstructions of the reflection coefficient for small ϵ suggest that this is indeed the case.* In Figure 1.3 we plot the reflection coefficient as a function of $|k|$ for the Gaussian potential $A(x,y) = \mathrm{e}^{-(x^2+y^2)}$ with $S(x,y) \equiv 0$. The reflection coefficient was calculated by solving the direct scattering problem

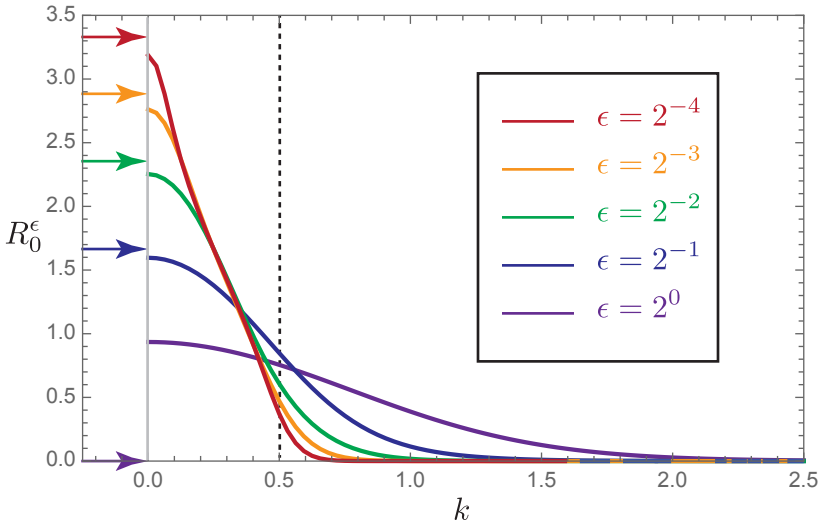

Figure 1.3 – Numerical calculations of the (radially symmetric and real-valued) reflection coefficient $R_0^\epsilon(k)$ for the Gaussian potential $q = A(x,y)\mathrm{e}^{\mathrm{i}S(x,y)/\epsilon}$ with $S(x,y) \equiv 0$ and $A(x,y) = \mathrm{e}^{-(x^2+y^2)}$, plotted as a function of $k > 0$ for several values of $\epsilon > 0$. The dotted vertical line at $k = 1/2$ is the numerically-predicted threshold below which the eikonal problem does not have a smooth global solution and the support of the reflection coefficient appears to concentrate with decreasing ϵ. Also indicated with arrows on the vertical axis are the corresponding values of the relatively accurate approximate formula $2\sqrt{\ln(\epsilon^{-1})}$ for $R_0^\epsilon(0)$ as predicted by Theorem 1.2.6.

(1.3)–(1.4) numerically using the scheme of [22] summarized in Section 7.3. These plots show that as $\epsilon \downarrow 0$ the support of the reflection coefficient $R_0^\epsilon(k)$ appears to reduce to a bounded region as $\epsilon \downarrow 0$, perhaps the domain $|k| \leq \frac{1}{2}$. Now, as will be explained in Section 5.1.2, Theorem 1.2.1 predicts the existence of a global solution of the eikonal problem (1.6)–(1.7) if $|k| > 1$ for the potential $A(x,y) = \mathrm{e}^{-(x^2+y^2)}$ with $S(x,y) \equiv 0$, but our numerical calculations described in Section 8.1 suggest that this is not a sharp bound, and moreover they suggest that the correct value at which singularities first form in $f(x,y;k)$ is again $|k| = \frac{1}{2}$, exactly as is known to be true for the Lorentzian potential. *Therefore, like in the one-dimensional problem,*

we expect that the existence of singularities in the solution of the eikonal problem (1.6)–(1.7) *leads to a nontrivial reflection coefficient in the semiclassical limit*.

Despite this connection with the one-dimensional problem, it is worth dwelling on the stark qualitative differences between the asymptotic behavior of $R_0^\epsilon(k)$ for the two-dimensional problem as illustrated in Figure 1.3 and that of $R_0^\epsilon(\lambda)$ for the one-dimensional problem as for $\lambda_- < \lambda < \lambda_+$ (and $R_0^\epsilon(\lambda) = o(1)$ as $\epsilon \downarrow 0$ for $\lambda \in \mathbb{R} \setminus [\lambda_-, \lambda_+]$). Apparently, $R_0^\epsilon(k)$ is real-valued, non-oscillatory, and develops a growing peak near $k = 0$ as $\epsilon \downarrow 0$, while $R_0^\epsilon(\lambda)$ is complex, rapidly oscillatory, and essentially of unit modulus within its asymptotic support. *Moreover, it seems obvious to the eye that as $\epsilon \downarrow 0$, $R_0^\epsilon(k)$ is converging pointwise to a real, radially-symmetric function with compact support on the disk $|k| \leq \frac{1}{2}$ and that blows up as $|k| \downarrow 0$.*

We do not yet have a good explanation for most of these interesting features of $R_0^\epsilon(k)$. However, motivated by the numerical observation of the growth of $R_0^\epsilon(k)$ near $k = 0$, in Chapter 6 we show how the solution of the direct spectral problem can be calculated for small ϵ at $k = 0$ for radially symmetric potentials A (and $S \equiv 0$). This analysis is based on a radial ordinary differential equation, and it results in an asymptotic formula for $R_0^\epsilon(0)$ that we prove is accurate as $\epsilon \downarrow 0$.

Theorem 1.2.6. *Suppose that $S(x, y) \equiv 0$ and that $A = A(r = \sqrt{x^2 + y^2})$, where $A(r)$ is a continuous nonincreasing function with $A(r) > 0$ for all $r > 0$ such that the function $rA(r)$ has a single maximum. Assume further that for some positive constants $L \leq U$, b and p, the inequalities $Le^{-br^p} \leq A(r) \leq Ue^{-br^p}$ hold for r sufficiently large. Then $R_0^\epsilon(0) = 2(b^{-1}\ln(\epsilon^{-1}))^{1/p}(1 + o(1))$ as $\epsilon \downarrow 0$.*

The Gaussian $A(r) = e^{-r^2}$ satisfies the hypotheses of Theorem 1.2.6 with $L = U = b = 1$ and $p = 2$, and we conclude that $R_0^\epsilon(0) = 2\sqrt{\ln(\epsilon^{-1})}(1 + o(1))$ as $\epsilon \downarrow 0$. The divergence of this approximation as $\epsilon \downarrow 0$ explains the rising peak at $k = 0$ seen in Figure 1.3; the exact values of the approximate formula for $R_0^\epsilon(0)$ are indicated with arrows for comparison. The heuristic analysis in Section 6.1 leading to the proof of Theorem 1.2.6 indicates that a similar approximation of $R_0^\epsilon(0)$ holds true for compactly supported amplitude functions $A = A(r)$, in which $(b^{-1}\ln(\epsilon^{-1}))^{1/p}$ is replaced with the largest value of $r > 0$ in the support of A, which in this case is independent of ϵ. The proof of Theorem 1.2.6 is given in Section 6.2, and in Section 6.3 we show how the direct spectral problem (1.3)–(1.4) can be solved explicitly in terms of special functions when $S(x, y) \equiv 0$ and A is a positive multiple of the characteristic function of the disk of radius ρ centered at the origin yielding the rigorous (but specialized to this particular example) result that $R_0^\epsilon(0) = 2\rho + o(1)$ as $\epsilon \downarrow 0$, consistent with the general principle for compactly supported radial amplitudes indicated above.

The analysis in Chapter 6 shows that the solution of the direct scattering problem (1.3)–

(1.4) at $k = 0$ for radial potentials $A = A(r)$ with $S \equiv 0$ is only consistent with the WKB expansion method in an annulus in the (x, y)-plane centered at the origin with an inner radius proportional to ϵ and an outer radius proportional to $r_{\text{Match}}(\epsilon)$, defined as the largest solution r of the equation $rA(r) = \epsilon$. In this case, the eikonal problem (1.6)–(1.7) has an exact radial solution that is smooth except for a conical singularity at the origin (this solution is described in Section 5.1.2). Our analysis shows that the ϵ-dependent problem (1.3)–(1.4) regularizes the effect of this singularity within a small neighborhood of the origin, and behaves as if $A \equiv 0$ for $r > r_{\text{Match}}(\epsilon)$. This observation suggests that if one wants to capture the behavior of the reflection coefficient for values of k of modulus sufficiently small that the eikonal problem does not have a global smooth solution, it may be necessary to construct the solution in nested approximately annular domains as is known to yield accurate approximations for $k = 0$. This is a subject for future investigation.

In Section 7 we provide new numerical algorithms for computing the eikonal function $f(x, y; k)$ and WKB amplitude $a_0(x, y; k)$, assuming that $|k|$ is sufficiently large. These algorithms are tested on the known exact solutions (1.12) and (1.13) respectively. One of the algorithms for computing the eikonal function $f(x, y; k)$ (a series-based method applicable to radial potentials with $S(x, y) \equiv 0$ that is described in Section 7.2) also gives a method of estimating the critical radius for $|k|$ below which singularities of some sort certainly appear in the eikonal function. This method predicts the threshold value of $|k| = \frac{1}{2}$ for the Gaussian $A(x, y) = \mathrm{e}^{-(x^2+y^2)}$ that matches with the numerical computations of $R_0^\epsilon(k)$ shown in Figure 1.3. We also briefly review the method proposed in an earlier work [22] of two of the authors for solving the ϵ-dependent direct scattering problem (1.3)–(1.4). In Section 8 we use the developed numerical methods to make quantitative comparisons with the WKB method and provide quantitative justification of Conjecture 1.2.3.

Chapter 2

Inverse scattering transformation

2.1 Inverse scattering method

The history of developing methods for solving non-linear integrable partial differential equations in mathematical physics as well as of constructing soliton solutions lead us to a famous result of Gardner, Green, Kruskal and Miura 1967, 1974, namely the inverse scattering method which was inspired by the Fourier transform for linear PDE's. In this chapter some classical results in theory of the intergable systems will be presented that can be also found in different variations (see, for example, [3]). To understand the underlying idea of the inverse scattering transform which is the main part of the algorithm, let us first have a look at the linear case. Consider the linearized KdV equation

$$u_t + u_{xxx} = 0, \tag{2.1}$$

and the following Cauchy problem

$$u(x,0) = u_0(x), \text{ where } u_0(x) \in L_2(\mathbb{R}).$$

One can apply a Fourier transformation to (2.1) and get an equation in the phase space

$$\tilde{u}_t - i\lambda^3 \tilde{u} = 0 \tag{2.2}$$

where λ is the Fourier variable.

It is easy to see that the general solution of (2.2) is

$$\tilde{u}(\lambda, t) = C(\lambda) e^{-i\lambda^3 t}$$

where $C(\lambda)$ will be identified from the initial conditions

$$C(\lambda) = \tilde{u}(\lambda, 0) = \int_{-\infty}^{+\infty} e^{i\lambda x} u(x, 0)\, \mathrm{d}x =: \mathcal{F}(u_0).$$

To get the solution of the original problem (2.1) one has to apply the Inverse Fourier Transform, thus

$$u(x, t) = \frac{1}{2\pi} \int_{-\infty}^{+\infty} e^{i\lambda x - i\lambda^3 t} C(\lambda)\, \mathrm{d}\lambda$$

The work of GGKM generalises this algorithm to some non-linear PDEs.

2.1.1 Isospectral deformation of the Schrödinger operator

Let's consider the following isospectral problem for Schrödinger operator

$$L\Phi = \frac{d^2\Phi}{dx^2} + u\Phi = \lambda\Phi, \tag{2.3}$$

i.e., one has to find a condition on the potential $u(x, t)$ such that the eigenvalues λ are t independent and further that Φ admits a time evolution $\Phi_t = A\Phi$ where A is a linear differential operator in x with its coefficients being functions of x and t (differential polynomials/rational functions in u). By differentiation of (2.3) with respect to t

$$L\Phi_t + L_t\Phi = \lambda\Phi_t \Leftrightarrow LA\Phi + u_t\Phi = \lambda A\Phi \Leftrightarrow u_t = [A, L].$$

Thus by choosing operators A one can construct Lax pairs for many equations. If we take A as an operator of third order, then compatibility conditions are equivalent to a KdV equation.

$$u_t - 6uu_x + u_{xxx} = 0, \quad \text{where } u = u(x, t). \tag{2.4}$$

Thereby for the KdV (2.4) equation the analogue of the FT will be the Scattering transform represented by the Schrödinger equation

$$\frac{d^2\Phi}{dx^2} + (\lambda + u)\Phi = 0.$$

Remark: we will consider that $\Phi \in L(\mathbb{R})$, $\lambda \in \mathbb{R}$, and u is such that $\int_{-\infty}^{+\infty}(1 + |x|)|u(x)|\, \mathrm{d}x < \infty$. Furthermore we will give a detailed proof of this choice.

2.1.2 Jost solutions

The eigenvalue problem (2.3) for the Schrödinger operator has formal solutions with the following asymptotic properties:

$$\psi_1(x,k) = e^{-ikx} + o(1), \quad \psi_2(x,k) = e^{ikx} + o(1), \quad \text{when} \quad x \to +\infty \tag{2.5}$$

$$\phi_1(x,k) = e^{-ikx} + o(1), \quad \phi_2(x,k) = e^{ikx} + o(1), \quad \text{when} \quad x \to -\infty \tag{2.6}$$

provided by a decaying condition on potential $u(x,t)$, where $\lambda = k^2$ such that $\Im(\lambda) > 0$ and $\Im(k) > 0$.

One has to notice that (2.3) as a second order linear equation has a two dimensional basis of solutions. Scattering methods help us to determine a potential $u(x,t)$ essentially supported at some neighbourhood of the origin by sending test waves from positive or negative infinity and detecting reflected waves. The role of these test waves in this case will be played by Jost functions (2.5), i.e., the solution of the spectral problem with a zero potential. For this purpose the aim is to study the relation between Jost solutions at negative and positive infinity. This information is contained in the transition matrix between two bases $\{\psi_1, \psi_2\}$ and $\{\phi_1, \phi_2\}$. It can be denoted

$$T(k) = \begin{pmatrix} a(k) & b(k) \\ c(k) & d(k) \end{pmatrix}.$$

For all real $k \neq 0$ the transformation matrix $T(k)$ is a pseudo-unitary matrix, i.e.

$$T(k) = \begin{pmatrix} a(k) & \bar{b}(k) \\ b(k) & \bar{a}(k) \end{pmatrix}$$

and $\det T(k) = |a(k)|^2 + |b(k)|^2 = 1$.

Proof. One can notice that the Wronskian of two independent solutions of the Schrödinger equation does not depend on x, namely

$$\frac{d}{dx} W(\phi_1, \phi_2) = \frac{d}{dx} W(\psi_1, \psi_2) = 0, \tag{2.7}$$

$$\begin{aligned} \frac{d}{dx} W(\phi_1, \phi_2) = \frac{d}{dx} \det \begin{pmatrix} \phi_1 & \phi_2 \\ \phi_1' & \phi_2' \end{pmatrix} &= \frac{d}{dx} \left(\phi_1' \phi_2' + \phi_1 \phi_2'' - \phi_2' \phi_1' - \phi_2 \phi_1'' \right) \\ &= \phi_1 \phi_2'' - \phi_2 \phi_1'' = \phi_1 (\lambda + u) \phi_2 - \phi_2 (\lambda - u) \phi_1 = 0. \end{aligned}$$

The same computation works for ψ_1 and ψ_2. Thus

$$W(\phi_1, \phi_2) = \lim_{x\to\infty} W(\phi_1, \phi_2) = W(e^{-ikx}, e^{-ikx}) = 2ik$$
$$W(\psi_1, \psi_2) = \lim_{x\to\infty} W(\psi_1, \psi_2) = W(e^{-ikx}, e^{-ikx}) = 2ik.$$

Taking into account that

$$W(\phi_1, \phi_2) = |(a(k)|^2 + |b(k)|^2) W(\phi_1, \phi_2) \tag{2.8}$$

and the symmetry of the coefficients $a = \bar{c}, \quad b = \bar{d}$ provided by

$$\phi_1 = \bar{\phi}_2, \quad \psi_1 = \bar{\psi}_2$$

and

$$\phi_1 = a\psi_1 + b\bar{\psi}_1$$
$$\bar{\phi}_1 = c\psi_1 + d\bar{\psi}_1$$

one can finish the proof.

Remark. Only the coefficients $r(k) = \frac{b(k)}{a(k)}$ and $t(k) = \frac{1}{a(k)}$ have a physical meaning – they are called the reflection coefficient and the transmission coefficient respectively.
Thus we presented the so called direct map from potential to scattering data. The analytic properties of the scattering data will enable us to complete the resolution of the problem.

1. The complex valued function $a(k)$ defined for all real $k \neq 0$ admits its analytic continuation on the upper half plane $\Im(k) > 0$, has only simple zeros and asymptotic behaviour

$$a(k) = 1 + \left(\frac{1}{k}\right), \quad \text{when} \quad |k| \to \infty.$$

2. For $\Im(k) > 0 \quad a(k) = 0$ if and only if $\lambda = k^2$ is an eigenvalue of the Schrödinger operator.

$$W(\phi_1, \psi_2) = \lim_{x\to+\infty} (ik(a(k)e^{-ikx} + b(k)e^{ikx})e^{ikx} - (-ika(k)e^{-ikx} + ikb(k)e^{ikx})e^{ikx}) =$$
$$\lim_{x\to+\infty} = (ik(a(k) + b(k)e^{2ikx} + a(k) - b(k)e2ikx)) = 2ika(k).$$

This means that for all $k \in \mathbb{R}$ but $k \neq 0$

$$a(k) = \frac{W(\phi_1(x,k), \psi_2(x,k))}{2ik}. \tag{2.9}$$

This equality gives us motivation to study the analytic continuation and analytic properties of the Jost solutions. Let us recall that the Green function for the Schrödinger equation (2.3) is

$$G(x,y,\lambda) = \begin{cases} -\frac{\sin k(x-y)}{k}, & x > y \\ 0, & x \leq y \end{cases}.$$

Thus the Jost solutions should satisfy

$$\phi_1 = e^{-ikx} + \int_{-\infty}^{x} G(x-y)u(y)\phi_1 dy \tag{2.10}$$

$$\begin{aligned} \phi_2 &= e^{ikx} + \int_{-\infty}^{x} G(x-y)u(y)\phi_2 dy \\ \psi_1 &= e^{-ikx} + \int_{x}^{+\infty} G(x-y)u(y)\psi_1 dy \\ \psi_2 &= e^{ikx} + \int_{x}^{+\infty} G(x-y)u(y)\psi_2 dy \end{aligned}$$

One can check it by straight forward computations. For simplicity one has to apply a normalization condition assuming that $k \in \mathbb{R}$

$$\begin{aligned} \chi_1(x,k) &= e^{ikx}\phi_1, \\ \chi_2(x,k) &= e^{ikx}\psi_1. \end{aligned}$$

Multiplying (2.10) by the factor e^{ikx} one gets

$$\begin{aligned} &\chi_1(x,k) = 1 - \textstyle\int_{-\infty}^{x} e^{ikx}\frac{\sin k(x-y)}{k}u(y)\phi_1(y)dy = \\ &1 - \textstyle\int_{-\infty}^{x} e^{ikx}\frac{e^{ik(x-y)}-e^{-ik(x-y)}}{2ik}u(y)\phi_1(y)dy = 1 + \int_{-\infty}^{x}\frac{e^{ik(x-y)}-1}{2ik}u(y)\chi_1(x,k). \end{aligned} \tag{2.11}$$

The same computations for $\chi_2(x,k)$ give us

$$\chi_2(x,k) = 1 - \int_{x}^{+\infty}\frac{e^{ik(x-y)}-1}{2ik}u(y)\chi_2(x,k).$$

One can notice that the kernel in the integral equation (2.11) is bounded provided that $\Im(k) > 0$, indeed

$$|e^{2ik(x-y)}| = e^{-2\Im k(x-y)} < 1, \quad (x-y) > 0. \tag{2.12}$$

Consider that the potential $\psi(x,k)$ is rapidly decaying as $|x| \to \infty$, thus (2.11) is a Volterra integral equation and according to the theory (see [44], for example) it can be solved for any $k \in \mathbb{C}$ such that $\Im(k) > 0$ in the case of χ_1 (or $\Im(k) < 0$ for χ_2). In other words, χ_1 is an analytic function in the upper-half of the complex plane, whereas χ_2 is an analytic function in the lower half of the complex plane. This gives us that ϕ_1 and ψ_1 admit analytic continuation into the lower half and upper half of the complex plane respectively. The same arguments work in a case of ϕ_2 and ψ_2 by looking at the integral equations for $e^{-ikx}\phi_2$ and $e^{-ikx}\psi_2$ and it can be shown that ψ_2 and ϕ_2 are analytic functions for all $k \in \mathbb{C}$ such that $\Im(k) > 0$ and $\Im(k) < 0$ respectively. Finally, to prove that $a(k)$ is an analytic function in the upper half of the complex plane, one has to remember that the Wronskian of two analytic functions is an analytic function and apply this fact to formula (2.9).

3. On the domain $\Im(k) > 0$ the coefficient $a(k)$ becomes zero if and only if $\lambda = k^2$ is a point of the discrete spectrum of the Schrödinger operator, since at the points where $a(k)$ becomes zero, which means that the Jost functions become proportional, namely $\psi_1(x,k_0) = \alpha\phi_1(x,k_0)$. To show that these functions are solutions of the Schrödinger problem, it is sufficient to prove that the integrals converge for not only real values of k.

$$|\phi_1(x,k_0)| \sim |e^{-ik_0x}| = |e^{\Im(k_0)x}| \to 0 \text{ when } x \to -\infty$$

provided that $\Im(k) > 0$. And

$$|\phi_1(x,k_0)| = |\alpha||\psi_1(x,k_0)| \sim |\alpha||e^{ik_0x}| = |\alpha|e^{-\Im(k_0)x} \to 0 \text{ when } x \to +\infty$$

under the same condition on k.
One can notice that the reflection and transmission coefficients uniquely define the transition matrix $T(k)$ for all $k > 0$, therefore they completely define the continuous spectrum of the Schrödinger operator. Indeed, to recover the matrix $T(k)$ at the points of the continuous spectrum it is sufficient to keep only information about the coefficient $r(k)$ when $\Im(k) > 0$, and the points of the discrete spectrum of the Schrödinger operator, which is a finite collection of points on the upper-half plane are corresponding to the zeros of $a(k)$. In other words, it was shown that the eigenvalues of the scattering operator and the Schrödinger operator are the same. Since $a(k)$ can be expressed via r(k) in the following way, with similar formulas for $b(k)$:

$$|a(k)|^2 = \frac{1}{1 - |r(k)|^2},$$

$$\arg[a(k)] = \frac{1}{i}\sum_{n=1}^{N} \ln\frac{k-i\kappa}{k+i\kappa} - \frac{1}{\pi}\int_{-\infty}^{+\infty} \frac{\ln|a(\nu)|}{\nu-k}d\nu.$$

We have finished the construction of the spectral data. For each $n = 1, 2, ...N$ one has to fix an eigenfunction $\phi(x, i\kappa_n)$ and study its asymptotic:

$$\phi(x, i\kappa_n) = b_n\psi(x, i\kappa_n) = b_n e^{-\kappa x} + o(1) \text{ for } x \to +\infty$$

and the set of spectral data will be defined as follows:

$$\text{the function } r(k), \text{ where } k > 0 \text{ and the set of points } \{\kappa_n,\ b_n\}, \text{ where } n = 1, 2, ..., N.$$

2.1.3 The time evotution of spectral data.

1. Evolution of the isospectral deformation of the Schrödinger equation corresponding to the continuous spectrum is described by the Gardner-Green-Kruskal-Miura equations:

$$\dot{a}(k,t) = 0, \quad \dot{b}(k,t) = 8ik^3 b(k,t).$$

To prove this one has to use the second equation of the Lax pair for KDV equation. This corresponds to the operator A having the following form

$$A = -4\partial_x^3 + 6u\partial_x - 3u_x.$$

Let us first consider the asymptotic of the Jost solution ϕ_1 and ϕ_2 for each t. It is obvious that the operators L and $\partial_t - A$ commute which implies that the operator $\partial_t - A$ acts invariantly on the space of eigenfunctions of L. Thus with respect to the basis of L at $-\infty$ the following can be seen as

$$(\partial_t - A)\phi_1 = c_1(k,t)\phi_1(x,t,k) + c_2(k,t)\phi_2(x,t,k).$$

Taking the limit of A at $-\infty$ one get

$$A \sim -4\partial_x^3$$

which leads to

$$4ik^3\phi_1(x,t,k) \sim c_1(k,t)\phi_1(x,t,k) + c_2(k,t)\phi_2(x,t,k) \text{ when } x \to -\infty.$$

As for the potential u is rapidly decaying at infinity, and the asymptotic of the Jost functions remain the same as $t \to -\infty$, the coefficient $c_2(k,t) = 0$, thus

$$(\partial_t - A)\phi_1 = 4ik^3\phi_1(x,t,k). \tag{2.13}$$

Considering the asymptotic of this expression at $+\infty$ one get

$$\left(\frac{\partial a(t,k)}{\partial t} + 4ik^3 a(t,k)\right)e^{-ikx} + \left(\frac{\partial b(t,k)}{\partial t} - 4ik^3 b(t,k)\right)e^{ikx} \sim 4ik^3(a(t,k)e^{-ikx} + b(t,k)e^{ikx}).$$

2. The time evolution of the scattering data corresponding to the discrete spectrum is

$$\dot{\kappa}_n = 0, \quad \dot{b}_n = 8\kappa_n^3 b_n(t), \text{ where } n = 1, ..., N.$$

Since a priori, we are considering the isospectral deformation of the Schrödinger operator, this means that the κ_n are constants. Knowing the time evolution(2.13) of the solution proportional to e^{-ikx} at $x \to -\infty$ we one can study its asymptotic at $x \to +\infty$ at the point $k = i\kappa_n$

$$\frac{\partial b(t,k)}{\partial t} - 4i\kappa_n^3 b(t,k) \sim 4\kappa_n^3 e^{-\kappa_n x} \tag{2.14}$$

which proves the second equation of (2.1.3). Thus the time evolution of all elements of scattering data can be written in a following way:

$$\begin{aligned} r(k,0) &\to r(k,0)e^{8ik^3t} \\ \kappa_n &\to \kappa_n \\ b_n(0) &\to b_n(0)e^{8\kappa^3 t} \end{aligned}$$

where $k > 0$, $n = 1, ..., N$.

2.1.4 Solution of the inverse problem

Reduction of the differential equations to integral equations of Volterra type allows to use the well developed theory of Volterra equations [44]. Thus one can look for the solution of (2.10) in the form

$$\psi_2(x,k) = e^{ikx} + \int_x^{+\infty} K(x,y)e^{ikx}dy \tag{2.15}$$

where $K(x,y)$ is a real function as $y \geq x$ and $k \in \mathbb{R}$. This solution also holds true as $k \in \mathbb{C}$ provided that ϕ_2 admits analytic continuation in the upper half plane. Remembering that ϕ_1

can be represented as a linear combination of the basis functions at $-\infty$ one gets

$$\phi_1(x,k) = a(k)\phi_1(x,k) + b(k)\psi_2(x,k).$$

Dividing this expression by $a(k)$, subtracting e^{-ikx}, multiplying by e^{iky} and finally integrating (fixing $y \in \mathbb{R}$) with respect to k one gets,

$$\int_{-\infty}^{+\infty} \left(\frac{\phi_1(x,k)e^{iky}}{a(k)} - e^{ik(x-y)} \right) dk = \int_{-\infty}^{+\infty} e^{iky} \left(\phi_1(x,k) - e^{-ikx} + r(k)\phi_2(x,k) \right) dk \tag{2.16}$$

Then one can compute the residue at simple zeroes of $a(k)$, namely at points κ_n where $n = 1, ..., N$:

$$\int_{-\infty}^{+\infty} \left(\frac{\phi_1(x,k)e^{iky}}{a(k)} - e^{ik(x-y)} \right) dk = 2\pi i \sum_{n=1}^{N} \operatorname*{res}_{k=i\kappa_n} \left(\frac{\phi_1(x,k)e^{iky}}{a(k)} \right) =$$
$$2\pi i \sum_{n=1}^{N} \frac{\phi_1(x,i\kappa_n)e^{-\kappa_n y}}{a'(i\kappa_n)} = 2\pi i \sum_{n=1}^{N} \frac{b_n \psi_2(x,i\kappa_n)e^{-\kappa_n y}}{a'(i\kappa_n)}.$$

Then one can compute the integral using the residue theorem taking into account that the integral in the semi-circle tends to zero as the radius goes to infinity and (2.15):

$$2\pi i \sum_{n=1}^{N} \frac{\phi_1(x,i\kappa_n)e^{-\kappa_n y}}{a'(i\kappa_n)} = 2\pi i \sum_{n=1}^{N} \frac{b_n e^{-\kappa_n (x+y)}}{a'(i\kappa_n)} + 2\pi i \int_x^{+\infty} \left(K(x,z) \sum_{n=1}^{N} \frac{b_n e^{-\kappa_n (y+z)}}{a'(i\kappa_n)} \right) dz.$$

To compute the right-hand part of (2.16) one can use that for $k \in \mathbb{R}$

$$\phi_1(x,k) = \bar{\psi}_2(x,k) = e^{-ik} + \int_x^{+\infty} K(x,y)e^{-iky} dy.$$

This leads to

$$\int_{-\infty}^{\infty} e^{iky} \left(\psi_1(x,k) - e^{-ikx} + r(k)\psi_2(x,k) \right) dk =$$
$$\int_{-\infty}^{+\infty} e^{iky} \left(\int_x^{+\infty} K(x,z)e^{-ikz} dz \right) dk + \int_{-\infty}^{+\infty} \left(r(k)e^{ik(x+y)} + r(k) \int_x^{+\infty} K(x,z) \right) e^{ik(y+z)} dk.$$

Noticing that the function $K(x,y)$ is only defined for $y \geq x$, one can see that the first integral in the last expression is nothing but a composition of Fourier transform and Inverse Fourier transform, indeed:

$$\int_{-\infty}^{+\infty} e^{iky} \left(\int_x^{+\infty} K(x,z)e^{-ikz} dz \right) dk = 2\pi K(x,y). \tag{2.17}$$

Thus for $y \geq x$ the equation (2.16) has the form

$$2\pi\left(-\sum_{n=1}^{N}\frac{b_n e^{-\kappa_n(x+y)}}{a'(i\kappa_n)}-\frac{1}{2\pi}\int_{-\infty}^{+\infty}r(k)e^{ik(x+y)}dk\right)=$$
$$2\pi K(x,y)+2\pi\int_x^{+\infty}K(x,z)\left(\sum_{n=1}^{N}\frac{b_n e^{-\kappa_n(y+z)}}{a'(i\kappa_n)}+\frac{1}{2\pi}r(k)e^{ik(y+z)}dk\right)dz$$

Introducing the notation $F(x)=\sum_{n=1}^{N}\frac{b_n e^{-\kappa_n(y+z)}}{a'(i\kappa_n)}+\frac{1}{2\pi}r(k)e^{ik(y+z)}dk$ finally one gets

$$K(x,y)+F(x+y)=\int_x^{+\infty}K(x,z)F(y+z)dz=0,\ \text{where } y\geq x. \tag{2.18}$$

This integral equation is called the Gelfand-Levitan-Marchenko equation.

2.1.5 Reconstruction formula

The last step is to find a reconstruction formula for the the potential $u(x)$ using evolved spectral data.

One can show using the analytic properties of the Jost solutions that the function $\theta(x,k)=e^{-ikx}\psi_2$ has the following asymptotic behaviour as $|k|\to\infty,\quad \Im(k)>0$

$$\theta(x,k)=1+\frac{1}{2ik}\int_x^{+\infty}u(y)dy+o(\frac{1}{k}). \tag{2.19}$$

Thus one can deduce

$$u(x)=\frac{\partial}{\partial x}\left(\lim_{|k|\to\infty}2ik\left(\theta(x,k)-1\right)\right)=\frac{\partial}{\partial x}\left(\lim_{|k|\to\infty}2ik\left(e^{-ikx}\psi_2-1\right)\right). \tag{2.20}$$

According to 2.15 one gets

$$2ik\left(e^{-ikx}\psi_2-1\right)=-2ik\int_x^{+\infty}K(x,y)e^{ik(y-x)}dy=-2\int_x^{+\infty}K(x,y)\frac{\partial}{\partial y}e^{ik(y-x)}=$$
$$-2K(x,y)\frac{\partial}{\partial y}e^{ik(y-x)}\Big|_x^{+\infty}+2\int_x^{+\infty}K_y(x,y)e^{ik(y-x)}dy=2K(x,x)+2\int_x^{+\infty}K_y(x,y)e^{ik(y-x)}dy.$$

Taking the limit $k\to\infty$ while $\Im(x)>0$ means that the last integral tends to 0. Finally, we get the formula for the potential of the Schrödinger operator

$$u(x)=-2\frac{d}{dx}K(x,x),$$

where $K(x,y)$ is a solution of the Gelfand-Levitan-Marchenko equation (2.18).

2.1.6 Reflectionless potentials

In this section we will consider the inverse scattering problem in the case of potentials $u(x)$ which do not produce any reflection, that is $r(k) \equiv 0$ for $k \in \mathbb{R}$. These potentials are called reflectionless. One can notice that $r(k) \equiv 0$ if and only if $b(k) = 0$, thus as a consequence one gets that $a(k) \equiv 0$ for $k \in \mathbb{R}$. The coefficient $a(k)$ is an analytic function in the upper half plane with zeroes coinciding with the discrete spectrum of the Schrödinger equation. The uniqueness theorem provides that $a(k)$ could be only proportional to the function

$$\gamma \sum_{n=1}^{N} \frac{k - i\kappa_n}{k + i\kappa_n}. \tag{2.21}$$

But knowing that the function $a(k) \to 1$ when $k \to \infty$ one gets that the coefficient $\gamma = 1$. Given that $b(k)$ is identically zero the kernel $F(x)$ in the GLM equation simply becomes the sum of exponents

$$F(x) = \sum_{n=1}^{N} \beta_n e^{-\kappa_n x}, \text{ where } \beta_n = \frac{b_n}{ia'(i\kappa_n)}. \tag{2.22}$$

We will seek the solution of the GLM equation (2.18) as a sum of exponents:

$$K(x,y) = \sum_{n=1}^{N} K_n(x) e^{-\kappa_n y},$$

and substituting this expansion in (2.18) the integral

$$\int_x^{+\infty} K(x,z)F(y+z)dz = \sum_{m,n=1}^{N} K_m(x)\beta_n e^{-\kappa_n y} \int_x^{+\infty} e^{-(\kappa_n+\kappa_m)z}dz = \sum_{m,n=1}^{N} K_m(x)\frac{\beta_n e^{-(\kappa_n+\kappa_m)x}}{\kappa_n+\kappa_m}$$

the GLM (2.18) becomes

$$\sum_{n=1}^{N} K_n(x)e^{-\kappa_n y} + \sum_{n=1}^{N} \beta_n(x)e^{-\kappa_n(x+y)} + \sum_{m,n=1}^{N} K_m(x)\frac{\beta_n e^{-(\kappa_n+\kappa_m)x}}{\kappa_n+\kappa_m} = 0. \tag{2.23}$$

As far as the left part of the equation for any fixed x is a linear combination of $e^{-\kappa_n y}$ with different exponents, the last equation is equivalent to the system:

$$K_n(x) + \sum_{m=1}^{N} K_m(x)\frac{\beta_n e^{-(\kappa_n+\kappa_m)x}}{\kappa_n+\kappa_m} = -\beta_n e^{-\kappa_n x}. \tag{2.24}$$

One can see that this system is linear. Let us denote by $A(x) = (A_{nm}(x))$ the following matrix:

$$A_{nm}(x) = \delta_{nm} + \frac{\beta_n e^{-(\kappa_n+\kappa_m)x}}{\kappa_n + \kappa_m}. \tag{2.25}$$

This system can solved by the Kramer's method:

$$K_n(x) = \frac{\det A^{(n)}(x)}{detA(x)}. \tag{2.26}$$

Thus one gets

$$K(x,x) = \frac{1}{\det A(x)} \sum_{n=1}^{N} \det A^{(n)}(x) e^{-\kappa_n x}. \tag{2.27}$$

Then remembering the rule of derivation of the determinant we find that

$$K(x,x) = \frac{d}{dx} \ln \det A(x).$$

And finally, using the inverse formula we get an explicit expression for the potential

$$u(x) = -2\frac{d^2}{dx^2} \ln \det A(x).$$

2.1.7 Interaction of solitons

Time evolution for the matrix $A(x,t)$ is given by

$$A_{nm}(x) = \delta_{nm} + \frac{\beta_n e^{-(\kappa_n+\kappa_m)x + 8\kappa_n^3 t}}{\kappa_n + \kappa_m}$$

where $\beta_n = \beta_n(0) = const$. Then the corresponding solution of the KdV equation can be found by

$$u(x,t) = -2\frac{d^2}{dx^2} \ln \det A(x,t).$$

These solutions are called multi-soliton solutions.

One can easily compute the well-known one soliton solution taking $N = 1$:

$$u(x,t) = -2\frac{\partial^2}{\partial x^2} \ln\left(1 + \frac{\beta e^{-2x+8\kappa^3 t}}{2\kappa}\right) = -2\frac{4\gamma\kappa^2}{(e^{x\kappa} + \gamma e^{-\kappa x})^2} = \frac{2\kappa^2}{ch^2(\kappa(x - 4\kappa^2 t + \delta))},$$

where $\delta = \frac{1}{2\kappa} \ln \frac{\beta}{2\kappa}$.

Remark. The physical meaning of κ^2 - the velocity of the soliton (up to a coefficient) and the constant β is the phase of the latter. Now let us take $N = 2$ and $\kappa_2 > \kappa_1$. In this case the formula for the potential is

$$u = -\ln \frac{\partial^2}{\partial x^2} \left(\left(1 + \frac{\beta_1 e^{-2\kappa_1 x + 8\kappa_1^2 t}}{2\kappa_2} \right) \left(1 + \frac{\beta_2 e^{-2\kappa_2 x + 8\kappa_2^2 t}}{2\kappa_2} \right) - \frac{\beta_1 \beta - 2}{\kappa_1^2 + \kappa_2^2} e^{-2(\kappa_1+\kappa_2)x + 8(\kappa_1^3+\kappa_2^3)t} \right) =$$
$$= 2\frac{\partial}{\partial x} \left(\frac{-2\kappa_1 e^{\theta_1} - 2\kappa_2 e^{\theta_2 - 2(\kappa_1+\kappa_2)} B e^{\theta_1+\theta_2}}{1 + e^{theta_1} + e^{\theta+2} + B e^{\theta+1+\theta_2}} \right),$$

where $\theta_n = -2\kappa_n x + 8\kappa_n^3 t + \ln \frac{\beta_n}{2\kappa_n}$ for $n = 1, 2$, $B = \left(\frac{\kappa_2 - \kappa_1}{\kappa_2 + \kappa_1} \right)^2$. Let us assume that $\theta_1 = 0$, which is the case when $x \sim 4\kappa_1^2 t + \frac{1}{2\kappa_1} \ln \frac{\beta_1}{2\kappa_1}$, we get

$$\theta_2 = 8\kappa_2(\kappa_2^2 - \kappa_1^2)t + \ln \frac{\beta_2}{2\kappa_2} - \frac{\kappa_2}{\kappa_1} \ln \frac{\beta_1}{2\kappa_1}.$$

One can deduce that $\theta_2 \to -\infty$ along the line $\theta_1 = 0$ when $t \to -\infty$ which leads to

$$u(x,t) \sim -\frac{8\kappa_1^2 e^{\theta_1}}{1 + e^{\theta_1}} + 2 \left(\frac{-2\kappa_1^2 e^{\theta_1}}{1 + e^{\theta_1}} \right)^2 = -\frac{8\kappa_1^2 e^{\theta_1}}{(1 + e^{\theta_1})^2} = -\frac{2\kappa_1^2}{ch^2 \frac{\theta_1}{2}} = -\frac{2\kappa_1^2}{ch^2(\kappa_1(x - 4\kappa_1^2 t + \delta_1))},$$

where $\delta = \frac{1}{2\kappa_1} ln \frac{\beta_1}{2\kappa_1}$, that means that in the limit $t \to -\infty$ along the line $\theta_1 = 0$ one can observe a single soliton with the velocity $4\kappa_1^2$ and the amplitude $2\kappa_1^2$. Similarly, provided the same condition $\theta_1 = 0$ holds, one can study the limit $t \to +\infty$:

$$u(x,t) \sim -2\frac{d}{dx} \left(\frac{-2\kappa_2 e^{-\theta_1} - 2(\kappa_1 + \kappa_2)B}{e^{-\theta_1} + B} \right) = -\frac{2\kappa_1^2}{ch^2 \frac{\theta_1 + \ln B}{2}}.$$

Here one can see that in the limit $t \to +\infty$ along the line $\theta_1 = 0$ there is a single soliton moving with the velocity $4\kappa_1^2$ and the amplitude $2\kappa_1^2$ but with a shifted phase $\tilde{\delta}_1 = \delta_1 - \frac{\ln B}{2\kappa - 1}$. Symmetrically one can study the asymptotic behaviour of the solution for $t \pm \infty$ provided that $\theta = 0$: it will be again a single soliton with fixed parameters except for the phase, which is shifted. Summarising all these observations, one can conclude that with time the soliton with bigger amplitude is reaching the other one with smaller amplitude, then they interact and after that they continue moving with the same velocities, but they both get a phase shift.
Remark. One has to mention the properties of the solitons. Since the equation is non-linear generally speaking the linear combination of several different solitons will not be a solution of the equation. However the asymptotic for large time of a multi-soliton solution will be the same as a corresponding linear combination of the solitons. Thus one can say that on the set

of soliton solutions the KDV (2.4) has the property of asymptotic linearity.

This class of multi-soliton solutions is important not only as exact solutions of the KdV equation (2.4), but also because they describe the common asymptotic behaviour of its solutions. One can prove the following theorem:
Theorem: Let the initial data $u(x,0)$ satisfy the condition:

$$\int_{-\infty}^{+\infty} |u(x,0)|(1+|x|)dx < \infty. \tag{2.28}$$

Then the solution of the corresponding Cauchy problem for the KdV ((2.4)) for large times

$$u(x,t) = u_N(x,t) + O(\frac{1}{\sqrt{t}}), \text{ for } t \to +\infty, \tag{2.29}$$

where u_N is the N-soliton asymptotic solution, i.e., the solitons are ordered with the largest first determined by the discrete spectrum of the Schrödinger operator with potential $u(x,t)$.

2.2 Inverse scattering for the nonlinear Schrödinger equation

Among other equations that can be solved with IS the most prominent is the non-linear Schrödinger equation. In this part we briefly present the general construction which is similar to the case of KdV (2.4). The cubic nonlinear Schrödinger equation

$$iu_t(x,t) + \frac{1}{2}u_{xx}(x,t) + \sigma|u(x,t)|^2u(x,t) = 0 \tag{2.30}$$

where $\psi(x,t)$ is a complex-valued function. One can distinguish two cases: $\sigma = 1$ is called focusing and $\sigma = -1$ is respectively defocusing. Remarkably, changing the sign of the nonlinearity is affecting drastically the qualitative behaviour of the solution.
This equation possess a Lax pair:

$$\frac{\partial \Psi}{\partial x} = U\Psi = \begin{bmatrix} -i\lambda & u \\ -\bar{u} & i\lambda \end{bmatrix} \Psi \tag{2.31}$$

and

$$\frac{\partial \Psi}{\partial t} = W\Psi = \begin{bmatrix} -i\lambda^2 + i\frac{1}{2}|u|^2 & \lambda u + i\frac{1}{2}u_x \\ -\lambda\bar{u} + i\frac{1}{2}\bar{u} & i\lambda^2 - i\frac{1}{2}|u|^2 \end{bmatrix} \Psi. \tag{2.32}$$

The compatibility condition is

$$\frac{\partial U}{\partial t} - \frac{\partial V}{\partial x} + [U, V] = 0. \tag{2.33}$$

As in the case of KdV the goal is to study the properties of the solution of the equation corresponding to the Scattering operator U. Let suppose that $u(x,t)$ for a fixed t is a rapidly decreasing function as $x \to \pm\infty$. Then the Jost solutions are

$$j_1^-(x,\lambda) = \begin{bmatrix} e^{-i\lambda x} \\ 0 \end{bmatrix} + o(1), \text{ as } x \to -\infty$$

$$j_2^-(x,\lambda) = \begin{bmatrix} 0 \\ e^{i\lambda x} \end{bmatrix} + o(1), \text{ as } x \to -\infty$$

$$j_1^+(x,\lambda) = \begin{bmatrix} e^{-i\lambda x} \\ 0 \end{bmatrix} + o(1), \text{ as } x \to +\infty$$

$$j_2^+(x,\lambda) = \begin{bmatrix} 0 \\ e^{i\lambda x} \end{bmatrix} + o(1), \text{ as } x \to +\infty.$$

Denoting matrices $J^{\pm} = \left[j^1\pm, j^2\pm\right]$ and taking into account that the determinants of these matrices are constant, we introduce the scattering matrix $S(\lambda) = \begin{pmatrix} a(\lambda) & -\bar{b}(\lambda) \\ b(\lambda) & \bar{a}(\lambda) \end{pmatrix}$ in the following way

$$J^- = J^+ S. \tag{2.34}$$

Provided that $|a(\lambda)| + |b(\lambda)|^2 = 1$ one gets that the reflection coefficient

$$r(\lambda) = \frac{b(\lambda)}{a(\lambda)} \tag{2.35}$$

is uniquely determined by the scattering matrix $S(\lambda)$. Thus we get that the direct scattering map is the map $\mathcal{R} : u \to r$. In order to describe the inverse map $\mathcal{I} : r \to u$ one can introduce new normalized matrices $M^{\pm}(x,\lambda)$ based on the Jost solutions:

$$M^+ = \left[\frac{e^{i\lambda x}}{a(\lambda)} j_1^-, e^{-i\lambda x} j_2^+\right], \text{ for } \Im(\lambda) > 0$$

,

$$M^- = \left[e^{i\lambda x} j_1^+, \frac{e^{-i\lambda x}}{\bar{a}(\bar{\lambda})} j_2^- \right], \text{ for } \Im(\lambda) < 0.$$

The goal is to represent the inverse scattering map as a Riemann-Hilbert problem on matrices $M^{\pm}$ which is equivalent to the Gelfand-Levitan-Marchenko equations (as was done for the KdV example). Firstly, these matrices have the following properties:

1. It can be shown using the asymptotic properties of the Jost solutions and the scattering data that
$$\lim_{|\Im(\lambda)\to\infty|} M^{\pm} = \mathbb{I}. \tag{2.36}$$

2. Both matrices $M^{\pm}$ are analytic on the upper half and lower half plane respectively except for having simple poles at the points λ_n where $n = 1, ..., N$ such that $a(\lambda_n) = 0$.

3. Matrices $M^{\pm}$ take continuous boundary values on the real line. The relation between them is described by the jump matrix $V(x, \lambda)$ where $\lambda \in \mathbb{R}$:
$$M^+ = M^- V,$$
where $V(x, \lambda) = \begin{pmatrix} 1 + |r(\lambda)|^2 & e^{-2i\lambda x}\overline{r}(\lambda) \\ e^{2i\lambda x} r(\lambda) & 1 \end{pmatrix}$.

Remark. The solution of the problem is called Beals-Coifmann solution, which are functions of the complex argument λ whereas x is a fixed parameter. Thus we have presented all sufficient conditions to formulate a Riemann-Hilbert problem. This R-H problem can be solved by the steepest descent method and then the sought-for potential $u(x)$ can be computed from the formula

$$u(x) = 2i \lim_{\lambda\to\infty} \lambda M^{\pm}. \tag{2.37}$$

2.2.1 Time evolution

To derive the time dependence of the scattering data one has to come back to the case of time-dependent potential $u(x, t)$. Then the Jost functions (2.5) which are solutions of the system (2.31) generally cannot be solutions of the system corresponding to the second operator of the Lax pair (2.32) unless we find the proper multipliers:

$$J^{\pm}(x, t, \lambda) = \left[c_1^{\pm}(t, \lambda) j_{\pm}^1(x, \lambda), c_2^{\pm}(t, \lambda) j_{\pm}^2(x, \lambda) \right].$$

This can be done by solving (2.32) in the limit for $x \to \infty$ when the operator W becomes diagonal:

$$\frac{\partial \Psi}{\partial t} = \begin{bmatrix} -i\lambda^2 & 0 \\ 0 & i\lambda^2 \end{bmatrix} \Psi.$$

The general solution of this equation is

$$\Psi_0 = c_1(x,\lambda) \begin{bmatrix} e^{-i\lambda^2 t} \\ 0 \end{bmatrix} + c_2(x,\lambda) \begin{bmatrix} 0 \\ e^{i\lambda^2 t} \end{bmatrix}.$$

Thus one can find the time-dependent Jost functions:

$$J^{\pm}(x,t,\lambda) = \left[e^{-i\lambda^2 t} j^1_{\pm}(x,\lambda), e^{i\lambda^2 t} j^2_{\pm}(x,\lambda) \right].$$

The next goal is to find the differential equation in t on the scattering matrix $S(\lambda,t)$. The latter can be derived in the following way: one has to find the respective equation for the Jost matrix

$$\frac{\partial}{\partial t}(J^{\pm} e^{-i\lambda^2 t \sigma_3}) = W(J^{\pm} e^{-i\lambda^2 t \sigma_3}).$$

Simplifying this and denoting $\frac{\partial J^{\pm}(x,t,\lambda)}{\partial t} = J^{\pm}_t(x,t,\lambda)$ one gets

$$J^{\pm}_t(x,t,\lambda) = \left(i\lambda^2 \sigma_3 + W\right) J^{\pm}(x,t\lambda). \tag{2.38}$$

Differentiating with respect to t the definition of the scattering matrix (2.34), one gets

$$J^-_t(x,t,\lambda) = J^+_t(x,t,\lambda) S(\lambda,t) + J^+(x,t,\lambda) S_t(\lambda,t),$$

then one can use the equations to eliminate the derivatives of $J^{\pm}$

$$\left(i\lambda^2 \sigma_3 + W\right) J^-(x,t\lambda) = \left(i\lambda^2 \sigma_3 + W\right) J^+(x,t\lambda) + J^+(x,t,\lambda) S_t(\lambda,t),$$

then J^- can be also eliminated

$$\left(i\lambda^2 \sigma_3 + W\right) J^+(x,t,\lambda) S(\lambda,t) = \left(i\lambda^2 \sigma_3 + W\right) J^+(x,t,\lambda) S_(\lambda,t) + J^+(x,t,\lambda) S_t(\lambda,t).$$

Finally, multiplying by the inverse of the matrix J^+, one gets

$$S_t(\lambda, t) = i\lambda^2 \left[S, \sigma_3\right].$$

Then one can find the differential equations for the entries of the scattering matrix:

$$\begin{bmatrix} a(\lambda) & -\bar{b}(\lambda) \\ b(\lambda) & \bar{a}(\lambda) \end{bmatrix}_t = \begin{bmatrix} 0 & 2i\lambda^2\bar{b}(\lambda) \\ 2i\lambda^2 b(\lambda) & 0 \end{bmatrix}_t. \tag{2.39}$$

Thus, we can define the time evolution of the entries explicitly:

$$a(\lambda, t) = a(\lambda, 0), b(\lambda, t) = b(\lambda, 0)e^{2i\lambda^2 t}.$$

Finally, we can derive the time-dependence for the reflection coefficient:

$$r(\lambda, t) = e^{2i\lambda^2 t} r(\lambda, t).$$

To finish this part one has to also define the time evolution of the points of the discrete spectrum of the matrix $a(\lambda, t)$. First, as far as the function $a(\lambda, t)$ for $\lambda \in \mathbb{R}$ is constant in time one can deduce that its analytic continuation $a(\lambda, t)$ where $\Im(\lambda) > 0$ does not change as time evolves. This means that the zeros of $a(\lambda, t) = a(\lambda)$ in the upper-half plane are also constants in time. We denote these points of the discrete spectrum $\lambda_1, \lambda_2, ...\lambda_n$. We recall the main property of these points, that the Jost functions became proportional

$$j_1^-(x, \lambda_n, t) = c_n(t) j_2^+(x, \lambda_n, t). \tag{2.40}$$

To define the time dependence of the coefficients $c_n(t)$ we has to differentiate the previous equality:

$$\frac{\partial j_1^-}{\partial t} = c_n \frac{\partial j_2^+}{\partial t} + \frac{\partial c_n}{\partial t} j_2^+, \text{ where } \lambda = \lambda_n.$$

Substituting the evolution equations for the Jost functions (2.38)

$$\frac{\partial j_1^-}{\partial t} = (W + i\lambda^2 \mathbb{I}) j_1^-, \quad \frac{\partial j_2^+}{\partial t} = (W - i\lambda^2 \mathbb{I}) j_2^+$$

and denoting $\dot{c}_n = \frac{\partial c_n}{\partial t}$ one gets

$$(W + i\lambda^2 \mathbb{I}) j_1^- = c_n (W - i\lambda^2 \mathbb{I}) j_2^+ + \dot{c}_n j_2^+$$

Using (2.40) to exclude j_1^- and simplifying the equation one has

$$\dot{c}_n j_2^+ = 2i\lambda^2 c_n j_2^+.$$

Taking into account that j_2^+ is non zero we finally get

$$\dot{c}_n = 2i\lambda^2 c_n.$$

Solving this ODE we see that

$$c_n(t) = e^{2i\lambda^2} c_n(0).$$

Thus we have finished describing the evolution in time of all the elements of the scattering data.

2.2.2 Multisoliton solutions

We have presented two examples of the Inverse scattering method. One can see that the procedure of construction of the scattering data for the KdV and the non-linear cubic Schrödinger equation looks similar. We also have shown how this classic approach allows us to find a solution in an explicit form considering reflectionless potentials for the KdV equation. There is no surprise that $r(\lambda)$ can also be identically zero for some potentials of the cubic NLS. It turns out that these potentials also correspond to multisoliton solutions. Let us look at this in more detail. The first thing we can see when $R(\lambda) \equiv 0$ is that the jump matrix in the Riemann-Hilbert problem is the identity matrix, namely the boundary values of the $M^{\pm}$ coincide. We can conclude that these two matrices depend on one meromorphic function on the complex plane with $2n$ poles in $\lambda_1, \bar{\lambda}_1, \lambda_2, \bar{\lambda}_2, ..., \lambda_n, \bar{\lambda}_n$. This function should be of the form

$$M(x,\lambda,t) = \mathbb{I} + \sum_{n=1}^{N} \frac{A_n}{\lambda - \lambda_n} + \sum_{n=1}^{N} \frac{B_n}{\lambda - \bar{\lambda}_n},$$

where $A_(x,t)$ and $B_n(x,t)$ as $n = 1, ..., N$ are matrices which can found from the residue conditions:

$$res_{\lambda=\lambda_n} M(x,\lambda,t) = A_n(x,t), \quad res_{\lambda=\bar{\lambda}_n} M(x,\lambda,t) = B_n(x,t).$$

This implies that

$$A_n(x,t) = \begin{pmatrix} \alpha_n(x,t) & 0 \\ \beta_n(x,t) & 0 \end{pmatrix} \quad B_n(x,t) = \begin{pmatrix} 0 & \gamma_n(x,t) \\ 0 & \delta_n(x,t) \end{pmatrix}$$

while the non-zero columns of these matrices satisfy the following relations

$$\begin{pmatrix} \alpha_n(x,t) \\ \beta_n(x,t) \end{pmatrix} = \frac{c_n}{a'(\lambda)} e^{2i(\lambda_n x + \lambda_n t)} \left(\begin{pmatrix} 0 \\ 1 \end{pmatrix} + \sum_{m=1}^{N} \frac{1}{(\lambda_n - \lambda_m^*)} \begin{pmatrix} \gamma_n(x,t) \\ \delta_n(x,t) \end{pmatrix} \right)$$

and

$$\begin{pmatrix} \gamma_n(x,t) \\ \delta_n(x,t) \end{pmatrix} = -\frac{c_n}{a'(\lambda)} e^{-2i(\lambda_n x + \lambda_n t)} \left(\begin{pmatrix} 1 \\ 0 \end{pmatrix} + \sum_{m=1}^{N} \frac{1}{(\lambda_n^* - \lambda_m)} \begin{pmatrix} \alpha_n(x,t) \\ \beta_n(x,t) \end{pmatrix} \right).$$

This system is a linear system on functions $\alpha_n, \beta_n, \gamma_n, \delta_n$, and it has a unique solution if and only if the respective determinant does not vanish. Thus we can determine a matrix $M(x,t,\lambda)$ which allows us to reconstruct the potential $u(x,t)$ by the formula (2.37), namely

$$u(x,t) = 2i\lambda M_{12}(\lambda,x,t) = 2i \lim_{\lambda\to\infty} \lambda \sum_{n=1}^{N} \frac{\alpha(x,t)}{\lambda - \bar{\lambda}} = 2i \sum_{n=1}^{N} \alpha_n(x,t).$$

On can see that it is sufficient to find only functions α_n for $n = 1, ..., N$ and not all entries of the matrix $M(\lambda,x,t))$, which obviously reduces the computational effort. Let us consider, for example, N=1. Then we can derive from the system (1) the equation for α_1

$$\alpha_1(x,t) = -\frac{c_n}{a'(\lambda)} e^{-2i(\lambda_n x + \lambda_n t)} \left(1 - \frac{c_n e^{2i(\lambda_n x + \lambda_n t)}}{a'(\lambda)(\lambda - \bar{\lambda})^2} \right) \alpha_1(x,t).$$

Solving this equation and denoting $\lambda = a + ib$ one gets

$$\alpha_1(x,t) = be^{-2i(ax + (a^2+b^2)t + \phi)} \operatorname{sech}(2b(x - x_0 + 2ta)).$$

One can see that this 1-soliton solution is sort of similar to the solution of the KdV equation. We have seen the two cases of the equation describing the wave phenomena in $1+1$ dimensions and the natural question is too study the system with the similar properties 2+1 dimensions.

Chapter 3

Davey-Stewartson equation

Now we are ready to present the main object of this work, the system

$$\begin{aligned} iq_t + 2\left(\overline{\partial}^2 + \partial^2\right) q + (g + \overline{g})\, q = 0 \\ \overline{\partial} g + \partial\left(|q|^2\right) = 0, \end{aligned} \tag{3.1}$$

which was introduced in 1974 by Davey and Stewartson (DS) as equations describing the modulation of a 3-dimensional wave-packet. Although this equation was derived in a context of fluid dynamics, later applications in non-linear optics were discovered. This system of equations in $2+1$ dimension is completely integrable: it admits a Lax factorisation, has a Hamiltonian structure and therefore has its action-angle variables, possesses Darboux-Bäcklund transformations and a Hirota representation. Also there exists an associated inverse scattering problem, which we are going to focus on in this work.

On the other hand the DS system can be viewed as a 2-dimensional generalisation of the non-linear Schrödinger equation. Indeed, if we introduce the following partial change of the coordinates by putting M=$\Re(g)$ and assuming M and q are independent of y then it appears that q is a solution of the corresponding cubic non-linear Schrödinger equation :

$$iq_t + q_{xx} \pm 2q|q|^2 = 0. \tag{3.2}$$

Similarly, one can consider the x-independent reduction of DS which will lead to another cubic non-linear Schrödinger equation with respect to the y variable.

3.1 Complete integrability of the Davey-Stewartson system

3.1.1 Hamiltonian structure

The lax pair for DS is derived through a generalised AKNS scheme

$$L = \begin{pmatrix} \partial_x + i\partial_y & -q \\ -q^* & \partial_x - i\partial_y \end{pmatrix}$$

$$B = \begin{pmatrix} \partial_x^2 + \frac{i}{2}\left(\partial_x - i\partial_y\right) g + \frac{1}{2}qq^* & iq^*\partial_y + \frac{1}{2}\left(\partial_x + i\partial_y\right) q^* \\ iq^*\partial_y + \frac{1}{2}\left(\partial_x + i\partial_y\right) q^* & \partial_x^2 + \frac{i}{2}\left(\partial_x - i\partial_y\right) g - \frac{1}{2}qq^* \end{pmatrix}.$$

3.1.2 Inverse scattering method

To introduce the spectral operator we will rewrite the first operator from the Lax pair using the notations $\partial = \frac{1}{2}\left(\frac{\partial}{\partial x} - i\frac{\partial}{\partial y}\right)$ and $\overline{\partial} = \frac{1}{2}\left(\frac{\partial}{\partial x} + i\frac{\partial}{\partial y}\right)$. The inverse scattering transform associated with the elliptic system is

$$\frac{\partial \Psi}{\partial \bar{z}} = Q\bar{\Psi} \tag{3.3}$$

where

$$Q = \begin{pmatrix} 0 & q \\ \pm q & 0 \end{pmatrix}$$

and $\Psi(z,k) = e^{i\bar{k}z/2}\mu(z,k)$; also we require that

$$\lim_{|z|\to\infty} \mu(z,k) = I. \tag{3.4}$$

In order to define the scattering matrix we will rewrite the problem in terms of a regularized matrix $\mu = \mu(z,k)$. Thus the eigenfunctions of the scattering operator, namely the entries of the matrix μ, are bounded. On gets

$$\partial\mu = e^{kz-\bar{k}\bar{z}}Q\bar{\mu} \tag{3.5}$$

together with the boundary condition (3.4) on μ. Let us assume that the potential $q \in \mathscr{S}(\mathbb{C})$ then one can invert the operator to rewrite the matrix equation in terms of the integral oper-

ator

$$\mu = I + \frac{1}{2\pi}\int\limits_{\mathbb{C}} \frac{e^{kz-\bar{k}\bar{z}}Q\bar{\mu}}{z-w} d_{\mathbb{C}}w. \tag{3.6}$$

Therefore we have the following integral equations:

$$\mu_{11} = I + \frac{1}{2\pi}\int\limits_{\mathbb{C}} \frac{e^{kz-\bar{k}\bar{z}}Q_{12}\bar{\mu}_{21}}{z-w} d_{\mathbb{C}}w \tag{3.7}$$

$$\mu_{12} = I + \frac{1}{2\pi}\int\limits_{\mathbb{C}} \frac{e^{kz-\bar{k}\bar{z}}Q_{21}\bar{\mu}_{11}}{z-w} d_{\mathbb{C}}w \tag{3.8}$$

$$\mu_{21} = I + \frac{1}{2\pi}\int\limits_{\mathbb{C}} \frac{e^{kz-\bar{k}\bar{z}}Q_{12}\bar{\mu}_{22}}{z-w} d_{\mathbb{C}}w \tag{3.9}$$

$$\mu_{22} = I + \frac{1}{2\pi}\int\limits_{\mathbb{C}} \frac{e^{kz-\bar{k}\bar{z}}Q_{21}\bar{\mu}_{12}}{z-w} d_{\mathbb{C}}w. \tag{3.10}$$

The scattering matrix

$$T(k) = \begin{pmatrix} 0 & T_{12}(k) \\ T_{21}(k) & 0 \end{pmatrix}$$

can be derived by differentiating these integral equations (3.7) with respect to k

$$\partial_k \mu = \frac{1}{2\pi}\int\limits_{\mathbb{C}} Q\frac{\partial_k(e^{kw-\bar{k}\bar{w}}\bar{\mu})}{z-w} d_{\mathbb{C}}w,$$

namely

$$\partial_k \mu_{11} = I + \frac{1}{2\pi}\int\limits_{\mathbb{C}} Q_{12}\frac{\partial_k(e^{kw-\bar{k}\bar{w}}\bar{\mu}_{21})}{z-w} d_{\mathbb{C}}w$$

$$\partial_{\bar{k}} \mu_{12} = \frac{1}{2\pi}\int\limits_{\mathbb{C}} Q_{21}\frac{\partial_{\bar{k}}(e^{kw-\bar{k}\bar{w}}\bar{\mu}_{11})}{z-w} d_{\mathbb{C}}w$$

$$\partial_{\bar{k}} \mu_{21} = \frac{1}{2\pi}\int\limits_{\mathbb{C}} Q_{12}\frac{\partial_{\bar{k}}(e^{kw-\bar{k}\bar{w}}\bar{\mu}_{22})}{z-w} d_{\mathbb{C}}w$$

$$\partial_k \mu_{22} = I + \frac{1}{2\pi}\int\limits_{\mathbb{C}} Q_{21}\frac{\partial_k(e^{kw-\bar{k}\bar{w}}\bar{\mu}_{12})}{z-w} d_{\mathbb{C}}w.$$

Let us define the elements of $T(k)$ as follows

$$T_{12}(k) = \frac{i}{2\pi} \int_{\mathbb{C}} e^{-(kw-\bar{k}\bar{w})} Q_{12} \bar{\mu}_{22} d_{\mathbb{C}} w$$
$$T_{21}(k) = \frac{i}{2\pi} \int_{\mathbb{C}} e^{-(kw-\bar{k}\bar{w})} Q_{21} \bar{\mu}_{11} d_{\mathbb{C}} w.$$

One can notice that

$$\partial_k (e^{kz-\bar{k}\bar{z}} \bar{\mu}_{21}) = e^{kz-\bar{k}\bar{z}} T_{21} \mu_{22} \tag{3.11}$$
$$\partial_k \mu_{11} = \bar{T}_{21} \mu_{12} \tag{3.12}$$
$$\partial_k (e^{kz-\bar{k}\bar{z}} \bar{\mu}_{12}) = e^{kz-\bar{k}\bar{z}} T_{12} \mu_{11} \tag{3.13}$$
$$\partial_k \mu_{22} = \bar{T}_{12} \mu_{21}, \tag{3.14}$$

which can be rewritten as a D-bar problem

$$\partial_{\bar{k}} \nu = e^{kz-\bar{k}\bar{z}} T \bar{\nu}$$

by introducing the matrix

$$\nu = \begin{pmatrix} \bar{\mu}_{11} & \mu_{12} e^{kz-\bar{k}\bar{z}} \\ \mu_{21} e^{kz-\bar{k}\bar{z}} & \bar{\mu}_{22} \end{pmatrix}.$$

The boudary condition is given by (3.6)

$$\lim_{|k|\to\infty} \nu = I \tag{3.15}$$

The scattering matrix can be computed by

$$T_{12}(k) = \lim_{|z|\to\infty} \frac{iz}{2} \mu_{12}(z,k)$$
$$T_{21}(k) = \lim_{|z|\to\infty} \frac{iz}{2} \mu_{21}(z,k).$$

Again this system of equations can be written in terns of the integral operators

$$\nu = I + \frac{1}{2\pi} \int_{\mathbb{C}} T \frac{e^{k'z-\bar{k}'\bar{z}} \bar{\nu}}{k-k'} d_{\mathbb{C}} k'.$$

One can show that the scattering data evolve in time

$$\partial_t T(k) = -\frac{k^2 - \bar{k^2}}{2} T(k).$$

One can see the corresponding inverse problem appears to be the same type of D-bar problem provided that the function $r(t,k) = T_{12}$ plays the role of the potential. Namely, one can see that inverse-scattering problem is

$$\begin{aligned} \overline{\partial}_k \nu_1 &= \tfrac{1}{2}\overline{R(k,t)}\overline{\nu}_2 \\ \overline{\partial}_k \nu_2 &= \tfrac{1}{2}\overline{R(k,t)}\overline{\nu}_1 \end{aligned}$$

where $R(k,t) = e^{\bar{k}z - kz} r(k,t)$ and where the solution $\nu_j = \nu_j(k,t)$ is sought that satisfies

$$\lim_{|k|\to\infty} \nu_1(k,t) = 1 \quad \text{and} \quad \lim_{|k|\to\infty} \nu_2(k,t) = 0.$$

Finally, the reconstruction formula is

$$q(z,t) = 2 \lim_{|k|\to\infty} \overline{k\, \nu_2(k,t)}.$$

Schematically, these steps can be represented by the following diagram:

$$\begin{array}{ccc} Q(0) & \xrightarrow{\quad S \quad} & r(k,0) \\ \downarrow & & \downarrow \\ Q(t) & \xleftarrow{S^{-1}} & \partial_t r = -\frac{k^2 - \bar{k^2}}{2} r \end{array} .$$

One can see that the rigorous study of the inverse problem comes down to the theory of the integral operators in proper functional spaces. Perry showed that the inverse scattering problem, consequently the Cauchy problem for the defocusing DS, is globally well-posed in $H^{(1,1)}(\mathbb{C})$, existence and uniqueness of the global solution are shown. Recently in 2017 Nachman proved the same result in L_2.

Before we will move to the asymptotic framework of the D-bar problem we will introduce a learning example of a D-bar problem in case of the compact support potential.

3.1.3 Potentials of compact support

Let us consider the D-bar equation (3.3) using polar coordinates (r, ϕ) with the potential $q = 1$ for $r \leq 1$ and zero otherwise. We first study the case $k = 0$. There we have for $r \leq 1$

$$m_r + \frac{i}{r} m_\phi = (\bar{m} + 1) e^{-i\phi}. \tag{3.16}$$

Differentiating once with respect to $\bar{z}$, we get

$$m_{rr} + \frac{1}{r} m_r + \frac{1}{r^2} m_{\phi\phi} = m + 1. \tag{3.17}$$

We write the solution in the form of a Fourier series $m = \sum_{n \in \mathbb{Z}} a_n(r) e^{in\phi}$ which implies

$$a_n' - \frac{n}{r} a_n = \bar{a}_{-n-1} + \delta_{n,-1} \tag{3.18}$$

and

$$a_n'' + \frac{1}{r} a_n' - \frac{n^2}{r^2} a_n = a_n + \delta_{n0}. \tag{3.19}$$

Note that the a_n must be even (odd) functions of r for even (odd) n in order to get smooth solutions (in x and y) near $r = 0$.

Equations (3.19) are Fuchsian with the only finite pole at $r = 0$. Thus we can represent the solutions as a series in r which will converge on the whole unit disk. For $n = 0$ we get

$$a_0(r) = \sum_{m=0}^{\infty} \alpha_{2m}^0 r^{2m} \tag{3.20}$$

with constants α_m^0 given by

$$\alpha_2^0 = \frac{1}{4}(1 + \alpha_0^0), \quad \alpha_{2m}^0 = \frac{1}{4m^2} \alpha_{2m-2}^0 = \frac{1}{4m^2(2m-2)^2 \dots 4}(1 + \alpha_0^0). \tag{3.21}$$

For $n > 0$ we get

$$a_n(r) = \sum_{m=0}^{\infty} \alpha_{2m}^n r^{2m+n} \tag{3.22}$$

with

$$\alpha_{2m}^n = \frac{1}{4m(m+n)} \alpha_{2m-2}^n. \tag{3.23}$$

For $n < 0$ we get

$$a_n(r) = \sum_{m=0}^{\infty} \alpha_{2m}^n r^{2m-n} \tag{3.24}$$

with

$$\alpha_{2m}^{n} = \frac{1}{4m(m-n)}\alpha_{2m-2}^{n}. \tag{3.25}$$

3.2 Semicalssical limit

In this section we want to study the D-bar problem with a small real parameter ϵ. This rescaling can be understood in too different ways:
1. one can consider the coefficient ϵ only in the initial data, i.e., by an appropriate changing of the coordinates it is possible to make the equation and respectively D-bar problem independent of ϵ,
2. or one can focus on ϵ independent initial data and ϵ that appears in the equation itself.
Now we can repeat the formalism of the Inverse scattering but taking in account the ϵ factor. We start with the defocusing DSII and introducing following change of variables $z = \frac{\tilde{z}}{\epsilon}$. Therefore the semiclassical defocusing DSII will be

$$\begin{aligned} i\epsilon q_t + 2\epsilon^2\left(\bar{\partial}^2 + \partial^2\right) q + (g + \bar{g})\, q = 0 \\ \bar{\partial} g + \partial\left(|q|^2\right) = 0, \end{aligned} \tag{3.26}$$

where the initial data

$$q(x, y, 0) = A(x, y, 0) e^{iS(x,y,0)/\epsilon}. \tag{3.27}$$

The D-bar problem for DS will be as follows

$$\epsilon\bar{\partial}\mu_1 = \frac{1}{2} e^{\frac{\bar{k}\bar{z}-kz}{\epsilon}} q\bar{\mu}_1 \tag{3.28}$$

$$\epsilon\bar{\partial}\mu_2 = \frac{1}{2} e^{\frac{\bar{k}\bar{z}-kz}{\epsilon}} q\bar{\mu}_2. \tag{3.29}$$

Nevertheless the asymptotic condition (3.4) remains unchanged, namely $\mu_1 \to 1$ and $\mu_2 \to 0$ as $|z| \to \infty$.

The reflection coefficient is

$$r(k) = \frac{1}{\pi\epsilon}\int\int e_{\frac{k}{\epsilon}}(z) q(z) \bar{\mu}_1(z) dA(z). \tag{3.30}$$

One can invert the D-bar operator and formally write a solution for 3.29 taking into ac-

count the asymptotic conditions for μ_1 and μ_2

$$\mu_1 = 1 + \frac{1}{2\epsilon}\bar{\partial}^{-1}\left(e_{\frac{k}{\epsilon}}(\cdot)\, q(\cdot)\, \bar{\mu}_2(\cdot)\right) = 1 + T\mu_2$$
$$\mu_2 = \frac{1}{2\epsilon}\bar{\partial}^{-1}\left(e_{\frac{k}{\epsilon}}(\cdot)\, q(\cdot)\, \bar{\mu}_1(\cdot)\right) = T\mu_1$$

where we denote $e_{\frac{k}{\epsilon}} = e^{\frac{\bar{k}\bar{z}-kz}{\epsilon}}$. Thus we get a system

$$\mu_1 = 1 + T\mu_2$$
$$\mu_2 = T\mu_1.$$

Let us solve it with respect to μ_1 and μ_2 respectively

$$\mu_1 = 1 + T^2\mu_1 \Rightarrow \mu_1 - T^2\mu_1 = 1 \Rightarrow (1 - T^2)\mu_{=}1 \Rightarrow \mu_1 = (1 - T^2)^{-1}1 \tag{3.31}$$

$$\mu_2 = T\mu_1 = T(1 + T\mu_2) = T1 + T^2\mu_2 \Rightarrow \mu_2 = \left(1 - T^2\right)^{(-1)} T1 \tag{3.32}$$

To obtain the inverse system we need to compute derivatives of the functions μ_1 and μ_2 with respect to the k variable. First, to calculate the following

$$\bar{\partial}_k\mu_1 = \bar{\partial}_k\left[(1 - T^2)^{-1}1\right]$$

we use the differentiation rule for operators

$$\bar{\partial}_k\left[\left(1 - T^2\right)^{-1}\right] = (1 - T^2)^{-1}\bar{\partial}_k T^2(1 - T^2)^{-1}.$$

This leads to

$$\bar{\partial}_k\mu_1 = (1 - T^2)^{-1}\bar{\partial}_k T^2(1 - T^2)^{-1}1,$$

where the key point is to calculate the derivative of the square of the operator T,

$$\bar{\partial}_k T^2 f = \frac{1}{4\pi^2 e^2}\bar{\partial}_k\left[\int\int \frac{e_{\frac{k}{\epsilon}}(w)q(w)}{w - z}\int\int \frac{\overline{e_{\frac{k}{\epsilon}}(\zeta)q(\zeta)}f(\zeta)}{\bar{\zeta} - \bar{w}}dA(\zeta)dA(w)\right]$$

Taking into account that

$$e_{\frac{k}{\epsilon}}(w)e_{-\frac{k}{\epsilon}}(\zeta) = e^{\frac{\bar{k}\bar{w}-kw}{\epsilon}+\frac{k\zeta-k\bar{\zeta}}{\epsilon}} = e^{\frac{\bar{k}}{\epsilon}(\bar{w}-\bar{\zeta})+\frac{k}{\epsilon}(\zeta-w)}$$

it is easy to see that

$$\bar{\partial}_k e_{\frac{k}{\epsilon}}(w)e_{-\frac{k}{\epsilon}}(\zeta) = \frac{1}{\epsilon}(\bar{w}-\bar{\zeta})e^{\frac{\bar{k}}{\epsilon}(\bar{w}-\bar{\zeta})+\frac{k}{\epsilon}(\zeta-w)} = \frac{1}{\epsilon}(\bar{w}-\bar{\zeta})e_{\frac{k}{\epsilon}}(w)e_{-\frac{k}{\epsilon}}(\zeta),$$

$$= -\frac{1}{4\pi^2\epsilon^3}\left[\int\int \frac{e_{\frac{k}{\epsilon}}(w)q(w)}{w-z}\int\int \overline{e_{\frac{k}{\epsilon}}(\zeta)q(\zeta)}f(\zeta)dA(\zeta)dA(w)\right].$$

We introduce following notation

$$F\left[\bar{q}f\right]\left(\frac{k}{2\epsilon}\right) = \int\int \overline{e_{\frac{k}{\epsilon}}(\zeta)q(\zeta)}f(\zeta)dA(\zeta)$$

which leads to

$$\bar{\partial}_k T^2 f = \frac{1}{4\pi\epsilon^3}F\left[\bar{q}f\right]\left(\frac{k}{2\epsilon}\right)\bar{\partial}^{-1}\left(e_{\frac{k}{\epsilon}}q\right). \tag{3.33}$$

Now we use this formula (3.33) and the expression (3.31) for μ_1

$$\bar{\partial}_k\mu_1 = (1-T^2)^{-1}\bar{\partial}_k T^2\mu_1 = \frac{1}{4\pi\epsilon^3}(1-T^2)^{-1}F\left[\bar{q}\mu_1\right]\left(\frac{k}{2\epsilon}\right)\bar{\partial}^{-1}\left(e_{\frac{k}{\epsilon}}q\right).$$

Using the formula for reflection coefficient (3.30), definition of T and formula for μ_2 we get

$$\bar{\partial}_k\mu_1 = (1-T^2)^{-1}\frac{1}{4\pi\epsilon^3}\epsilon\pi\bar{r}(k)\bar{\partial}^{-1}\left(e_{\frac{k}{\epsilon}}q\right) = \frac{\bar{r}(k)}{2\epsilon}(1-T^2)^{-1}T1 = \frac{\bar{r}(k)}{2\epsilon}\mu_2.$$

Let us write the first equation of the inverse system

$$\bar{\partial}_k\mu_1 = \frac{\bar{r}(k)}{2\epsilon}\mu_2. \tag{3.34}$$

We can use the following procedure to check the second equation of the inverse system. For this purpose one has to compute the following expression

$$\left(\partial_k + \frac{z}{\epsilon}\right)\mu_2 = \left(\partial_k + \frac{z}{\epsilon}\right)T\mu_1.$$

Remembering the definition of the operator T and expression for μ_1 one gets

$$\left(\partial_k + \frac{z}{\epsilon}\right) T\mu_1 = \left(\partial_k + \frac{z}{\epsilon}\right) \frac{1}{2\epsilon\pi} \int\int \frac{e_{\frac{k}{\epsilon}}(w) q(w) \bar{\mu}_1(w)}{z-w} dA(w) =$$
$$\frac{1}{2\epsilon\pi} \int\int \left(-\frac{w}{\epsilon}\right) \frac{e_{\frac{k}{\epsilon}}(w) q(w) \bar{\mu}_1(w)}{z-w} dA(w) +$$
$$\frac{1}{2\epsilon\pi} \int\int \frac{e_{\frac{k}{\epsilon}}(w) q(w) \partial_k \bar{m} u_1(w)}{z-w} dA(w) + \frac{1}{2\epsilon\pi} \int\int \frac{z}{\epsilon} \frac{e_{\frac{k}{\epsilon}}(w) q(w) \bar{\mu}_1(w)}{z-w} dA(w) =$$
$$\frac{1}{2\epsilon^2\pi} F[q\bar{\mu}_1]\left(\frac{k}{2\epsilon}\right) + T\left[\bar{\partial}_k \mu_1\right].$$

Using the definition of the reflection coefficient and the first equation for the inverse system one gets

$$\frac{1}{2\epsilon} r(k) + T\left[\frac{1}{2\epsilon} \bar{r}(k) \mu_2\right] =$$
$$\frac{1}{2\epsilon} r(k) + \frac{1}{2\epsilon} r(kT\mu_2) = \frac{1}{2\epsilon} r(k) + \frac{1}{2\epsilon} r(k)(mu_1 - 1) = \frac{r(k)}{2\epsilon} \mu_1$$

The last step is to implement the following change of coordinates:

$$\nu_1 = \mu_1,$$
$$\nu_2 = e^{\frac{\bar{k}z - kz}{\epsilon}} \bar{\mu}_2$$

Then the system has the form

$$\bar{\partial}_k \nu_1 = \frac{\bar{r}(k)}{2\epsilon} \bar{\nu}_2$$
$$\bar{\partial}_k \nu_2 = \frac{\bar{r}(k)}{2\epsilon} \bar{\nu}_1$$

3.2.1 Studying the direct problem with the semiclassical initial data

We can rewrite the D-bar (3.29) problem as the following system of equations

$$\begin{aligned} \epsilon\bar{\partial}\psi_1 &= \tfrac{1}{2} A(x,y) e^{iS(x,y)/\epsilon} \psi_2 \\ \epsilon\partial\psi_2 &= \tfrac{1}{2} A(x,y) e^{-iS(x,y)/\epsilon} \psi_1, \end{aligned} \tag{3.35}$$

by substituting the initial data in the form (3.27). Where $\psi_j(z,k) = e^{i\bar{k}z/\epsilon} \mu_j(z,k)$ for $j = 1, 2$. We will consider the amplitude $A(x,y) \in \mathcal{S}$ as a strictly positive fonction and the phase $S(x,y)$ as a real-valued function which is asymptotically linear, i.e., $S(x,y) \to wz + \bar{w}\bar{z}$ as

$|z| \to \infty$ where $w \in \mathbb{C}$. Then we can simplify the system by removing the factors $e^{iS(x,y)/\epsilon}$ by

$$\begin{bmatrix} \psi_1 \\ \psi_2 \end{bmatrix} = e^{iS(x,y)\sigma_3/(2\epsilon)} \begin{bmatrix} \chi_1 \\ \chi_2 \end{bmatrix}, \tag{3.36}$$

then (3.35) transforms to

$$\epsilon \begin{bmatrix} \bar{\partial} & 0 \\ 0 & \partial \end{bmatrix} \begin{bmatrix} \chi_1 \\ \chi_2 \end{bmatrix} = \frac{1}{2} \begin{bmatrix} -i\bar{\partial}S & A \\ A & i\partial S \end{bmatrix} \begin{bmatrix} \chi_1 \\ \chi_2 \end{bmatrix}. \tag{3.37}$$

The solution χ_1 and χ_2 should be constructed in way having a common phase but amplitudes could be different, namely

$$\chi_j = e^{f(x,y)/\epsilon}\phi_j, \quad j = 1, 2, \tag{3.38}$$

$$\epsilon \begin{bmatrix} \bar{\partial} & 0 \\ 0 & \partial \end{bmatrix} \begin{bmatrix} \phi_1 \\ \phi_2 \end{bmatrix} = \frac{1}{2} \begin{bmatrix} -i\bar{\partial}S - 2\bar{\partial}f & A \\ A & i\partial S - 2\partial f \end{bmatrix} \begin{bmatrix} \phi_1 \\ \phi_2 \end{bmatrix}. \tag{3.39}$$

Now, we can apply a standard perturbation scheme in the limit $\epsilon \to 0$. Obviously the phase functions ϕ_1 and ϕ_2 should be entire series in ϵ

$$\phi_1 = \sum_{n=0}^{\infty} \phi_1^{(n)}(x, y)\epsilon^n \tag{3.40}$$

$$\phi_2 = \sum_{n=0}^{\infty} \phi_2^{(n)}(x, y)\epsilon^n. \tag{3.41}$$

Substituting the series in (4.6) and comparing the coefficient of each power of ϵ we get the following system:

$$\begin{aligned} \frac{1}{2} \begin{bmatrix} -i\bar{\partial}S - 2\bar{\partial}f & A \\ A & i\partial S - 2\partial f \end{bmatrix} \begin{bmatrix} \phi_1^0 \\ \phi_2^0 \end{bmatrix} &= \begin{bmatrix} 0 \\ 0 \end{bmatrix} \\ \begin{bmatrix} \bar{\partial} & 0 \\ 0 & \partial \end{bmatrix} \begin{bmatrix} \phi_1^{n-1} \\ \phi_2^{n-1} \end{bmatrix} = \frac{1}{2} \begin{bmatrix} -i\bar{\partial}S - 2\bar{\partial}f & A \\ A & i\partial S - 2\partial f \end{bmatrix} \begin{bmatrix} \phi_1^n \\ \phi_2^n \end{bmatrix}, \text{ for } n \geq 1 \end{aligned} \tag{3.42}$$

Now it is more convenient to introduce the following notation to write all the equations in matrix form:

$$\Phi^n(x, y, k) = \begin{bmatrix} \phi_1^n \\ \phi_2^n \end{bmatrix}. \tag{3.43}$$

Firstly, the necessary condition that provides the existence of the solution for the first system in (3.42) system is the matrix

$$\mathbf{M}(x,y) := \frac{1}{2}\begin{bmatrix} -i\bar{\partial}S - 2\bar{\partial}f & A \\ A & i\partial S - 2\partial f \end{bmatrix} \tag{3.44}$$

which is supposed to be singular.
This statement is equivalent to

$$\det \mathbf{M}(x,y) := \det \frac{1}{2}\begin{bmatrix} -i\bar{\partial}S - 2\bar{\partial}f & A \\ A & i\partial S - 2\partial f \end{bmatrix} = 0, \tag{3.45}$$

a scalar equation, which is called the eikonal equation

$$\left[2\bar{\partial}f + i\bar{\partial}S\right]\left[2\partial f - i\partial S\right] = A^2. \tag{3.46}$$

The boundary condition for the new functions can be simply derived from (3.4)

$$\begin{aligned} \lim_{|z|\to\infty} \phi_1 e^{f/\epsilon} e^{iS/(2\epsilon)} e^{-kz/\epsilon} &= 1 \\ \lim_{|z|\to\infty} \phi_2 e^{f/\epsilon} e^{-iS/(2\epsilon)} e^{-\bar{k}\bar{z}/\epsilon} &= 0. \end{aligned} \tag{3.47}$$

This leads to the asymptotic condition for f

$$\lim_{|z|\to\infty} \left(f + i\frac{1}{2}S - kz\right) = 0. \tag{3.48}$$

The second observation is we should always verify that the corresponding vector solution always belongs to the span$\mathbf{M}(x,y)$.
One can notice that

$$\Phi^{(0)}(x,y) = \alpha(x,y)\begin{bmatrix} -i\bar{\partial}S + 2\bar{\partial}f \\ A \end{bmatrix}. \tag{3.49}$$

To summarize the procedure: one has to find the function $f(x,y)$ that satisfies the asymptotic condition so that the determinant of the matrix $M(x,y)$ vanishes for all $x, y \in \mathbb{R}$. And then the asymptotic expansion for the small ϵ can be computed using the recurrent formulas (3.42). Here we should recall that the spectral parameter k does not show up in the eikonal equation but since the asymptotic condition on $f(x,y)$ does depend on k the solution will be

k dependent, too. Let us assume that

$$\Phi^{(0)}(x,y,k) = \frac{1}{2k}\alpha^0(x,y,k)\begin{bmatrix} -i\bar{\partial}S + 2\bar{\partial}f \\ A \end{bmatrix}. \tag{3.50}$$

Remembering the resolvability condition for the non-homogeneous linear system one gets

$$\begin{bmatrix} \bar{\partial} & 0 \\ 0 & \partial \end{bmatrix}\Phi^n(x,y,k) \in \text{span}\begin{bmatrix} -i\bar{\partial}S - 2\bar{\partial}f \\ A \end{bmatrix}. \tag{3.51}$$

It can be rewritten as

$$\det\left(\begin{bmatrix} \bar{\partial} & 0 \\ 0 & \partial \end{bmatrix}\Phi^n(x,y,k), \begin{bmatrix} -i\bar{\partial}S - 2\bar{\partial}f \\ A \end{bmatrix}\right) = 0. \tag{3.52}$$

If we assume that this condition is true then the general solution for each fixed n will be

$$\Phi^{(n)}(x,y;k) = \Phi_{\mathrm{p}}^{(n)}(x,y;k) + \frac{\alpha_n(x,y;k)}{2k}\begin{bmatrix} 2\partial f(x,y;k) - \mathrm{i}\partial S(x,y) \\ A(x,y) \end{bmatrix}, \quad n = 1,2,3,\ldots, \tag{3.53}$$

where $\Phi_{\mathrm{p}}^{(n)}(x,y;k)$ a particular solution. Here we got a scalar equation which is easily seen to be a scalar linear equation for the $\alpha^n(x,y,k)$. By using the linearity property of the determinant we derive the following identity

$$\det\left(\begin{bmatrix} -i\bar{\partial}S - 2\bar{\partial}f \\ A \end{bmatrix}, \begin{bmatrix} \bar{\partial} & 0 \\ 0 & \partial \end{bmatrix}\Phi_{\mathrm{p}}^{(n)}(x,y;k)\right) = -\det\left(\begin{bmatrix} -i\bar{\partial}S - 2\bar{\partial}f \\ A \end{bmatrix}, \begin{bmatrix} \bar{\partial} & 0 \\ 0 & \partial \end{bmatrix}\frac{\alpha^n}{2k}\begin{bmatrix} -i\bar{\partial}S - 2\bar{\partial}f \\ A \end{bmatrix}\right) \tag{3.54}$$

and this together with the asymptotic condition on $\alpha(x,y,k)$ which can be derived from

$$\lim_{z\to\infty}\Phi^0 = \begin{bmatrix} 1 \\ 0 \end{bmatrix} \tag{3.55}$$

and

$$\lim_{z\to\infty}\Phi^n = \begin{bmatrix} 0 \\ 0 \end{bmatrix} \text{ for } n = 1,2,\ldots \tag{3.56}$$

should determine completely $\Phi^n(x,y,k)$. So that we have the following asymptotic conditions

$$\lim_{z\to\infty}\alpha^0(x,y,k) = 1, \quad \lim_{z\to\infty}\alpha^n(x,y,k) = 0, \text{ for } n = 1,2,\ldots \tag{3.57}$$

By direct computation one can derive

$$\det\left(\begin{bmatrix}-i\bar{\partial}S-2\bar{\partial}f\\ A\end{bmatrix},\begin{bmatrix}\bar{\partial}&0\\0&\partial\end{bmatrix}\frac{\alpha^n}{2k}\begin{bmatrix}-i\bar{\partial}S-2\bar{\partial}f\\ A\end{bmatrix}\right)=-\frac{1}{2k}\mathcal{L}\alpha^n \tag{3.58}$$

where the operator $\mathcal{L}$ is defined as an operator corresponding to the determinant of the matrix $M(x,y)$. Finally one can write the formula for the reflection coefficient

$$r(k)=2\lim_{z\to\infty} ze^{-2i\Im kz/\epsilon}.\phi_2(x,\bar{y},k) \tag{3.59}$$

Now we want to remember that here we can only find the approximation of the solution with respect to some order N of epsilon. Now we are interested in computing the corresponding order of decay of the reflection coefficient. Let us suppose that the WKB approximation was found and can be represented as follows

$$\Phi(x,y,k)=\sum_{n=1}^{N}\Phi^n(x,y,k)+\tilde{\Phi}(x,y,k) \tag{3.60}$$

where $\tilde{\Phi}(x,y,k)$ is a remainder. And let us suppose also that the remainder is $o(\epsilon^N)$. Comparing the formula for the reflection coefficient and its known properties one can conclude that $\phi_2^n=o(\frac{1}{z})$ which implies that the reflection coefficient has an asymptotic behaviour of $o(\epsilon^N)$ as $\epsilon\to 0$.

Chapter 4

WKB Method for Calculating the Reflection Coefficient

4.1 WKB formalism

If the initial data is given in the form (1.4), then (1.3) takes the form of a linear system of partial differential equations with highly oscillatory coefficients:

$$\epsilon \mathcal{D}\boldsymbol{\psi} = \frac{1}{2}\begin{bmatrix} 0 & A(x,y)\mathrm{e}^{\mathrm{i}S(x,y)/\epsilon} \\ A(x,y)\mathrm{e}^{-\mathrm{i}S(x,y)/\epsilon} & 0 \end{bmatrix}\boldsymbol{\psi}, \quad \boldsymbol{\psi} = \begin{bmatrix}\psi_1 \\ \psi_2\end{bmatrix}, \quad \mathcal{D} := \begin{bmatrix}\overline{\partial} & 0 \\ 0 & \partial\end{bmatrix}. \tag{4.1}$$

Let us assume for simplicity that $A(x,y)$ is a strictly positive Schwartz-class function, and that the real-valued phase is asymptotically linear: $S(x,y) = wz + \overline{wz} + O(1)$ as $z \to \infty$ for some $w \in \mathbb{C}$, in the sense that

$$\partial S(x,y) \to w \quad \text{and} \quad \overline{\partial} S(x,y) \to \overline{w}, \quad z \to \infty. \tag{4.2}$$

The parameter $w \in \mathbb{C}$ has the effect of introducing a shift of the value of the spectral parameter $k \in \mathbb{C}$. Indeed if $S = wz + \overline{wz} + \tilde{S}$ and $\tilde{\boldsymbol{\psi}}(z;k)$ corresponds to $(A, \tilde{S})$ while $\boldsymbol{\psi}(z;k)$ corresponds to (A, S), then $\tilde{\psi}_1(z;k - \mathrm{i}w) = \psi_1(z;k)\mathrm{e}^{-\mathrm{i}wz/\epsilon}$ and $\tilde{\psi}_2(z;k-\mathrm{i}w) = \psi_2(z;k)\mathrm{e}^{\mathrm{i}\overline{wz}/\epsilon}$. Without loss of generality, we will therefore assume throughout this paper that $w = 0$. For classical solutions of (4.1) we require $\boldsymbol{\psi} \in C^1(\mathbb{R}^2)$, and similarly for $\boldsymbol{\chi}$ and $\boldsymbol{\phi}$ to be defined shortly.

The oscillatory factors $\mathrm{e}^{\pm \mathrm{i}S(x,y)/\epsilon}$ can be removed from the coefficients in (4.1) by the substitution

$$\boldsymbol{\psi} = \mathrm{e}^{\mathrm{i}S(x,y)\sigma_3/(2\epsilon)}\boldsymbol{\chi} \tag{4.3}$$

leading to the equivalent system

$$\epsilon \mathcal{D}\boldsymbol{\chi} = \frac{1}{2}\begin{bmatrix} -\mathrm{i}\bar{\partial}S & A \\ A & \mathrm{i}\partial S \end{bmatrix}\boldsymbol{\chi}. \tag{4.4}$$

This problem is not directly amenable to a perturbation approach, because if $\epsilon = 0$ there can only exist nonzero solutions $\boldsymbol{\chi}$ if the coefficient matrix on the right-hand side is singular, which can be assumed to be a non-generic (with respect to $(x, y) \in \mathbb{R}^2$) phenomenon.

One way around this difficulty is to introduce a complex scalar field $f : \mathbb{R}^2 \to \mathbb{C}$ and make an exponential gauge transformation of the form

$$\boldsymbol{\chi} = \mathrm{e}^{f(x,y)/\epsilon}\boldsymbol{\phi}. \tag{4.5}$$

This transforms (4.4) into the form

$$\epsilon \mathcal{D}\boldsymbol{\phi} = \mathbf{M}(x, y)\boldsymbol{\phi}, \tag{4.6}$$

where $\mathbf{M}(x, y)$ is the ϵ-independent matrix

$$\mathbf{M}(x, y) := \frac{1}{2}\begin{bmatrix} -\mathrm{i}\bar{\partial}S - 2\bar{\partial}f & A \\ A & \mathrm{i}\partial S - 2\partial f \end{bmatrix}. \tag{4.7}$$

Now we have both the vector unknown $\boldsymbol{\phi}$ and the scalar unknown f, but we may now take advantage of the extra degree of freedom by choosing f in such a way that the augmented coefficient matrix $\mathbf{M}(x, y)$ on the right-hand side of (4.6) is singular for all $(x, y) \in \mathbb{R}^2$. A direct calculation shows that the condition $\det(\mathbf{M}(x, y)) = 0$ is precisely the eikonal equation (1.6) for f. If f is any solution of this nonlinear partial differential equation, it follows that there exist nonzero solutions of (4.6) when $\epsilon = 0$, and such a solution can be used as the leading term in a formal asymptotic power series expansion in powers of ϵ.

Next recall the asymptotic normalization conditions for (1.4) on the functions ψ_j as $z \to \infty$, which in terms of $\boldsymbol{\phi}$ imply

$$\begin{aligned} \lim_{|z|\to\infty} \phi_1 \mathrm{e}^{f/\epsilon}\mathrm{e}^{\mathrm{i}S/(2\epsilon)}\mathrm{e}^{-kz/\epsilon} &= 1 \\ \lim_{|z|\to\infty} \phi_2 \mathrm{e}^{f/\epsilon}\mathrm{e}^{-\mathrm{i}S/(2\epsilon)}\mathrm{e}^{-\bar{k}\bar{z}/\epsilon} &= 0 \end{aligned} \tag{4.8}$$

Since S is real, and since the second limit is zero, these two conditions can be combined to

read

$$\lim_{|z|\to\infty} \boldsymbol{\phi} \exp\left(\frac{1}{\epsilon}\left[f + \frac{\mathrm{i}}{2}S - kz\right]\right) = \begin{bmatrix}1\\0\end{bmatrix}. \tag{4.9}$$

Since we want to be able to accurately represent $\boldsymbol{\phi}$ using asymptotic power series in ϵ, in particular we want $\boldsymbol{\phi}$ to have simple asymptotics as $z \to \infty$, so we now impose on the eikonal function f the normalization condition (1.7). Under this condition, (4.9) becomes simply

$$\lim_{|z|\to\infty} \boldsymbol{\phi} = \begin{bmatrix}1\\0\end{bmatrix}. \tag{4.10}$$

Since the conditions (1.6)–(1.7) on the eikonal function f explicitly involve the spectral parameter $k \in \mathbb{C}$, we denote any solution of the eikonal problem by $f = f(x, y; k)$. Similarly, the matrix $\mathbf{M}$ defined in (4.7) now depends on k via f and will be denoted $\mathbf{M}(x, y; k)$, a singular matrix for all $(x, y) \in \mathbb{R}^2$.

Given a suitable value of $k \in \mathbb{C}$ and a corresponding solution $f(x, y; k)$ of the eikonal problem (1.6)–(1.7), we may now try to determine the terms in an asymptotic power series expansion of $\boldsymbol{\phi} = \boldsymbol{\phi}^\epsilon(x, y; k)$:

$$\boldsymbol{\phi}^\epsilon(x, y; k) \sim \sum_{n=0}^{\infty} \boldsymbol{\phi}^{(n)}(x, y; k)\epsilon^n, \quad \epsilon \to 0. \tag{4.11}$$

Substituting into (4.6) and matching the terms with the same powers of ϵ one finds firstly that

$$\boldsymbol{\phi}^{(0)}(x, y; k) \in \ker(\mathbf{M}(x, y; k)) = \operatorname*{span}_{\mathbb{C}(x,y)} \begin{bmatrix} 2\partial f(x, y; k) - \mathrm{i}\partial S(x, y) \\ A(x, y) \end{bmatrix}. \tag{4.12}$$

This determines $\boldsymbol{\phi}^{(0)}(x, y; k)$ up to a scalar multiple, which in general can depend on $(x, y) \in \mathbb{R}^2$ and $k \in \mathbb{C}$. We may therefore write $\boldsymbol{\phi}^{(0)}(x, y; k)$ in the form

$$\boldsymbol{\phi}^{(0)}(x, y; k) = \frac{\alpha_0(x, y; k)}{2k} \begin{bmatrix} 2\partial f(x, y; k) - \mathrm{i}\partial S(x, y) \\ A(x, y) \end{bmatrix} \tag{4.13}$$

for a scalar field $\alpha_0(x, y; k)$ to be determined. Then from the higher-order terms one obtains the recurrence relations:

$$\mathbf{M}(x, y; k)\boldsymbol{\phi}^{(n+1)}(x, y; k) = \mathcal{D}\boldsymbol{\phi}^{(n)}(x, y; k), \quad n = 0, 1, 2, 3, \ldots. \tag{4.14}$$

As $\mathbf{M}(x, y; k)$ is singular, at each order there is a solvability condition to be enforced, namely

that

$$\mathcal{D}\boldsymbol{\phi}^{(n)}(x,y;k) \in \operatorname{ran}(\mathbf{M}(x,y)) = \operatorname*{span}_{\mathbb{C}(x,y)} \begin{bmatrix} -\mathrm{i}\bar{\partial}S(x,y) - 2\bar{\partial}f(x,y;k) \\ A(x,y) \end{bmatrix}, \quad n = 0,1,2,3,\ldots, \tag{4.15}$$

which we write in Wronskian form as

$$\det\left(\begin{bmatrix} -\mathrm{i}\bar{\partial}S(x,y) - 2\bar{\partial}f(x,y;k) \\ A(x,y) \end{bmatrix}, \mathcal{D}\boldsymbol{\phi}^{(n)}(x,y;k) \right) = 0, \quad n = 0,1,2,3,\ldots. \tag{4.16}$$

Assuming that (4.16) holds for a given n, the general solution of (4.14) is

$$\boldsymbol{\phi}^{(n)}(x,y;k) = \boldsymbol{\phi}_{\mathrm{p}}^{(n)}(x,y;k) + \frac{\alpha_n(x,y;k)}{2k} \begin{bmatrix} 2\partial f(x,y;k) - \mathrm{i}\partial S(x,y) \\ A(x,y) \end{bmatrix}, \quad n = 1,2,3,\ldots, \tag{4.17}$$

where

$$\boldsymbol{\phi}_{\mathrm{p}}^{(n)}(x,y;k) := \frac{2\partial\phi_2^{(n-1)}(x,y;k)}{\mathrm{i}\partial S(x,y) - 2\partial f(x,y;k)} \begin{bmatrix} 0 \\ 1 \end{bmatrix} \tag{4.18}$$

is a particular solution and $\alpha_n(x,y;k)$ is a scalar field to be determined parametrizing the homogeneous solution.

The calculation of the terms in the formal series (4.11) therefore has been reduced to the sequential solution of the scalar equation (4.16) for $\alpha_{n-1}(x,y;k)$, for $n = 1,2,3,\ldots$. We interpret the boundary condition (4.10) in light of the formal series (4.11) as:

$$\lim_{|z|\to\infty} \boldsymbol{\phi}^{(0)}(x,y;k) = \begin{bmatrix} 1 \\ 0 \end{bmatrix}, \quad \lim_{|z|\to\infty} \boldsymbol{\phi}^{(n)}(x,y;k) = \mathbf{0}, \quad n = 1,2,3,\ldots. \tag{4.19}$$

Taking into account (1.7), (4.2) for $w = 0$, and (4.19) we require the solution of (4.16) subject to the boundary condition:

$$\lim_{|z|\to\infty} \alpha_n(x,y;k) = \begin{cases} 1, & n = 0 \\ 0, & n = 1,2,3,\ldots. \end{cases} \tag{4.20}$$

A direct calculation shows that (suppressing the arguments)

$$\det\left(\begin{bmatrix} -\mathrm{i}\bar{\partial}S - 2\bar{\partial}f \\ A \end{bmatrix}, \mathcal{D}\frac{\alpha_n}{2k} \begin{bmatrix} 2\partial f - \mathrm{i}\partial S \\ A \end{bmatrix} \right) = -\frac{1}{2k}\mathcal{L}\alpha_n \tag{4.21}$$

where the differential operator $\mathcal{L}$ is defined in (1.10). Therefore, assuming $k \neq 0$, taking $n = 0$ in (4.16) and using (4.13) immediately yields (1.10) for α_0, which by (4.20) is to be solved subject to the boundary condition $\alpha_0 \to 1$ as $|z| \to \infty$. Similarly, taking $n > 0$ in (4.16) and using (4.17) gives a related non-homogeneous equation

$$\begin{aligned} \mathcal{L}\alpha_n &= 2k \det\left(\begin{bmatrix} -\mathrm{i}\bar{\partial}S - 2\bar{\partial}f \\ A \end{bmatrix}, \mathcal{D}\boldsymbol{\phi}_{\mathrm{P}}^{(n)}\right) \\ &= 2k(-\mathrm{i}\bar{\partial}S - 2\bar{\partial}f)\partial\left[\frac{2\partial\phi_2^{(n-1)}}{\mathrm{i}\partial S - 2\partial f}\right], \quad n = 1, 2, 3, \ldots, \end{aligned} \tag{4.22}$$

which by (4.20) is to be solved subject to the boundary condition $\alpha_n \to 0$ as $|z| \to \infty$. We remark that under the conditions of Theorem 1.2.1 the denominator $\mathrm{i}\partial S - 2\partial f$ is bounded away from zero, so we may expect that the forcing term on the right-hand side is a smooth function of $(x, y) \in \mathbb{R}^2$ that decays as $|z| \to \infty$ due in part to the fact that $\mathrm{i}\bar{\partial}S + 2\bar{\partial}f \to 0$ as $|z| \to \infty$. Therefore, invertibility of $\mathcal{L}$ on a suitable space of decaying functions is sufficient to guarantee the existence of all terms of the WKB expansion.

Now we give the proof (based on Conjecture 1.2.3) of Corollary 1.2.4. Observe that using (1.5), (1.7), (4.3), and (4.5), the reflection coefficient $R_0^\epsilon(k)$ can be written in terms of the (well-defined for all $(x, y) \in \mathbb{R}^2$, $k \in \mathbb{C}$, and $\epsilon > 0$) solution $\boldsymbol{\phi}^\epsilon(x, y; k)$ of (4.6) and (4.10) as

$$R_0^\epsilon(k) = 2 \lim_{z\to\infty} z\mathrm{e}^{-2\mathrm{i}\mathrm{Im}(kz)/\epsilon}\overline{\phi_2^\epsilon(x, y; k)}. \tag{4.23}$$

Suppose that the WKB expansion can be successfully and uniquely constructed through terms of order ϵ^N, in which case we may write $\boldsymbol{\phi}^\epsilon(x, y; k)$ unambiguously in the form

$$\boldsymbol{\phi}^\epsilon(x, y; k) = \sum_{n=0}^{N} \boldsymbol{\phi}^{(n)}(x, y; k)\epsilon^n + \tilde{\boldsymbol{\phi}}^{(N),\epsilon}(x, y; k). \tag{4.24}$$

Suppose also that the remainder term $\tilde{\boldsymbol{\phi}}^{(N),\epsilon}(x, y; k) = o(\epsilon^N)$ uniformly in $(x, y) \in \mathbb{R}^2$. Then, since the rapidly oscillatory factor $\mathrm{e}^{-2\mathrm{i}\mathrm{Im}(kz)/\epsilon}$ is bounded despite having no limit as $|z| \to \infty$ unless $k = 0$, the (known) existence of $R_0^\epsilon(k)$ for all $k \in \mathbb{C}$ and $\epsilon > 0$ implies that $\phi_2^{(n)}(x, y; k) = o(z^{-1})$ as $|z| \to \infty$ for all $n = 0, 1, 2, \ldots, N$, and we conclude that $R_0^\epsilon(k) = o(\epsilon^N)$ as $\epsilon \downarrow 0$. This is rather obvious for the case of $N = 0$; indeed, replacing ϕ_2^ϵ with its leading-order approximation $\phi_2^{(0)}(x, y; k) = \alpha_0(x, y; k)A(x, y)/(2k)$ yields under the assumption that $\tilde{\boldsymbol{\phi}}^{0,\epsilon}(x, y; k)$ is uniformly $o(1)$ the approximate formula

$$R_0^\epsilon(k) = \frac{1}{\bar{k}} \lim_{z\to\infty} z\mathrm{e}^{-2\mathrm{i}\mathrm{Im}(kz)/\epsilon}\overline{\alpha_0(x, y; k)}A(x, y) + o(1) = o(1) \tag{4.25}$$

(the explicit limit is zero because $\alpha_0 \to 1$ and A is Schwartz-class).

4.1.1 Some notes on rigorous analysis

Assuming for a given $k \in \mathbb{C} \setminus \{0\}$ that the terms $\boldsymbol{\phi}^{(0)}, \ldots, \boldsymbol{\phi}^{(N)}$ have been determined, the error term $\tilde{\boldsymbol{\phi}}^{(N),\epsilon}(x, y; k)$ in (4.24) satisfies the equation

$$[\epsilon\mathcal{D} - \mathbf{M}]\, \tilde{\boldsymbol{\phi}}^{(N),\epsilon} = \epsilon^{N+1} \boldsymbol{\gamma}^{(N)}(x, y; k), \quad \boldsymbol{\gamma}^{(N)}(x, y; k) := -\mathcal{D}\boldsymbol{\phi}^{(N)}. \tag{4.26}$$

Note that $\boldsymbol{\gamma}^{(N)}(x, y; k)$ is independent of $\epsilon > 0$ and is, for each $(x, y) \in \mathbb{R}^2$, a vector in $\mathrm{ran}(\mathbf{M}(x, y; k))$ as a consequence of the equation (cf., (4.16)) satisfied by $\alpha_N(x, y; k)$.

In general, the singularly-perturbed differential operator $\epsilon\mathcal{D} - \mathbf{M}$, although certainly invertible on suitable spaces ultimately as a consequence of Fredholm theory and vanishing lemma described in [34, Lemma 2.3], will have a very large inverse when ϵ is small. Controlling this inverse is obviously the fundamental analytical challenge in establishing the validity of the WKB expansion.

Here we offer only the following advice to assist in the necessary estimation: the inverse $(\epsilon\mathcal{D} - \mathbf{M})^{-1}$ need only be controlled on the subspace of vector-valued functions $\boldsymbol{\gamma}^{(N)}$ that lie pointwise in the $\mathbb{C}^2(x, y)$ subspace $\mathrm{ran}(\mathbf{M}(x, y; k))$. Such uniform control would automatically imply that the norm of $\tilde{\boldsymbol{\phi}}^{(N),\epsilon}$ is $O(\epsilon^{N+1})$, as continuing the WKB expansion to higher order would suggest.

Chapter 5

The Eikonal Problem

In this section, we consider the problem of how to construct solutions of the eikonal problem consisting of the nonlinear equation (1.6) and the boundary condition (1.7). We also consider the related problem of finding the leading-order WKB amplitude function $\alpha_0(x, y; k)$.

5.1 Global existence of $f(x, y; k)$ and $\alpha_0(x, y; k)$ for $|k|$ sufficiently large

We first consider solving the eikonal problem (1.6)–(1.7) for $f(x, y; k)$. To study a function that tends to zero at infinity, we define

$$g(x, y; k) := f(x, y; k) - kz + \mathrm{i}\frac{1}{2}S(x, y), \tag{5.1}$$

upon which (1.6) can be rearranged to read

$$\bar{\partial} g = \frac{u}{4(k - \mathrm{i}v + \partial g)}, \quad \text{where } u := A^2 \text{ and } v := \partial S. \tag{5.2}$$

Differentiation via the operator ∂ and assuming that g is twice continuously differentiable gives an equation for $b = \partial g - \mathrm{i}v$:

$$\bar{\partial} b = -\mathrm{i}\bar{\partial} v + \partial \left[\frac{u}{4(k + b)} \right]. \tag{5.3}$$

Since we expect $\partial g \to 0$, and we may assume $v = \partial S \to 0$ as $|z| \to \infty$, we may invert $\overline{\partial}$ with the solid Cauchy transform $\overline{\partial}^{-1}$ defined by

$$\overline{\partial}^{-1} F(x,y) := -\frac{1}{\pi} \iint_{\mathbb{R}^2} \frac{F(x',y')\,\mathrm{d}\mathbb{A}(x',y')}{(x'-x)+\mathrm{i}(y'-y)}, \tag{5.4}$$

for a suitable function $F : \mathbb{R}^2 \to \mathbb{C}$, where $\mathrm{d}\mathbb{A}(x,y)$ denotes the area differential in the plane. And hence obtain the fixed-point equation

$$b = F(b), \tag{5.5}$$

where F is the nonlinear mapping

$$F(b) := -\mathrm{i}v + \mathcal{B}\left[\frac{u}{4(k+b)}\right], \tag{5.6}$$

in which $\mathcal{B}$ denotes the *Beurling transform* defined by $\mathcal{B} := \overline{\partial}^{-1}\partial = \partial\overline{\partial}^{-1}$.

We will seek a solution $b \in \mathrm{W}(\mathbb{R}^2)$, where $\mathrm{W}(\mathbb{R}^2)$ denotes the *Wiener space* [13] defined as the completion of the Schwartz space $\mathscr{S}(\mathbb{R}^2)$ under the norm

$$\|b\|_{\mathrm{W}} := \iint_{\mathbb{R}^2} |\hat{b}(\xi_x,\xi_y)|\,\mathrm{d}\xi_x\,\mathrm{d}\xi_y, \quad \hat{b}(\xi_x,\xi_y) := \frac{1}{4\pi^2}\iint_{\mathbb{R}^2} b(x,y)\mathrm{e}^{-\mathrm{i}(\xi_x x+\xi_y y)}\,\mathrm{d}x\,\mathrm{d}y, \tag{5.7}$$

i.e., the Wiener norm is just the L^1 norm in the Fourier transform domain. Observe that since the inverse Fourier transform is given by

$$b(x,y) = \iint_{\mathbb{R}^2} \hat{b}(\xi_x,\xi_y)\mathrm{e}^{\mathrm{i}(\xi_x x+\xi_y y)}\,\mathrm{d}\xi_x\,\mathrm{d}\xi_y, \tag{5.8}$$

it follows that whenever b is a function with a nonnegative Fourier transform $\hat{b}(\xi_x,\xi_y) \geq 0$, the Wiener norm is given simply by the value of b at the origin: $\|b\|_{\mathrm{W}} = b(0,0)$. By the Riemann-Lebesgue lemma, functions in $\mathrm{W}(\mathbb{R}^2)$ are continuous and decay to zero as $|z| \to \infty$, and $\|b\|_\infty \leq \|b\|_{\mathrm{W}}$. A key property of the Wiener space is that it is a Banach algebra as a

consequence of the convolution theorem:

$$\begin{aligned}\|b_1 b_2\|_{\mathrm{W}} &= \iint_{\mathbb{R}^2} |\widehat{b_1 b_2}(\xi_x,\xi_y)|\,\mathrm{d}\xi_x\,\mathrm{d}\xi_y \\ &= \iint_{\mathbb{R}^2} |\hat{b}_1 * \hat{b}_2(\xi_x,\xi_y)|\,\mathrm{d}\xi_x\,\mathrm{d}\xi_y \\ &= \iint_{\mathbb{R}^2} \left| \iint_{\mathbb{R}^2} \hat{b}_1(\xi_x',\xi_y')\hat{b}_2(\xi_x-\xi_x',\xi_y-\xi_y')\,\mathrm{d}\xi_x'\,\mathrm{d}\xi_y' \right| \mathrm{d}\xi_x\,\mathrm{d}\xi_y \\ &\leq \iint_{\mathbb{R}^2}\iint_{\mathbb{R}^2} |\hat{b}_1(\xi_x',\xi_y')||\hat{b}_2(\xi_x-\xi_x',\xi_y-\xi_y')|\,\mathrm{d}\xi_x\,\mathrm{d}\xi_y\,\mathrm{d}\xi_x'\,\mathrm{d}\xi_y' \\ &= \|b_1\|_{\mathrm{W}}\|b_2\|_{\mathrm{W}}.\end{aligned} \tag{5.9}$$

Another important property obvious from the definition (5.7) is scale invariance: if $b \in \mathrm{W}(\mathbb{R}^2)$ and for $\rho > 0$, $b_\rho(x,y) := b(x/\rho, y/\rho)$, then $\|b_\rho\|_{\mathrm{W}} = \|b\|_{\mathrm{W}}$ for all $\rho > 0$. The Wiener space is also well-behaved with respect to the Beurling transform, whose action in the Fourier domain is given by

$$\widehat{\mathcal{B}b}(\xi_x,\xi_y) = -\frac{\xi_x + \mathrm{i}\xi_y}{\xi_x - \mathrm{i}\xi_y}\hat{b}(\xi_x,\xi_y), \tag{5.10}$$

so as the Fourier multiplier has unit modulus for all $(\xi_x,\xi_y) \in \mathbb{R}^2$, $|\widehat{\mathcal{B}b}(\xi_x,\xi_y)| = |\hat{b}(\xi_x,\xi_y)|$, and therefore

$$\|\mathcal{B}b\|_{\mathrm{W}} = \|b\|_{\mathrm{W}}, \quad \forall b \in \mathrm{W}(\mathbb{R}^2). \tag{5.11}$$

While all of these properties are useful to us, it is really the combination of the Banach algebra property (5.9) with the unitarity of the Beurling transform expressed in (5.11) that makes $\mathrm{W}(\mathbb{R}^2)$ a useful space for us to work with when dealing with nonlinear problems involving the operator $\mathcal{B}$ such as (5.5)–(5.6).

To view (5.5)–(5.6) as a fixed-point equation on $\mathrm{W}(\mathbb{R}^2)$, we first assume that $u \in \mathrm{W}(\mathbb{R}^2)$ and $v \in \mathrm{W}(\mathbb{R}^2)$. We then need to guarantee that $F(b) \in \mathrm{W}(\mathbb{R}^2)$ provided that $b \in \mathrm{W}(\mathbb{R}^2)$. We write $F(b)$ in the slightly-modified form

$$F(b) = -\mathrm{i}v + \frac{1}{4k}\mathcal{B}u + \mathcal{B}\left[\frac{1}{4}u\left(\frac{1}{k+b} - \frac{1}{k}\right)\right]. \tag{5.12}$$

Due to (5.9) and (5.11), it is sufficient that $b \mapsto (k+b)^{-1} - k^{-1}$ takes $\mathrm{W}(\mathbb{R}^2)$ into itself. This will be the case provided that $|k|$ is sufficiently large. Indeed, consider the geometric series

$$\frac{1}{k+b} - \frac{1}{k} = \frac{1}{k}\cdot\frac{1}{1-(-b/k)} - \frac{1}{k} = -\sum_{n=1}^{\infty}\left(-\frac{1}{k}\right)^{n+1} b^n. \tag{5.13}$$

Since due to the homogeneity property of the norm and the Banach algebra property (5.9),

$$\left\| \left(-\frac{1}{k} \right)^{n+1} b^n \right\|_{\mathrm{W}} = \frac{1}{|k|^{n+1}} \|b^n\|_{\mathrm{W}} \leq \frac{\|b\|_{\mathrm{W}}^n}{|k|^{n+1}}, \quad n = 1, 2, 3, \ldots, \tag{5.14}$$

the geometric series on the right-hand side of (5.13) converges in the Wiener space $\mathrm{W}(\mathbb{R}^2)$ provided that $|k| > \|b\|_{\mathrm{W}}$. Moreover, given any $B > 0$, under the condition $\|b\|_{\mathrm{W}} \leq B$ and $|k| > B$ we have $(k+b)^{-1} - k^{-1} \in \mathrm{W}(\mathbb{R}^2)$ with

$$N_k[b] := \left\| \frac{1}{k+b} - \frac{1}{k} \right\|_{\mathrm{W}} \leq \sum_{n=1}^{\infty} \frac{\|b\|_{\mathrm{W}}^n}{|k|^{n+1}} \leq \sum_{n=1}^{\infty} \frac{B^n}{|k|^{n+1}} = \frac{1}{|k| - B} - \frac{1}{|k|} = \frac{B}{|k|(|k| - B)}. \tag{5.15}$$

Under the same conditions, an estimate for the action of the nonlinear operator F given by (5.6) is

$$\|F(b)\|_{\mathrm{W}} \leq \|v\|_{\mathrm{W}} + \frac{\|u\|_{\mathrm{W}}}{4(|k| - B)}, \quad \|b\|_{\mathrm{W}} \leq B, \quad |k| > B. \tag{5.16}$$

It follows that F is a mapping from the closed B-ball in $\mathrm{W}(\mathbb{R}^2)$ into itself provided that k and B are chosen so that

$$\|v\|_{\mathrm{W}} + \frac{\|u\|_{\mathrm{W}}}{4(|k| - B)} \leq B \quad \text{and} \quad |k| > B. \tag{5.17}$$

This proves the following result.

Lemma 5.1.1. *Suppose that u and v are functions in the Wiener space $\mathrm{W}(\mathbb{R}^2)$ with $\|u\|_{\mathrm{W}} > 0$. Then, for every $B > \|v\|_{\mathrm{W}}$, the mapping $b \mapsto F(b)$ defined by* (5.6) *takes the closed B-ball in $\mathrm{W}(\mathbb{R}^2)$ into itself if*

$$|k| \geq B + \frac{\|u\|_{\mathrm{W}}}{4} \cdot \frac{1}{B - \|v\|_{\mathrm{W}}} > B. \tag{5.18}$$

We next consider under what additional conditions the mapping F defines a contraction on the B-ball in $\mathrm{W}(\mathbb{R}^2)$. Suppose that $b, b' \in \mathrm{W}(\mathbb{R}^2)$ with $\|b\|_{\mathrm{W}} \leq B$ and $\|b'\|_{\mathrm{W}} \leq B$. Then,

$$\begin{aligned} \|F(b') - F(b)\|_{\mathrm{W}} &= \left\| \mathcal{B} \left[\frac{u}{4(k+b')} - \frac{u}{4(k+b)} \right] \right\|_{\mathrm{W}} \\ &= \left\| \frac{u}{4(k+b')} - \frac{u}{4(k+b)} \right\|_{\mathrm{W}} \\ &= \frac{1}{4} \left\| \frac{(b'-b)u}{(k+b')(k+b)} \right\|_{\mathrm{W}}. \end{aligned} \tag{5.19}$$

Adding and subtracting k^{-1} from $(k+b')^{-1}$ and $(k+b)^{-1}$, the triangle inequality and the

Banach algebra property (5.9) give

$$\|F(b') - F(b)\|_{\mathrm{W}} \leq \frac{1}{4}\|u\|_{\mathrm{W}} \left(\frac{1}{|k|^2} + \frac{N_k[b']}{|k|} + \frac{N_k[b]}{|k|} + N_k[b']N_k[b] \right) \|b' - b\|_{\mathrm{W}}, \tag{5.20}$$

where the notation in the parentheses is defined in (5.15). Using the inequality (5.15) and the given bounds on b and b', we therefore get

$$\|F(b') - F(b)\|_{\mathrm{W}} \leq \frac{\|u\|_{\mathrm{W}}}{4(|k| - B)^2} \|b' - b\|_{\mathrm{W}}. \tag{5.21}$$

Combining this estimate with Lemma 5.1.1, we have proved the following.

Lemma 5.1.2. *Suppose that u and v are functions in the Wiener space $\mathrm{W}(\mathbb{R}^2)$. Then, for every $B > \|v\|_{\mathrm{W}}$, the mapping $b \mapsto F(b)$ defined by* (5.6) *is a contraction mapping on the closed B-ball in $\mathrm{W}(\mathbb{R}^2)$ if k satisfies the inequality* (1.8).

Now we may give the proof of Theorem 1.2.1.

Proof of Theorem 1.2.1. Because $u \in \mathrm{W}(\mathbb{R}^2)$ and $v \in \mathbb{R}^2$, the given condition on k implies, via the contraction mapping theorem and Lemma 5.1.2, the existence of a unique solution b of the fixed-point equation $b = F(b)$ with $\|b\|_{\mathrm{W}} \leq B$. To obtain f from b, recall that $f = g + kz + \frac{1}{2}\mathrm{i}S$ where $\partial g = b + \mathrm{i}v = F(b) + \mathrm{i}v$. Applying ∂^{-1} as defined by the conjugate solid Cauchy transform and using $\partial^{-1}\mathcal{B} = \overline{\partial}^{-1}$, we obtain

$$g = \overline{\partial}^{-1}\left[\frac{u}{4(k+b)}\right]. \tag{5.22}$$

Because $\|b\|_\infty \leq \|b\|_{\mathrm{W}} \leq B$, the condition (1.8) on k implies that $(k+b)^{-1} \in L^\infty(\mathbb{R}^2)$, so since $u \in L^p(\mathbb{R}^2)$ and $u \in \mathrm{W}(\mathbb{R}^2) \subset L^\infty(\mathbb{R}^2)$, g is $\overline{\partial}^{-1}$ applied to a function that is in $L^{p'}(\mathbb{R}^2)$ for every $p' \geq p$. It follows from [5, Theorem 4.3.11] that g is continuous and tends to zero as $|z| \to \infty$, proving the asymptotic boundary condition (1.7). Now, as $\partial g = b + \mathrm{i}v \in \mathrm{W}(\mathbb{R}^2)$, in particular ∂g is continuous. Furthermore, $\overline{\partial} g = \mathcal{B}^{-1}\partial g$ so since $\mathcal{B}^{-1}$ maps $\mathrm{W}(\mathbb{R}^2)$ onto itself, $\overline{\partial} g$ is also in $\mathrm{W}(\mathbb{R}^2)$ and hence continuous. It follows that g is actually of class $C^1(\mathbb{R}^2)$, and so is $f = g + kz + \frac{1}{2}\mathrm{i}S$. Therefore f is a classical solution of (1.6). Finally, the estimate (1.9) follows from $\|b\|_{\mathrm{W}} \leq B$ because $b = \partial f - k - \frac{1}{2}\mathrm{i}v = \partial f - k - \frac{1}{2}\mathrm{i}\partial S$. As b is the unique Wiener space solution of the fixed-point equation $b = F(b)$ with $\|b\|_{\mathrm{W}} \leq B$, f is the only classical solution of (1.6) satisfying the condition (1.9). QED

Some comments:

— The lower bound (1.8) on $|k|$ that implies existence of a global solution depends on B, and it is attractive to try to choose B in order to guarantee a solution for $|k|$ as small as possible. The lower bound on $|k|$ is continuous with respect to B and grows both as $B \downarrow \|v\|_{\mathrm{W}}$ and as $B \uparrow \infty$, guaranteeing a strictly positive minimum value depending only on $\|u\|_{\mathrm{W}}$ and $\|v\|_{\mathrm{W}}$. There exists a solution of the eikonal problem (1.6)–(1.7) with the desired asymptotics whenever $|k|$ exceeds this minimum value. When $v = 0$, the lower bound for $|k|$ can be made as small as $\sqrt{\|u\|_{\mathrm{W}}}$ by taking the optimal value of $B = \frac{1}{2}\sqrt{\|u\|_{\mathrm{W}}}$.

— The contraction mapping theorem guarantees that there is exactly one solution within the B-ball in $\mathrm{W}(\mathbb{R}^2)$. There could in principle be other solutions as well, with larger Wiener norms.

Next, we consider the existence of the leading-order WKB amplitude $a_0(x, y; k)$. We will show that under the same conditions that a unique f is determined for sufficiently large $|k|$, we also obtain a suitable function a_0 solving (1.10) under the boundary condition $a_0 \to 1$ as $|z| \to \infty$. That this problem has a solution when $|k|$ is sufficiently large is the content of Theorem 1.2.2 which we now prove.

Proof of Theorem 1.2.2. Multiplying (1.10) by A and using the eikonal equation (1.6) gives

$$(2\bar{\partial}f + \mathrm{i}\bar{\partial}S)\left[A\partial(Aa_0) + (2\partial f - \mathrm{i}\partial S)\bar{\partial}((2\partial f - \mathrm{i}\partial S)a_0)\right] = 0. \tag{5.23}$$

We can choose to satisfy this equation by equating the second factor to zero; multiplying through by $2a_0$ (assuming $a_0 \neq 0$) we obtain the equation

$$\bar{\partial}((2\partial f - \mathrm{i}v)^2 a_0^2) + \partial(ua_0^2) = 0, \quad u := A^2 \text{ and } v := \partial S. \tag{5.24}$$

Now in terms of the quantity b satisfying the fixed point equation $b = F(b)$ (5.5)–(5.6) equivalent to the eikonal problem (1.6)–(1.7), we have $2\partial f - \mathrm{i}v = 2(k + b)$, so the equation for a_0 can be written as

$$4\bar{\partial}((k + b)^2 a_0^2) + \partial(ua_0^2) = 0. \tag{5.25}$$

Noting that since $b \in \mathrm{W}(\mathbb{R}^2)$ decays to zero as $|z| \to \infty$, we have $(k + b)^2 a_0^2 \to k^2$ as $|z| \to \infty$, and taking this into account we invert the operator $\bar{\partial}$ and obtain

$$4(k + b)^2 a_0^2 = 4k^2 - \mathcal{B}(ua_0^2). \tag{5.26}$$

Now, to get into the Wiener space, we seek a_0^2 in the form $a_0^2 = 1 + m$ with $m \in \mathrm{W}(\mathbb{R}^2)$. Thus

the problem becomes

$$m - \mathcal{K}m = h, \quad \mathcal{K}m := -\frac{\mathcal{B}(um)}{4(k+b)^2}, \quad h := -\frac{8kb + 4b^2 + \mathcal{B}(u)}{4(k+b)^2}. \tag{5.27}$$

Now observe that under the inequality (1.8), we have $h \in \mathrm{W}(\mathbb{R}^2)$ with

$$\|h\|_{\mathrm{W}} \leq \frac{8|k|B + 4B^2 + \|u\|_{\mathrm{W}}}{4(|k| - B)^2}. \tag{5.28}$$

Also, since

$$\|\mathcal{K}m\|_{\mathrm{W}} \leq \frac{\|u\|_{\mathrm{W}}}{4(|k| - B)^2}\|m\|_{\mathrm{W}}, \tag{5.29}$$

the inequality (1.8) implies that the operator norm of $\mathcal{K}$ on $\mathrm{W}(\mathbb{R}^2)$ satisfies $\|\mathcal{K}\|_{\mathrm{W}} < 1$. Hence $1 - \mathcal{K}$ has a bounded inverse on $\mathrm{W}(\mathbb{R}^2)$ given by the Neumann series $1 + \mathcal{K} + \mathcal{K}^2 + \cdots$. QED

We remark that this proof shows the bounded invertibility of the linear differential operator $\mathcal{L}$ defined in (1.10) on a space of functions whose squares differ from unity by a function in $\mathrm{W}(\mathbb{R}^2)$.

5.1.1 Existence of $f(x,y;k)$ for $|z|$ sufficiently large given arbitrary $k \neq 0$.

Proof of Theorem 1.2.5. Let $n \in \mathrm{W}(\mathbb{R}^2)$ be a function with compact support in the unit disk satisfying $n(0,0) = 1$, and suppose that $\partial n \in \mathrm{W}(\mathbb{R}^2)$ as well. For $\rho > 0$, denote by $n_\rho \in \mathrm{W}(\mathbb{R}^2)$ the function defined by $n_\rho(x,y) := n(x/\rho, y/\rho)$. Then for each $h \in \mathrm{W}(\mathbb{R}^2)$, $n_\rho h \to h$ in $\mathrm{W}(\mathbb{R}^2)$ as $\rho \to \infty$. Indeed, we have

$$\begin{aligned} \|n_\rho h - h\|_{\mathrm{W}} &:= \iint_{\mathbb{R}^2} |\widehat{n_\rho h}(\xi_x, \xi_y) - \hat{h}(\xi_x, \xi_y)| \, \mathrm{d}\xi_x \, \mathrm{d}\xi_y \\ &= \iint_{\mathbb{R}^2} |\widehat{n_\rho} * \hat{h}(\xi_x, \xi_y) - \hat{h}(\xi_x, \xi_y)| \, \mathrm{d}\xi_x \, \mathrm{d}\xi_y. \end{aligned} \tag{5.30}$$

Also, note that $\widehat{n_\rho}(\xi_x, \xi_y) = \rho^2 \hat{n}(\rho\xi_x, \rho\xi_y)$ behaves as an approximate delta function when ρ is large, having unit integral on $\mathbb{R}^2$ independently of ρ. Since $\hat{n}, \hat{h} \in L^1(\mathbb{R}^2)$, it follows from (5.30) that $\|n_\rho h - h\|_{\mathrm{W}} \to 0$ as $\rho \to \infty$; see [26, Theorem 2.16]. Therefore $(1 - n_\rho)h \to 0$ in $\mathrm{W}(\mathbb{R}^2)$ as $\rho \to \infty$, and $(1 - n_\rho)h$ agrees exactly with h for $|z| > \rho$.

Given $k \neq 0$, we use the function $1 - n_\rho$ for ρ sufficiently large (given k) to modify the functions u and v appearing in the fixed-point iteration for (1.6)–(1.7) in such a way that the inequality (1.8) holds and therefore Theorem 1.2.1 applies to the modified u and v. Con-

cretely, given ρ we set

$$\tilde{u} := (1 - n_\rho)u \quad \text{and} \quad \tilde{S} := (1 - n_\rho)S. \tag{5.31}$$

Recalling $v = \partial S$, the latter definition implies that

$$\tilde{v} := \partial\tilde{S} = (1 - n_\rho)v - \frac{1}{\rho}S\partial n(x/\rho, y/\rho). \tag{5.32}$$

Note that the second term above has a Wiener norm of order $O(\rho^{-1})$ because $\partial n \in \mathrm{W}(\mathbb{R}^2)$ and S differs from a function in $\mathrm{W}(\mathbb{R}^2)$ by a constant, so the claim follows from the scale invariance and Banach algebra properties of the Wiener space. The value of ρ will be chosen as follows. Choose $B \in (0, \frac{1}{2}|k|)$. Then take $\rho > 0$ so large that $\|\tilde{u}\|_{\mathrm{W}} \leq |k|B$ and $\|\tilde{v}\|_{\mathrm{W}} \leq \frac{1}{2}B$. It then follows that $B > \|\tilde{v}\|_{\mathrm{W}}$, and that

$$B + \frac{1}{4} \cdot \frac{\|\tilde{u}\|_{\mathrm{W}}}{B - \|\tilde{v}\|_{\mathrm{W}}} < \frac{1}{2}|k| + \frac{1}{2}|k| = |k| \tag{5.33}$$

and

$$B + \frac{1}{2}\sqrt{\|\tilde{u}\|_{\mathrm{W}}} < \frac{1}{2}|k| + \frac{1}{2\sqrt{2}}|k| < |k| \tag{5.34}$$

so the inequality (1.8) holds true. Therefore, by Theorem 1.2.1, there is a unique global classical solution $\tilde{f}(x, y; k)$ of (1.6)–(1.7), in which $u = A^2$ is replaced with $\tilde{u}$ and S is replaced with $\tilde{S}$, that satisfies $\|\partial\tilde{f} - k - \frac{1}{2}\mathrm{i}\tilde{v}\|_{\mathrm{W}} \leq B$. Since $\tilde{u}(x, y) = u(x, y) = A(x, y)^2$ and $\tilde{S}(x, y) = S(x, y)$ both hold for $|z| > \rho$ due to the compact support in the unit disk of n, the construction of $f(x, y; k)$ given $k \neq 0$ is finished upon defining $f := \tilde{f}$ for $|z| > \rho$. According to Theorem 1.2.2, corresponding to $\tilde{f}$ defined on $\mathbb{R}^2$ there is a unique classical solution $\tilde{\alpha}_0$ of (1.10) with the appropriate substitutions for which $\tilde{\alpha}_0 \to 1$ as $|z| \to \infty$, and defining $\alpha_0 := \tilde{\alpha}_0$ for $|z| > \rho$ finishes the proof. QED

5.1.2 Series solutions of the eikonal problem

Here, we develop a method based on infinite series that reproduces some of the above results by different means, and that can lead to an effective, sometimes explicit, solution of the eikonal problem.

Series expansions of $f(x, y; k)$ for $S(x, y) = 0$

Suppose that $S(x, y) \equiv 0$. If also $A(x, y) \equiv 0$, then the exact solution of the eikonal problem (1.6)–(1.7) is $f(x, y; k) = kz$ regardless of the value of $k \in \mathbb{C}$. This fact suggests a perturbative approach to the latter problem in which, for fixed k, a measure of the amplitude

$A(x,y)$ is taken to be the small parameter. Such an approach is to be contrasted with that of Section 5.1 in which for fixed A and S, k was taken to be a large parameter.

Let $\delta > 0$ be a parameter, and consider the $S \equiv 0$ form of the eikonal equation (1.6) in which $A^2/4$ is replaced with δA^2:

$$\overline{\partial} f(x,y;k) \partial f(x,y;k) = \delta A(x,y)^2. \tag{5.35}$$

We try to solve (5.35) by a formal series

$$f(x,y;k) \sim kz + \sum_{n=1}^{\infty} \delta^n f_n(x,y;k), \quad \delta \to 0, \tag{5.36}$$

where the coefficient functions $f_n(x,y;k)$ are to be determined. Since the leading term builds in the leading asymptotics of $f(x,y;k)$ for large $|z|$, we insist that $f_n(x,y;k) \to 0$ as $|z| \to \infty$ for all n for consistency with (1.7). We intend to set $\delta = \frac{1}{4}$ once these have been determined and then assess the possible convergence of the series.

Substituting the series (5.36) into (5.35) and collecting together the terms with the same powers of δ yields the following hierarchy of equations:

$$\overline{\partial} f_1(x,y;k) = \frac{1}{k} A(x,y)^2, \tag{5.37}$$

and

$$\overline{\partial} f_n(x,y;k) = -\frac{1}{k} \sum_{\ell=1}^{n-1} \overline{\partial} f_\ell(x,y;k) \partial f_{n-\ell}(x,y;k), \quad n = 2,3,4,\ldots, \tag{5.38}$$

The boundary condition $f_n(x,y;k) \to 0$ as $|z| \to \infty$ requires that we invert $\overline{\partial}$ on the right-hand side by the solid Cauchy transform (5.4), however in certain situations the inversion can be carried out explicitly. We will make this procedure effective in the special case that A is a function with radial symmetry below in Section 5.1.2.

Setting $u_n := k^{-1}\overline{\partial} f_n$, the hierarchy (5.37)–(5.38) becomes

$$u_1 = k^{-2} A(x,y)^2, \quad u_n = -\sum_{\ell=1}^{n-1} u_\ell \mathcal{B} u_{n-\ell}, \quad n = 2,3,4,\ldots. \tag{5.39}$$

The space $\mathrm{W}(\mathbb{R}^2)$ is a convenient choice to analyze the terms u_n for the same reasons as in the preceding study of the fixed point problem (5.5)–(5.6), namely the combination of nonlinearity with the presence of the Beurling transform $\mathcal{B}$ in the recurrence relation (5.39). Using the triangle inequality in the space $\mathrm{W}(\mathbb{R}^2)$ along with the Banach algebra property

(5.9) and the identity (5.11), we then get

$$\|u_n\|_{\mathrm{W}} \leq \sum_{\ell=1}^{n-1} \|u_\ell\|_{\mathrm{W}} \|u_{n-\ell}\|_{\mathrm{W}}, \quad n = 2, 3, 4, \ldots. \tag{5.40}$$

Now we renormalize u_n as follows: $u_n = \|u_1\|_{\mathrm{W}}^n v_n$, such that (5.40) becomes

$$\|v_1\|_{\mathrm{W}} = 1, \quad \|v_n\|_{\mathrm{W}} \leq \sum_{\ell=1}^{n-1} \|v_\ell\|_{\mathrm{W}} \|v_{n-\ell}\|_{\mathrm{W}}, \quad n = 2, 3, 4, \ldots. \tag{5.41}$$

Recall the *Catalan numbers* that satisfy the recurrence relation

$$C_n = \sum_{\ell=0}^{n-1} C_\ell C_{n-1-\ell}, \quad n = 1, 2, 3, 4, \ldots \tag{5.42}$$

subject to the initial condition $C_0 = 1$. Explicitly, the Catalan numbers are given by the formula

$$C_n = \frac{(2n)!}{(n+1)!n!}, \quad n \geq 0. \tag{5.43}$$

From these definitions, we see that

$$\|v_n\|_{\mathrm{W}} \leq C_{n-1} = \frac{(2n-2)!}{n!(n-1)!}, \quad n \geq 1. \tag{5.44}$$

Now we consider the convergence of the series (using $\delta = 1/4$)

$$\sum_{n=1}^{\infty} \delta^n \bar{\partial} f_n = k \sum_{n=1}^{\infty} 4^{-n} u_n = k \sum_{n=1}^{\infty} (\tfrac{1}{4}\|u_1\|_{\mathrm{W}})^n v_n. \tag{5.45}$$

Since, by Stirling's formula,

$$C_{n-1} = \frac{4^n}{4\sqrt{\pi} n^{3/2}} (1 + O(n^{-1})), \quad n \to \infty, \tag{5.46}$$

the series (5.45) is convergent in the space $\mathrm{W}(\mathbb{R}^2)$ provided that $\|u_1\|_{\mathrm{W}} \leq 1$, i.e., that

$$|k|^2 \geq \|A^2\|_{\mathrm{W}}. \tag{5.47}$$

Under this assumption on $|k|$, we then set

$$f(x, y; k) = kz + \bar{\partial}^{-1} \sum_{n=1}^{\infty} \delta^n \bar{\partial} f_n(x, y) = kz + k\bar{\partial}^{-1} \sum_{n=1}^{\infty} \frac{1}{4^n} u_n(x, y), \tag{5.48}$$

under the additional assumption that $\bar{\partial}^{-1}$ makes sense when applied to the particular element of $W(\mathbb{R}^2)$ given by the convergent series. Note that the assumption (5.47) on k coincides with (1.8) in the case that $v = 0$ and $B = \frac{1}{2}\sqrt{\|u\|_W}$. As has been pointed out, the latter is the optimal choice of B given $v = 0$ in (1.8).

Explicit inversion of $\bar{\partial}$ for $A(x,y)$ radially symmetric

Specializing further, let us now suppose that $A(x,y)$ is a radially-symmetric function, that is,

$$A(x,y) = a(m), \quad m := x^2 + y^2 = z\bar{z} \tag{5.49}$$

for a suitable function $a : \mathbb{R}_+ \to \mathbb{R}_+$. We will show how in this case the iterative construction of series terms f_n can be made explicit, avoiding the solution of partial differential equations or convolution with the Cauchy kernel (cf., (5.4)) at each order.

In Chapter 6 we will be interested in the solution of the eikonal problem (1.6)–(1.7) for radial phase-free potentials at $k = 0$, so before implementing the series procedure described in Section 5.1.2 we briefly discuss this special case. With $S \equiv 0$ and A given in the form (5.49), observe that for $k = 0$ one may seek f as a function of $m = x^2 + y^2 = z\bar{z}$ alone by writing $f(x,y;0) = F(m)$ by analogy with (5.49). The eikonal equation (1.6) for $S \equiv 0$ and A of the form (5.49) then becomes simply

$$4mF'(m)^2 = a(m)^2. \tag{5.50}$$

This equation has two solutions that are smooth for all $m > 0$ and that decay to zero as $m \to \infty$:

$$F(m) = \pm\frac{1}{2}\int_m^\infty \frac{a(\mu)}{\mu^{1/2}}\,\mathrm{d}\mu = \pm\int_{m^{1/2}}^\infty a(s^2)\,\mathrm{d}s. \tag{5.51}$$

On the other hand, both of these solutions $f(x,y;0) = F(x^2+y^2)$ exhibit conical singularities at the origin $r = 0$ unless $a(0) = 0$.

Now we return to the series approach described in Section 5.1.2. The equation (5.37) for f_1 in the current setting reads

$$\bar{\partial} f_1 = \frac{1}{k} a(z\bar{z})^2. \tag{5.52}$$

This equation is easily integrated under the condition that f_1 should be smooth at the origin:

$$f_1 = \frac{1}{kz}\int_0^{z\bar{z}} a(m)^2\,\mathrm{d}m. \tag{5.53}$$

Assuming that $a \in L^2(\mathbb{R}_+)$, we see easily that

$$|f_1| \leq \frac{\|a\|_2^2}{|kz|}, \tag{5.54}$$

an estimate that provides decay as $z \to \infty$. Assuming also that a is continuous down to $m = 0$ shows that

$$f_1 = \frac{a(0)^2}{k}\bar{z} + o(|z|), \quad z \to 0, \tag{5.55}$$

indicating that f_1 is smooth near $z = 0$ as well. We next claim that for all $n = 1, 2, 3, \ldots$ it is consistent with (5.37) and (5.38) to write f_n in the form

$$f_n = \frac{G_n(m)}{(2n-1)(kz)^{2n-1}}, \quad m = z\bar{z}, \tag{5.56}$$

where G_n is a smooth function. (Precisely, the assertion is that $(2n-1)(kz)^{2n-1}f_n$ is a radial function of (x, y), i.e., depending only on the product $m = z\bar{z}$.) Indeed, this holds for $n = 1$ with

$$G_1(m) := \int_0^m a(\mu)^2 \, \mathrm{d}\mu. \tag{5.57}$$

Furthermore, substituting (5.56) into (5.38) gives a recurrence relation on the functions G_n:

$$G_n'(m) = \sum_{\ell=1}^{n-1} K_{n\ell} \left[(2(n-\ell)-1) G_\ell'(m) G_{n-\ell}(m) - m G_\ell'(m) G_{n-\ell}'(m) \right], \quad n \geq 2, \tag{5.58}$$

where

$$K_{n\ell} := \frac{2n-1}{(2\ell-1)(2(n-\ell)-1)}. \tag{5.59}$$

In order to ensure that f_n is smooth at the origin, we need to insist that G_n vanish at $m = 0$, and so once $G_n'(m)$ is known from (5.58), we obtain G_n itself by

$$G_n(m) = \int_0^m G_n'(\mu) \, \mathrm{d}\mu. \tag{5.60}$$

This guarantees only that $G_n(0) = 0$ but sufficiently high-order vanishing at $m = 0$ will be required to cancel the factor of z^{2n-1} in the denominator of f_n as given by (5.56). We will need $G_n(m) = O(m^{2n-1})$ as $m \to 0$ to have the necessary smoothness. We will also need to avoid rapid growth in $G_n(m)$ as $m \to \infty$ in order that f_n decay as $z \to \infty$. Although there is no additional freedom available once the recurrence (5.58) is solved and the integration constant is determined by (5.60), these additional properties of G_n are indeed present as can be confirmed in examples, to which we now proceed.

◁ Remark: The form (5.56) shows that, in polar coordinates $z = re^{i\phi}$, $f_n = \tilde{f}_n(r)e^{-i(2n-1)\phi}$, and thus the infinite series $f(x,y;k) - kz = \sum_{n=1}^{\infty} \delta^n f_n(x,y;k)$ is nothing but a Fourier series consisting of only negative odd harmonics $e^{-i\phi}$, $e^{-3i\phi}$, $e^{-5i\phi}$, etc. Another important observation clear from (5.56) and the fact that G_n is independent of k is that $f(x,y;k) - kz$ is a power series in negative odd powers of k with coefficients depending on $(x,y) \in \mathbb{R}^2$. These observations lead to a numerical approach to the eikonal problem for radial potentials with $S(x,y) \equiv 0$ that will be explained in Section 7.2. It is also clear that it is the asymptotic behaviour of $G_n(m)$ as $n \to \infty$ that determines for a given $|z|$ the minimum value of $|k|$ for which the series (5.36) converges. ▷

Example: Gaussian amplitude

Suppose that $A(x,y) = e^{-(x^2+y^2)}$, which we can write in the form (5.49) with $a(m) = e^{-m}$. Since the Fourier transform of $A(x,y)^2 = e^{-2(x^2+y^2)}$ by the definition (5.7) is $e^{-|\xi|^2/8}/(8\pi) > 0$ where $|\xi|^2 := \xi_x^2 + \xi_y^2$, it is easy to compute the Wiener norm of A^2 and we hence conclude that the series (5.45) is convergent in $W(\mathbb{R}^2)$ provided $|k| \geq \sqrt{\|A^2\|_W} = \sqrt{A(0,0)^2} = 1$. Later in Section 8.1 we will see convincing numerical evidence that this condition on k is not sharp, and that the related series (5.48) is convergent in $L^\infty(\mathbb{R}^2)$ for $|k| \geq \frac{1}{2}$.

Let us illustrate the analytical calculation of the terms in the series for this case. From (5.56)–(5.57) we have

$$G_1(m) = \int_0^m e^{-2\mu}\, d\mu = \frac{1}{2}\left[1 - e^{-2m}\right] \quad \Longrightarrow \quad f_1 = \frac{1 - e^{-2z\bar{z}}}{2kz}. \tag{5.61}$$

With G_1 determined, (5.58) for $n = 2$ reads

$$\begin{aligned} G_2'(m) &= 3G_1'(m)G_1(m) - 3mG_1'(m)^2 \\ &= 3e^{-2m}\frac{1}{2}\left[1 - e^{-2m}\right] - 3me^{-4m} \\ &= \frac{3}{2}e^{-2m} - \left[\frac{3}{2} + 3m\right]e^{-4m}, \end{aligned} \tag{5.62}$$

and hence using (5.60) we get

$$G_2(m) = \frac{3}{16}\left[1 - 4e^{-2m} + (3+4m)e^{-4m}\right]$$

$$\Longrightarrow \quad f_2 = \frac{1 - 4e^{-2z\bar{z}} + (3+4z\bar{z})e^{-4z\bar{z}}}{16(kz)^3}. \tag{5.63}$$

It can be checked by Taylor expansion that f_2 is smooth at the origin and it decays as $z \to \infty$.

This procedure can be continued explicitly to arbitrary order because one needs only to be able to integrate in closed form expressions of the form $m^p \mathrm{e}^{-2qm}$ for non-negative integers p and q:

$$\int_0^m \mu^p \mathrm{e}^{-2q\mu}\,\mathrm{d}\mu = \frac{p!}{(2q)^{p+1}}\left(1 - \mathrm{e}^{-2qm}\sum_{\ell=0}^{p}\frac{(2qm)^\ell}{\ell!}\right). \tag{5.64}$$

Unfortunately, it seems difficult to deduce a closed form expression for $G_n(m)$ for general $n \geq 2$ (and prove its correctness by an induction argument). Rather than proceed in this direction, we turn to another example of a radial amplitude function $A(x,y)$ for which this procedure yields dramatic results.

Example: Lorentzian amplitude

Suppose now that $A(x,y) = (1+x^2+y^2)^{-1}$, which can be written in the form (5.49) with $a(m) = (1+m)^{-1}$. Using the definition (5.7), the Fourier transform of $A(x,y)^2$ in this case turns out to be $|\xi|K_1(|\xi|)/(4\pi)$ where $|\xi| := \sqrt{\xi_x^2+\xi_y^2}$ and K_1 is a modified Bessel function of order 1 [11, §10.25]. By an integral representation formula [11, Eqn. 10.32.9] it is obvious that $K_1(|\xi|) > 0$, so again it is easy to calculate the Wiener norm of A^2 and hence observe that the series (5.45) converges in $\mathrm{W}(\mathbb{R}^2)$ whenever $|k| \geq \sqrt{\|A^2\|_{\mathrm{W}}} = \sqrt{A(0,0)^2} = 1$. Again, this condition is not sharp, and we will see so below, without the need to resort to numerics, by explicit calculation of the terms f_n given by (5.56).

Indeed, from (5.56)–(5.57) we have

$$G_1(m) = \int_0^m \frac{\mathrm{d}\mu}{(1+\mu)^2} = 1 - \frac{1}{1+m} = \frac{m}{1+m} \quad \Longrightarrow \quad f_1 = \frac{\overline{z}}{k(1+z\overline{z})}, \tag{5.65}$$

and we note that f_1 is smooth at the origin and decays as $z \to \infty$. We next claim that for general $n \geq 2$, the recurrence (5.58) and the normalization condition (5.60) are satisfied by taking G_n in the form

$$G_n(m) = C_{n-1}\left(\frac{m}{1+m}\right)^{2n-1}, \quad n \geq 1, \tag{5.66}$$

where $C_0, C_1, C_2, \ldots$ are suitably chosen constants. Indeed $G_n(0) = 0$ for all $n \geq 1$, so (5.60) is obviously satisfied regardless of the choice of the constants $\{C_k\}_{k=0}^{\infty}$. Also, the form (5.66) is clearly correct for $n = 1$ with the choice $C_0 = 1$. Moreover, substituting (5.66) into (5.58) shows that (5.66) is correct for general n, provided that the constants $\{C_k\}_{k=0}^{\infty}$ satisfy the recurrence (5.42) together with the initial condition $C_0 = 1$; i.e., the constant C_n is the n^{th} Catalan number, which is explicitly given by (5.43). Therefore, $G_n(m)$ has been determined

in closed form for all n, and it follows that

$$f_n = \frac{C_{n-1}}{2n-1}\left(\frac{1}{k}\cdot\frac{\overline{z}}{1+z\overline{z}}\right)^{2n-1}, \quad n \geq 1. \tag{5.67}$$

Note that f_n is smooth at the origin and decays as $z \to \infty$ for every $n \geq 1$.

With the terms f_n all explicitly determined, we directly analyze the convergence of the formal series (5.36) for f with $\delta = \frac{1}{4}$. Noting that by (5.46) we have

$$\frac{C_{n-1}}{2n-1} = \frac{4^n}{8\sqrt{\pi}n^{5/2}}(1+O(n^{-1})), \quad n \to \infty, \tag{5.68}$$

we see that the series (5.36) with $\delta = \frac{1}{4}$ converges exactly when

$$|k| \geq \frac{|z|}{1+|z|^2} \tag{5.69}$$

and diverges otherwise. Moreover, given any $\sigma > 1$, the convergence is absolute and uniform for k and z satisfying the condition

$$|k| \geq \sigma\frac{|z|}{1+|z|^2}. \tag{5.70}$$

Since the function on the right-hand side of (5.69) achieves its maximum value of $1/2$ at $|z| = 1$, we learn that if $|k| \geq 1/2$ the series on the right-hand side of (5.36) converges uniformly on $\mathbb{R}^2$ to a continuous function vanishing at infinity.

Proceeding further, the infinite series on the right-hand side of (5.36) can be summed in closed form [41] for those k and z for which it converges, yielding the explicit formula (1.12), in which the square root and the arcsin are both given by principal branches. This explicit expression for $g = f - kz$, which was originally defined as a function of W by a power series convergent for $|W| < 1$, defines an analytic continuation from the unit disk in the W-plane to the whole complex W-plane with the exception of two slits joining the points $W = \pm 1$ to infinity (we may choose the branch cuts to be the real intervals $-\infty < W \leq -1$ and $1 \leq W < +\infty$). Moreover, one can directly check that regardless of whether W is inside or outside of the unit disk, the explicit expression for $f(x,y;k)$ is an exact solution of the equation (1.6) in the case $S \equiv 0$ when $A(x,y) = (1+x^2+y^2)^{-1}$.

In this case, we can also solve explicitly for the scalar coefficient $\alpha_0(x,y;k)$, which completes the construction of the leading term $\boldsymbol{\phi}^{(0)}(x,y;k)$ in the WKB expansion. By direct

calculation using the definition of W given in (1.12),

$$\partial W = -kW^2 \quad \text{and} \quad \bar{z}^2\bar{\partial}W = kW^2. \tag{5.71}$$

Hence

$$\partial f = \frac{k}{2}\left(1 + (1-W^2)^{1/2}\right), \tag{5.72}$$

and from the relevant eikonal equation $\partial f \cdot \bar{\partial} f = \frac{1}{4}(1+z\bar{z})^{-2}$ we get

$$\bar{z}^2\bar{\partial} f = \frac{k}{2}\left(1 - (1-W^2)^{1/2}\right). \tag{5.73}$$

Writing (1.10) in the special case of $S \equiv 0$ (and hence $w = 0$) gives

$$A\bar{\partial}(\partial f \cdot \alpha_0) + \bar{\partial} f \cdot \partial(A\alpha_0) = 0 \tag{5.74}$$

as the equation to be solved by $\alpha_0(x, y; k)$ under the condition $\alpha_0(x, y; k) \to 1$ as $|z| \to \infty$. Since $A = kW/\bar{z}$ according to (1.12), and ∂f and $\bar{\partial} f$ are given by (5.72)–(5.73), (5.74) can be written as

$$W\bar{z}^2\bar{\partial}\left(\left(1 + (1-W^2)^{1/2}\right)\alpha_0\right) + \left(1 - (1-W^2)^{1/2}\right)\partial(W\alpha_0) = 0 \tag{5.75}$$

where we have used $k \neq 0$. Now using (5.71) it is clear that there is a solution of the form $\alpha_0 = \alpha_0(W)$, i.e., that α_0 depends on (x, y) only via W. Indeed, by the chain rule, the ansatz $\alpha_0 = \alpha_0(W)$ in (5.75) leads to the ordinary differential equation

$$W\frac{d}{dW}\left(\left(1 + (1-W^2)^{1/2}\right)\alpha_0(W)\right) - \left(1 - (1-W^2)^{1/2}\right)\frac{\mathrm{d}}{\mathrm{d}W}(W\alpha_0(W)) = 0 \tag{5.76}$$

after canceling kW^2. This can be rewritten in the equivalent form

$$\begin{aligned}\frac{\mathrm{d}}{\mathrm{d}W}\log\left(W(1-W^2)^{1/2}\alpha_0(W)^2\right) &= W^{-1}(1-W^2)^{-1/2} \\ &= \frac{\mathrm{d}}{\mathrm{d}W}\log\left(\frac{W}{1+(1-W^2)^{1/2}}\right).\end{aligned} \tag{5.77}$$

Integrating, exponentiating, and solving for α_0 gives

$$\alpha_0(W) = C\left((1-W^2)^{1/2}(1+(1-W^2)^{1/2})\right)^{-1/2} \tag{5.78}$$

where C is an integration constant. Since $|z| \to \infty$ means $W \to 0$, we need $C = \sqrt{2}$ to have

$\alpha_0 \to 1$ as $|z| \to \infty$, which gives (1.13).

◁ Remark: For this example, we can explain the gap between the general sufficient condition for convergence, namely $|k| \geq \sqrt{\|A^2\|_{\mathrm{W}}}$ which works out to $|k| \geq 1$ in this case, and the actual condition $|k| \geq 1/2$ obtained by direct analysis of the explicit terms in the series. Indeed, it is easy to check that when f_n is given by (5.67), the corresponding functions $u_n := k^{-1}\overline{\partial} f_n$ satisfy the identity $\mathcal{B}u_n = -\overline{z}^2 u_n$ for $n = 1, 2, 3, \ldots$. If this specialized information is used in (5.39), the recurrence becomes

$$u_1 = k^{-2}A(x,y)^2, \quad u_n = \overline{z}^2 \sum_{\ell=1}^{n-1} u_\ell u_{n-\ell}. \tag{5.79}$$

Therefore, introducing $w_n := \overline{z}^2 u_n$, we get a corresponding recurrence for $\{w_n\}_{n=1}^{\infty}$:

$$w_1 = k^{-2}\overline{z}^2 A(x,y)^2, \quad w_n = \sum_{\ell=1}^{n-1} w_\ell w_{n-\ell}. \tag{5.80}$$

This recurrence relation can be studied in exactly the same way as (5.39); one introduces v_n by the rescaling $w_n = \|w_1\|^n v_n$ (here we can use the $L^\infty(\mathbb{R}^2)$ norm in place of the Wiener norm if desired because we need only the Banach algebra property having dispensed with the Beurling transform), and obtains the estimate (5.44). Hence the condition for convergence of the series (5.45) now takes the form $\|w_1\| \leq 1$. Since by comparison with u_1, w_1 contains the additional factor of $\overline{z}^2$, it is easy to check that whereas $\|u_1\|_{\mathrm{W}} = \|u_1\|_\infty \leq 1$ reads $|k| \geq 1$, the condition $\|w_1\|_\infty \leq 1$ reads $|k| \geq \frac{1}{2}$. ▷

Chapter 6

A Specialized Method for Radial Potentials with $S \equiv 0$ and $k = 0$

Suppose $S \equiv 0$, and fix the spectral parameter to be $k = 0$. It is well known that in this case the corresponding Zakharov-Shabat scattering problem that arises in the one-dimensional setting with $\lambda = 0$ corresponding to $k = 0$, namely $\epsilon \boldsymbol{\psi}'(x) = A(x)\sigma_1 \boldsymbol{\psi}(x)$, can be solved explicitly by introducing a new coordinate m satisfying $m'(x) = A(x) > 0$. Indeed, this monotone change of independent variable reduces the problem to the constant-coefficient system $\epsilon \boldsymbol{\psi}'(m) = \sigma_1 \boldsymbol{\psi}(m)$. Unfortunately, similar reasoning fails in the setting of the two-dimensional Davey-Stewartson scattering problem (1.3).

In this section, we further assume that $A(x, y)$ is a function with radial symmetry, i.e., depending only on $|z|$, and show how the use of polar coordinates can be used to reduce the scattering problem to the study of a suitable ordinary differential equation. We then study this equation in the semiclassical limit and obtain a formula for the reflection coefficient in this special case.

We begin by writing the scattering problem (1.3) in polar coordinates (r, ϕ), where $z = x + \mathrm{i}y = r\mathrm{e}^{\mathrm{i}\phi}$ and $\overline{z} = r\mathrm{e}^{-\mathrm{i}\phi}$. In polar coordinates, the operators defined in (1.3) take the form

$$\partial = \frac{\mathrm{e}^{-\mathrm{i}\phi}}{2r}\left(r\frac{\partial}{\partial r} - \mathrm{i}\frac{\partial}{\partial \phi}\right) \quad \text{and} \quad \overline{\partial} = \frac{\mathrm{e}^{\mathrm{i}\phi}}{2r}\left(r\frac{\partial}{\partial r} + \mathrm{i}\frac{\partial}{\partial \phi}\right). \tag{6.1}$$

Therefore, with $S \equiv 0$ and $A = A(r)$ being a smooth function with $A'(0) = 0$, (1.3) becomes

$$\begin{aligned} \epsilon\frac{\mathrm{e}^{\mathrm{i}\phi}}{r}\left(r\psi_{1r} + \mathrm{i}\psi_{1\phi}\right) &= A(r)\psi_2 \\ \epsilon\frac{\mathrm{e}^{-\mathrm{i}\phi}}{r}\left(r\psi_{2r} - \mathrm{i}\psi_{2\phi}\right) &= A(r)\psi_1. \end{aligned} \tag{6.2}$$

It is then convenient to introduce new dependent variables by $w_1 := \psi_1$ and $w_2 = \bar{z}\psi_2$, so that the system takes the form

$$\begin{aligned} \epsilon r w_{1r} + \mathrm{i}\epsilon w_{1\phi} &= A(r) w_2 \\ \epsilon r w_{2r} - \mathrm{i}\epsilon w_{2\phi} &= r^2 A(r) w_1. \end{aligned} \tag{6.3}$$

If $k = 0$, then from normalization condition to (1.4) and (1.5), we see that the solution we seek has the property that $w_1 \to 1$ and $w_2 \to \frac{1}{2}\overline{R_0^\epsilon(0)}$ as $r \to \infty$, thereby recovering the reflection coefficient evaluated at the origin. Implicit is the assumption that w_j are smooth functions on the plane. We claim that in this situation, $w_j = w_j(r)$ are purely radial functions, reducing the problem to the study of the linear ordinary differential equations

$$\begin{aligned} \epsilon r \frac{\mathrm{d}w_1}{\mathrm{d}r} &= A(r) w_2 \\ \epsilon r \frac{\mathrm{d}w_2}{\mathrm{d}r} &= r^2 A(r) w_1. \end{aligned} \tag{6.4}$$

By the method of Frobenius, one can see that this system has a one-dimensional space of solutions that are bounded with zero derivative at $r = 0$, which is a regular singular point. Indeed, assuming that $A(r) = A(0) + O(r^2)$ as $r \downarrow 0$, the system (6.4) can be written in the form

$$\frac{\mathrm{d}}{\mathrm{d}r}\begin{bmatrix} w_1 \\ w_2 \end{bmatrix} = \left(\frac{1}{r}\begin{bmatrix} 0 & \epsilon^{-1}A(0) \\ 0 & 0 \end{bmatrix} + O(1) \right)\begin{bmatrix} w_1 \\ w_2 \end{bmatrix}, \quad r \downarrow 0 \tag{6.5}$$

and hence the only indicial exponent for the origin is zero with non-diagonalizable coefficient matrix; therefore every solution is a linear combination of a solution analytic at $r = 0$ proportional there to the nullvector $[1, 0]^\top$ and a second independent solution that diverges logarithmically at the origin. We can attempt to find $R_0^\epsilon(0)$ by normalizing an element of this subspace of solutions regular at the origin so that $w_1 \to 1$ as $r \to \infty$. Alternatively, we can take any nonzero element of this subspace and obtain $R_0^\epsilon(0)$ by the formula

$$R_0^\epsilon(0) = 2 \lim_{r\to\infty} \overline{w_2(r)}/\overline{w_1(r)}. \tag{6.6}$$

6.1 Riccati equation. Formal asymptotic analysis

The formula (6.6) in turn motivates us to study the Riccati equation for $Q := w_2/w_1$ implied by the coupled linear system (6.4) for $w_j(r)$:

$$\epsilon \frac{\mathrm{d}Q}{\mathrm{d}r} = \frac{A(r)}{r}\left(r^2 - Q^2\right). \tag{6.7}$$

If (6.7) is solved subject to the initial condition $Q(r) = O(r^2)$ as $r \downarrow 0$ (corresponding to the regular subspace at the origin for (6.4)), then the reflection coefficient $R_0^\epsilon(0)$ may be found as $R_0^\epsilon(0) = 2\lim_{r\to\infty} Q(r)$ (using the fact that $Q(r)$ is real-valued). Equivalently, we may introduce $X(r) := Q(r)/r$, which satisfies

$$\begin{aligned}\epsilon\frac{\mathrm{d}X}{\mathrm{d}r} &= -A(r)X^2 - \frac{\epsilon}{r}X + A(r)\\ &= -A(r)[X - X_+(r;\epsilon)][X - X_-(r;\epsilon)], \quad X(r) = O(r), \quad r \downarrow 0,\end{aligned} \tag{6.8}$$

for

$$X_\pm(r;\epsilon) := \frac{1}{2A(r)}\left[-\frac{\epsilon}{r} \pm \sqrt{\frac{\epsilon^2}{r^2} + 4A(r)^2}\right], \tag{6.9}$$

and from which one obtains $R_0^\epsilon(0)$ by

$$R_0^\epsilon(0) = 2\lim_{r\to\infty} rX(r). \tag{6.10}$$

Note that, given the solution $X(r;\epsilon)$ of (6.8), the solution of the original system (6.2) with the boundary conditions $\psi_1 \to 1$ and $\psi_2 = O(1/r)$ as $r \to \infty$ is given explicitly by

$$\begin{bmatrix}\psi_1\\ \psi_2\end{bmatrix} = \tilde{\alpha}_0 \begin{bmatrix}1\\ \mathrm{e}^{\mathrm{i}\phi}X(r;\epsilon)\end{bmatrix}\mathrm{e}^{f/\epsilon}, \quad \text{where} \quad f = -\int_r^{+\infty} A(r')\,\mathrm{d}r' \tag{6.11}$$

and

$$\tilde{\alpha}_0 = \exp\left(\frac{1}{\epsilon}\int_r^{+\infty}(1 - X(r';\epsilon))A(r')\,\mathrm{d}r'\right). \tag{6.12}$$

Suppose that $A(r)$ is nonincreasing. The nullclines for (6.8) are given by $X = X_\pm(r;\epsilon)$ (cf., (6.9)). We have $X_+(r;\epsilon) > 0 > X_-(r;\epsilon)$, and $\mathrm{d}X/\mathrm{d}r > 0$ for $X_-(r;\epsilon) < X < X_+(r;\epsilon)$ while $\mathrm{d}X/\mathrm{d}r < 0$ if either $X > X_+(r;\epsilon)$ or $X < X_-(r;\epsilon)$. The nullclines have the following asymptotic behavior for small ϵ:

- If $r \ll \epsilon$, then $X_+(r;\epsilon) = A(0)r/\epsilon + O((r/\epsilon)^3)$ while the lower nullcline satisfies $X_-(r;\epsilon) = -\epsilon/(A(0)r) + O(r/\epsilon)$.
- If $\epsilon \ll r$ and $rA(r) \gg \epsilon$, then $X_\pm(r;\epsilon) = \pm 1 + o(1)$.
- If $\epsilon \ll r$ and $rA(r) \ll \epsilon$, then $X_+(r;\epsilon) = [rA(r)/\epsilon](1 + o(1))$ while the lower nullcline satisfies $X_-(r;\epsilon) = -[\epsilon/(rA(r))](1 + o(1))$.

Since $X = X(r;\epsilon)$ tends to zero as $r \downarrow 0$ for fixed ϵ, only the nullcline $X_+(r,\epsilon)$ plays any role for small r (given $\epsilon > 0$ small). Moreover, since $\mathrm{d}X/\mathrm{d}r$ is explicitly proportional to ϵ^{-1}, $X(r;\epsilon)$ will very rapidly approach a small neighborhood of the nullcline $X = X_+(r;\epsilon)$ as r increases; therefore for moderate values of r in the regime where $r \gg \epsilon$ but $rA(r) \gg \epsilon$ (the

latter condition avoiding the "tail" of the amplitude function $A(r)$) we will have $X(r;\epsilon) \approx X_+(r;\epsilon) \approx 1$ for small ϵ. On the other hand, when $A(r)$ becomes small as r increases, then (6.8) can be approximated by the linear equation

$$\epsilon \frac{\mathrm{d}X}{\mathrm{d}r} = -\frac{\epsilon}{r} X \quad \text{with general solution} \quad X(r;\epsilon) = \frac{C(\epsilon)}{r}. \tag{6.13}$$

This approximation is exact wherever $A(r) \equiv 0$. The constant $C(\epsilon)$ can be determined by matching the approximate solution $X(r;\epsilon) \approx C(\epsilon)/r$ onto the approximation $X(r;\epsilon) \approx 1$ at an appropriate value of r, say $r = r_{\text{Match}}$. If $A(r)$ has compact support, then we take the breakpoint r_{Match} to be the positive support endpoint; otherwise we take the breakpoint $r = r_{\text{Match}}$ to be the root of the equation $rA(r) = \epsilon$ that is not small as $\epsilon \downarrow 0$. In the latter case, $r_{\text{Match}} \to \infty$ as $\epsilon \downarrow 0$ because A is nonincreasing and $A(r) \to 0$ as $r \to \infty$. Given $\epsilon \ll 1$ and the corresponding value of $r_{\text{Match}}(\epsilon) > 0$, we then determine $C = C(\epsilon)$ by setting $C/r_{\text{Match}} = 1$. See Figures 6.1–6.2 for further understanding of the solutions of the Riccati equation (6.8) and their relation to the nullcline $X = X_+(r;\epsilon)$ as ϵ decreases toward zero.

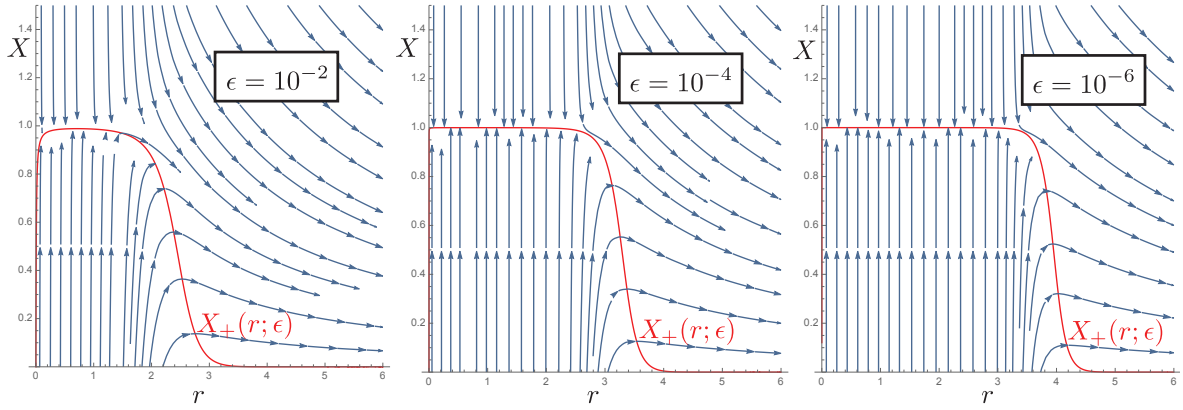

Figure 6.1 – The direction field of the Riccati equation (6.8) and its relation to the nullcline $X_+(r;\epsilon)$ in the case of a Gaussian amplitude $A(r) = \mathrm{e}^{-r^2}$. For small ϵ, the solution $X(r;\epsilon)$ departs from the nullcline $X = X_+(r;\epsilon)$ near its "shoulder," a feature that is increasingly well-defined as $\epsilon \to 0$ and is asymptotically located at $r = r_{\text{Match}}(\epsilon)$.

For the Gaussian example $A(r) = \mathrm{e}^{-r^2}$, the implications of the behavior of $X(r;\epsilon)$ can be seen also in numerical solutions at $k = 0$ of the direct spectral problem (1.3)–(1.4) carried out using the method described below in Section 7.3. See Figure 6.3.

Our formal approximation of $X(r;\epsilon)$ in the limit $\epsilon \downarrow 0$ is then as follows:

— For $r = O(\epsilon)$, $X(r;\epsilon)$ exhibits a rapid transition from the initial value $X(0;\epsilon) = 0$ to

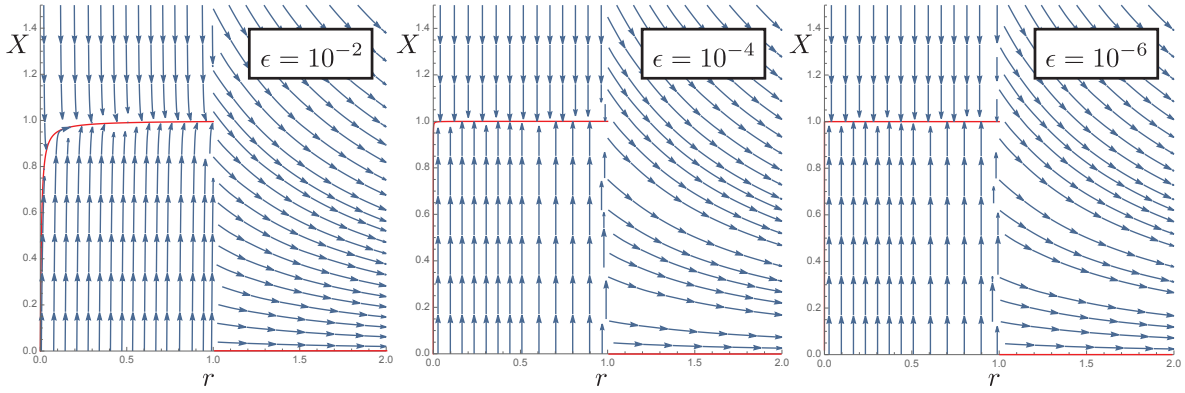

Figure 6.2 – The same as Figure 6.1 except for the potential $A(r) = \chi_{r\leq 1}(r)$. As in Figure 6.1, the (here, discontinuous) red curve is the nullcline $X = X_+(r;\epsilon)$. In this case for $r > 1$ we have $X_+(r;\epsilon) \equiv 0$ and $X(r;\epsilon) = C/r$ exactly.

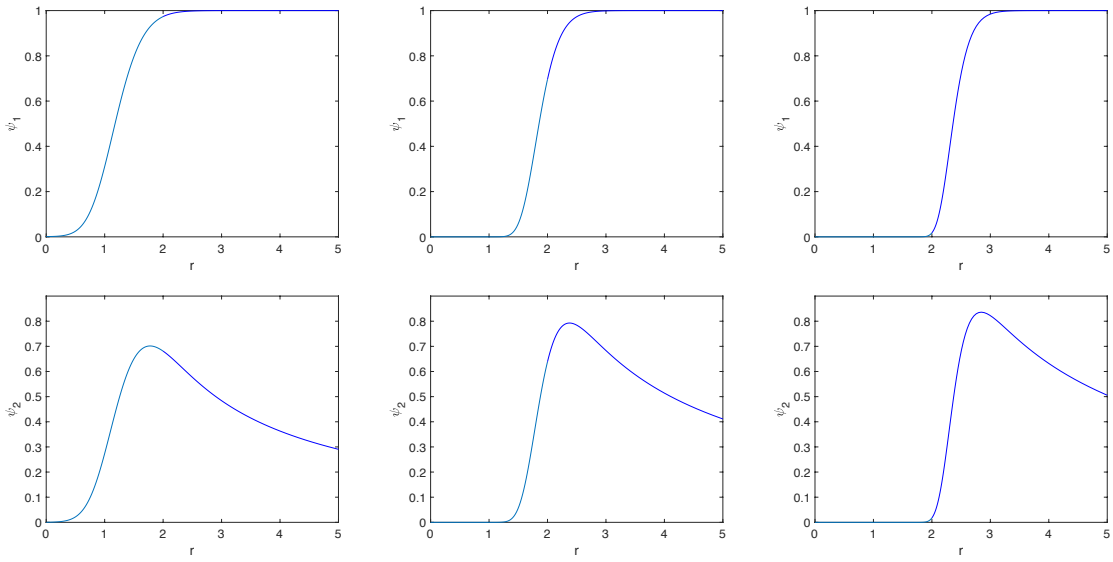

Figure 6.3 – Numerical solutions to the Dirac system (1.3) for the Gaussian potential $A(r) = \mathrm{e}^{-r^2}$ at $k = 0$ for the values $\epsilon = 10^{-1}, 10^{-2}, 10^{-3}$ from left to right. Upper row ψ_1, lower row $|\psi_2|$.

$X(r;\epsilon) \approx 1$.

— $X(r;\epsilon) \approx 1$ for $r \gg \epsilon$ but $r \leq r_{\mathrm{Match}}(\epsilon)$.

— $X(r;\epsilon) \approx r_{\mathrm{Match}}(\epsilon)/r$ for $r > r_{\mathrm{Match}}(\epsilon)$.

Recalling (6.10) to calculate the reflection coefficient at $k = 0$ gives

$$R_0^\epsilon(0) \approx 2r_{\text{Match}}(\epsilon), \quad \epsilon \downarrow 0. \tag{6.14}$$

◁ Remark: Given this asymptotic description of $X(r;\epsilon)$, from the formula (6.11)–(6.12) we can see that the solution of (6.2) for $k = 0$ is consistent with the approach based on the WKB method, *but only in the intermediate regime* $\epsilon \ll r \ll r_{\text{Match}}(\epsilon)$ where $X(r;\epsilon) \approx 1$. Note that the exponent f satisfies the eikonal equation (1.6) in the form (5.50) appropriate for radial potentials with $S \equiv 0$, and in particular the solution (5.51) with the lower sign is the one selected. Indeed, it is easily checked that the vector $[1, e^{i\phi}X(r;\epsilon)]^\top$ lies nearly in $\ker(\mathbf{M})$ wherever $X(r;\epsilon) \approx 1$. It should also be possible to prove that $\tilde{\alpha}_0$ given by (6.12) is $O(1)$ despite the explicit appearance of ϵ in the denominator of the exponent. Indeed, except perhaps in small intervals near $r = 0$ or near the "shoulder" or the nullcline $X_+(r;\epsilon)$, we will have $(1 - X(r;\epsilon))A(r) = O(\epsilon)$ for $r \gg \epsilon$ away from the "shoulder" because either $X(r;\epsilon) = 1 + O(\epsilon)$ (for $\epsilon \ll r \leq r_{\text{Match}}(\epsilon)$) or $0 < X(r;\epsilon) < 1$ and $A(r) < \epsilon/r$ (for $r \geq r_{\text{Match}}(\epsilon)$). Finally, $(1 - X(r;\epsilon))A(r) = O(1)$ near $r = 0$, so one expects that with a bit more work the integral in the exponent in (6.12) can be shown to be uniformly $O(\epsilon)$ for all $r > 0$. This observation may help motivate the correct way to generalize the WKB formalism so that it applies for $|k|$ below the threshold where the eikonal function develops singularities. ▷

6.1.1 Examples

Before turning to a rigorous proof, let us apply (6.14) in some examples.

Example 1: characteristic function of a disk. Suppose that A is an arbitrary positive multiple of the characteristic function of the disk of radius ρ. In this case $r_{\text{Match}} = \rho$, and therefore $R_0^\epsilon(0) \approx 2\rho$ in the limit $\epsilon \downarrow 0$. Observe that this result is independent of the amplitude of $A(r)$. We prove that this result is accurate by an explicit calculation involving modified Bessel functions in Section 6.3.

Example 2: Gaussian amplitude. Suppose that $A(r) = A_0 e^{-r^2}$. Then $r_{\text{Match}}(\epsilon)$ satisfies the equation $\ln(r_{\text{Match}}) + \ln(A_0) - r_{\text{Match}}^2 = -\ln(\epsilon^{-1})$, and so $r_{\text{Match}} \sim \sqrt{\ln(\epsilon^{-1})}$ as $\epsilon \downarrow 0$, and therefore also $R_0^\epsilon(0) \approx 2\sqrt{\ln(\epsilon^{-1})}$ in this limit. Again, the leading order asymptotic is independent of the amplitude A_0. We prove that this formula is accurate in the relative sense in Section 6.2 below.

6.2 Riccati equation. Rigorous analysis

Theorem 1.2.6 amounts to a more careful formulation of (6.14) under suitable conditions on the amplitude function $A(r)$.

Proof of Theorem 1.2.6. Given the graph $X = \varphi(r)$ in the (r, X)-plane of an arbitrary function $\varphi(\cdot)$, we may compare the slope of the vector field of the Riccati equation (6.8) evaluated at a point on the graph with the slope of the graph itself. If

$$\Delta X'\big|_{X=\varphi(r)} := \left[\frac{A(r)}{\epsilon}(1-\varphi(r)^2) - \frac{1}{r}\varphi(r)\right] - \varphi'(r) \tag{6.15}$$

is positive (negative) at a point $P = (r, \varphi(r))$, then the solution of (6.8) passing through P enters the region above (below) the graph $X = \varphi(r)$ as r increases. By choosing appropriate functions $\varphi(\cdot)$ and calculating the sign of $\Delta X'$ we will be able to obtain upper and lower bounds on the unique solution $X(r;\epsilon)$ of (6.8) satisfying $X(r;\epsilon) \to 0$ as $r \downarrow 0$ that are sufficiently strong to establish the asymptotic behavior of the reflection coefficient $R_0^\epsilon(0)$ given by (6.10) up to a relative error term that vanishes with ϵ.

To get started, we need to first locate the desired solution $X(r;\epsilon)$ for small $r > 0$. Using $A(r) = A(0) + o(r)$ and $X(r;\epsilon) \to 0$ as $r \downarrow 0$ we see that $X(r;\epsilon)$ actually satisfies the stronger condition $X(r;\epsilon) = A(0)r/(2\epsilon) + o(r)$ as $r \downarrow 0$ (the $o(r)$ error term depends on ϵ).

Now we look for simple bounds on the solution $X(r;\epsilon)$. Consider firstly the quantity $\Delta X'$ defined by (6.15) for the graph of the constant function $X = \varphi_1(r) := 1$. Obviously,

$$\Delta X'\big|_{X=\varphi_1(r)} = -1/r < 0, \quad \forall r > 0, \tag{6.16}$$

so all solutions of (6.8) cross the horizontal line $X = 1$ in the downward direction as r increases. (Equivalently, this horizontal line lies above the nullcline $X = X_+(r;\epsilon)$ for all $r > 0$.) Since for small r, the desired solution $X(r;\epsilon)$ certainly lies below this line, we obtain the inequality $X(r;\epsilon) < 1$ for all $r > 0$.

Next, observe that if $\epsilon < \frac{1}{2}A(0)$ we have the inequality $X(r;\epsilon) > r$ for sufficiently small $r > 0$. Computing the quantity $\Delta X'$ from (6.15) for the graph $X = \varphi_2(r) := r$ gives

$$\Delta X'\big|_{X=\varphi_2(r)} = \frac{A(r)}{\epsilon}(1-r^2) - 2. \tag{6.17}$$

Clearly, $\Delta X'|_{X=\varphi_2(r)} > 0$ holds for small $r > 0$ as a consequence of the inequality $\epsilon < \frac{1}{2}A(0)$, however it is equally clear that for $A(r)$ with exponential decay, $\Delta X'|_{X=\varphi_2(r)} < 0$ if r is sufficiently large given $\epsilon > 0$. Let $r_0(\epsilon)$ denote the smallest positive value of r for which

$\Delta X'|_{X=\varphi_2(r)} = 0$. It is easy to see that $r_0(\epsilon) = 1 - \epsilon A(1)^{-1} + o(\epsilon)$ as $\epsilon \to 0$. Therefore, since $X(r;\epsilon) > r$ for small $r > 0$ and since $\Delta X'$ for $X = \varphi_2(r) := r$ is positive for $0 < r < r_0(\epsilon)$, the lower bound $X(r;\epsilon) > r$ persists for all $r \in (0, r_0(\epsilon))$. In particular at $r = r_0(\epsilon)$ we learn that $X(r_0(\epsilon);\epsilon) \geq r_0(\epsilon) = 1 - \epsilon A(1)^{-1} + o(\epsilon)$. Combining this with the uniform upper bound $X(r;\epsilon) < 1$ puts the solution $X(r;\epsilon)$ in an $O(\epsilon)$ neighborhood of the nullcline $X = X_+(r;\epsilon)$ for $r = r_0(\epsilon) \approx 1$.

Now we try to get a lower bound on a larger interval, the length of which grows as $\epsilon \downarrow 0$. For any constant $\delta \in (0,1)$, we consider the horizontal line $X = \varphi_3(r) := 1 - \delta$ and compute $\Delta X'$ from (6.15) for this graph:

$$\Delta X'\big|_{X=\varphi_3(r)} = \frac{A(r)}{\epsilon}(2\delta - \delta^2) - \frac{1-\delta}{r}. \tag{6.18}$$

Since $2\delta - \delta^2 = \delta(1 + (1-\delta)) > 0$ and $A(1) > 0$ we have $\Delta X'|_{X=\varphi_3(r)} > 0$ for $r = r_0(\epsilon)$ and ϵ/δ sufficiently small. Because $rA(r)$ has a single maximum, the equation $\Delta X'|_{X=\varphi_3(r)} = 0$ has two roots when both δ and ϵ/δ are small, obtained from

$$rA(r) = \frac{\epsilon}{\delta} \cdot \frac{1-\delta}{2-\delta}. \tag{6.19}$$

(It is easy to see that these two roots coincide with the intersection points between the horizontal line $X = \varphi_3(r) := 1 - \delta$ and the graph of the nullcline $X = X_+(r;\epsilon)$.) One of the roots obviously satisfies $r = O(\epsilon/\delta)$ and hence is less than $r_0(\epsilon) \approx 1$. The other is large compared to $r_0(\epsilon)$ when ϵ/δ is small. Let us denote it by $r_1(\epsilon,\delta)$. Now, given the bounds on the solution $X(r;\epsilon)$ established so far for $r = r_0(\epsilon)$, the assumption that ϵ/δ is small implies in particular that $X(r_0(\epsilon);\epsilon) > 1 - \delta$, so since graphs of solutions of (6.8) cross the horizontal line $X = \varphi_3(r) := 1 - \delta$ in the upward direction for $r_0(\epsilon) \leq r < r_1(\epsilon,\delta)$, it follows that the lower bound $X(r;\epsilon) \geq 1 - \delta$ holds on the same interval.

To continue the lower bound for $r > r_1(\epsilon,\delta)$, we consider the graph $X = \varphi_4(r) := (1-\delta)r_1(\epsilon,\delta)/r$ and compute $\Delta X'$ for this graph from (6.15):

$$\Delta X'\big|_{X=\varphi_4(r)} = \frac{A(r)}{\epsilon}\left(1 - \frac{(1-\delta)^2 r_1(\epsilon,\delta)^2}{r^2}\right). \tag{6.20}$$

Obviously we have $\Delta X'|_{X=\varphi_4(r)} \geq 0$ for $r \geq r_1(\epsilon,\delta) > (1-\delta)r_1(\epsilon,\delta)$, so solutions of (6.8) cross the graph in the upwards direction provided $r \geq r_1(\epsilon,\delta)$. Moreover, since $X(r;\epsilon) \geq 1 - \delta$ holds at $r = r_1(\epsilon,\delta)$ the graph of the solution $X(r;\epsilon)$ lies above the graph of $X = \varphi_4(r) := (1-\delta)r_1(\epsilon,\delta)/r$ at $r = r_1(\epsilon,\delta)$, and therefore the lower bound $X(r;\epsilon) \geq (1-\delta)r_1(\epsilon,\delta)/r$ holds for all $r \geq r_1(\epsilon,\delta)$.

So far, the only upper bound we have is $X(r;\epsilon) < 1$; however we can obtain an upper bound proportional to r^{-1} for large r by considering the graph of the function

$$X = \varphi_5(r) := \left(r_{\text{Match}}(\epsilon) + \int_{r_{\text{Match}}(\epsilon)}^{r} \frac{sA(s)}{\epsilon}\, \mathrm{d}s \right) \frac{1}{r}. \tag{6.21}$$

Note that $\varphi_5(r_{\text{match}}(\epsilon)) = 1$ and that

$$\varphi_5(r) = \frac{C}{r}(1 + o(1)), \quad r \to \infty, \quad C := r_{\text{Match}}(\epsilon) + \int_{r_{\text{Match}}(\epsilon)}^{\infty} \frac{sA(s)}{\epsilon}\, \mathrm{d}s. \tag{6.22}$$

The $o(1)$ error term depends on ϵ but this dependence is irrelevant for the calculation of the reflection coefficient. Now, we calculate $\Delta X'$ from (6.15) for this graph:

$$\Delta X'\big|_{X=\varphi_5(r)} = -\frac{A(r)}{\epsilon} X(r)^2 < 0, \tag{6.23}$$

so trajectories of the Riccati equation (6.8) cross the graph of $X = \varphi_5(r)$ downwards. Since $X(r_{\text{Match}}(\epsilon);\epsilon) < 1$ and since $\varphi_5(r_{\text{Match}}(\epsilon)) = 1$, it follows that the inequality $X(r;\epsilon) < \varphi_5(r)$ holds for all $r \geq r_{\text{Match}}(\epsilon)$.

To sum up, we have shown that the unique solution $X(r;\epsilon)$ of the Riccati equation (6.8) for which $X(r;\epsilon) \to 0$ as $r \downarrow 0$ satisfies, if $\epsilon > 0$, $\delta > 0$, and ϵ/δ are all sufficiently small, the inequalities:

$$r < X(r;\epsilon) < 1, \quad 0 < r \leq r_0(\epsilon), \tag{6.24}$$

$$1 - \delta < X(r;\epsilon) < 1, \quad r_0(\epsilon) \leq r \leq r_1(\epsilon,\delta), \tag{6.25}$$

$$\frac{(1-\delta)r_1(\epsilon,\delta)}{r} < X(r;\epsilon) < 1, \quad r_1(\epsilon,\delta) \leq r \leq r_{\text{Match}}(\epsilon), \tag{6.26}$$

and finally,

$$\frac{(1-\delta)r_1(\epsilon,\delta)}{r} < X(r;\epsilon) < \left(r_{\text{Match}}(\epsilon) + \int_{r_{\text{Match}}(\epsilon)}^{r} \frac{sA(s)}{\epsilon}\, \mathrm{d}s \right) \frac{1}{r}, \quad r \geq r_{\text{Match}}(\epsilon). \tag{6.27}$$

See Figure 6.4. Setting $\delta = \delta(\epsilon) := 1/\ln(\epsilon^{-1})$, from (6.10) we then obtain the inequalities

$$\underline{R_0^\epsilon} := 2(1-\delta(\epsilon))r_1(\epsilon,\delta(\epsilon)) < R_0^\epsilon(0) < 2r_{\text{Match}}(\epsilon) + 2\int_{r_{\text{Match}}(\epsilon)}^{\infty} \frac{sA(s)}{\epsilon}\, \mathrm{d}s =: \overline{R_0^\epsilon}. \tag{6.28}$$

It remains to prove that the upper and lower bounds $\overline{R_0^\epsilon}$ and $\underline{R_0^\epsilon}$ may both be written in the form $2(b^{-1}\ln(\epsilon^{-1}))^{1/p}(1 + o(1))$ in the limit $\epsilon \downarrow 0$.

First consider the upper bound $\overline{R_0^\epsilon}$. The first term $2r_{\text{Match}}(\epsilon)$ can be found from the loga-

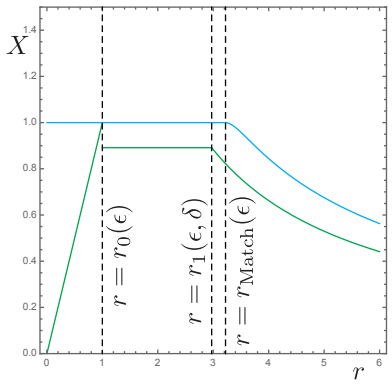

Figure 6.4 – The upper bounds (blue) and lower bounds (green) on the solution $X(r;\epsilon)$ in the case $A(r) = \mathrm{e}^{-r^2}$ for $\epsilon = 10^{-4}$ and $\delta = 1/\ln(\epsilon^{-1})$.

rithm of the defining relation for $r_{\mathrm{Match}}(\epsilon)$:

$$\ln(r_{\mathrm{Match}}(\epsilon)) + \ln(A(r_{\mathrm{Match}}(\epsilon))) = -\ln(\epsilon^{-1}). \tag{6.29}$$

Since $L\mathrm{e}^{-br^p} \leq A(r) \leq U\mathrm{e}^{-br^p}$ implies that $\ln(L) - br^p \leq \ln(A(r)) \leq \ln(U) - br^p$, it follows that for large r, $\ln(A(r)) = -br^p + O(1)$. Therefore,

$$\ln(r_{\mathrm{Match}}(\epsilon)) - br_{\mathrm{Match}}(\epsilon)^p + O(1) = -\ln(\epsilon^{-1}), \tag{6.30}$$

and it is clear that the dominant balance occurs between the terms $-br_{\mathrm{Match}}(\epsilon)^p$ and $-\ln(\epsilon)^{-1}$, showing that $r_{\mathrm{Match}}(\epsilon) = (b^{-1}\ln(\epsilon^{-1}))^{1/p}(1 + o(1))$ as $\epsilon \downarrow 0$. We estimate the (positive) second term in $\overline{R_0^\epsilon}$ as follows:

$$\begin{aligned}\int_{r_{\mathrm{Match}}(\epsilon)}^{\infty} \frac{sA(s)}{\epsilon}\,\mathrm{d}s &= \int_{r_{\mathrm{Match}}(\epsilon)}^{\infty} \frac{sA(s)}{r_{\mathrm{Match}}(\epsilon)A(r_{\mathrm{Match}}(\epsilon))}\,\mathrm{d}s \\ &\leq \frac{U}{L}\int_{r_{\mathrm{Match}}(\epsilon)}^{\infty} \frac{s\mathrm{e}^{-bs^p}}{r_{\mathrm{Match}}(\epsilon)\mathrm{e}^{-br_{\mathrm{Match}}(\epsilon)^p}}\,\mathrm{d}s \\ &= \frac{U}{L} r_{\mathrm{Match}}(\epsilon)\int_1^{\infty} t\mathrm{e}^{-br_{\mathrm{Match}}(\epsilon)^p(t^p-1)}\,\mathrm{d}t.\end{aligned} \tag{6.31}$$

It follows by dominated convergence that this upper bound is $o(r_{\mathrm{Match}}(\epsilon))$ in the limit $r_{\mathrm{Match}}(\epsilon) \uparrow \infty$, or equivalently, as $\epsilon \downarrow 0$. This proves that the upper bound satisfies $\overline{R_0^\epsilon} = 2(b^{-1}\ln(\epsilon^{-1}))^{1/p}(1 + o(1))$ as $\epsilon \downarrow 0$.

For the lower bound $\underline{R_0^\epsilon}$, since $\delta(\epsilon) = (\ln(\epsilon^{-1}))^{-1} \to 0$ as $\epsilon \downarrow 0$, it suffices to prove that $r_1(\epsilon, \delta(\epsilon)) = (b^{-1}\ln(\epsilon^{-1}))^{1/p}(1 + o(1))$ as $\epsilon \downarrow 0$. For this we return to the defining relation

(6.19) for $r_1(\epsilon,\delta)$ and take a logarithm:

$$\ln(r_1(\epsilon,\delta(\epsilon))) + \ln(A(r_1(\epsilon,\delta(\epsilon)))) \\ = \ln(\ln(\epsilon^{-1})) - \ln(\epsilon^{-1}) - \ln(2) + O((\ln(\epsilon^{-1}))^{-1}). \quad (6.32)$$

Again using $\ln(A(r)) = -br^p + O(1)$ as $r \uparrow \infty$, this becomes

$$\ln(r_1(\epsilon,\delta(\epsilon))) - br_1(\epsilon,\delta(\epsilon))^p = \ln(\ln(\epsilon^{-1})) - \ln(\epsilon^{-1}) + O(1). \quad (6.33)$$

As in the asymptotic calculation of $r_{\text{Match}}(\epsilon)$, the dominant balance is between $-br_1(\epsilon,\delta(\epsilon))^p$ and $-\ln(\epsilon^{-1})$ and therefore $r_1(\epsilon,\delta(\epsilon)) = (b^{-1}\ln(\epsilon^{-1}))^{1/p}(1+o(1))$ as $\epsilon \downarrow 0$ as desired. QED

The Gaussian $A(r) = \mathrm{e}^{-r^2}$ satisfies the hypotheses of Theorem 1.2.6 with $L = U = 1$, $b = 1$, and $p = 2$, and we are therefore guaranteed the corresponding relatively accurate approximation $R_0^\epsilon(0) = 2\sqrt{\ln(\epsilon^{-1})}(1+o(1))$ as $\epsilon \downarrow 0$. The upper and lower bounds $\overline{R_0^\epsilon}$ and $\underline{R_0^\epsilon}$ are compared with $2\sqrt{\ln(\epsilon^{-1})}$ and the numerical data for $R_0^\epsilon(0)$ from Figure 1.3 in Figure 6.5. It is worth noting that the decay of the relative error as $\epsilon \downarrow 0$ is extremely slow. Indeed, all

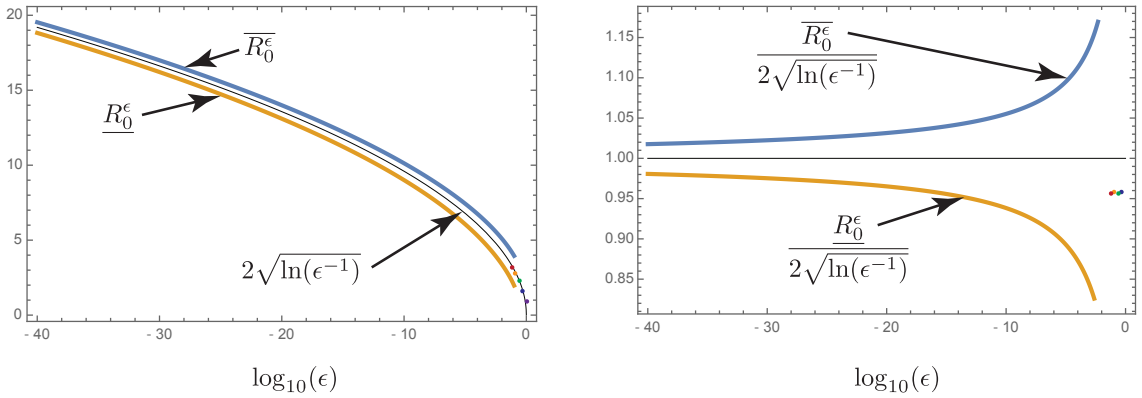

Figure 6.5 – The upper bound $\overline{R_0^\epsilon}$ and lower bound $\underline{R_0^\epsilon}$ for the Gaussian potential $A(r) = \mathrm{e}^{-r^2}$, compared with the approximation $2\sqrt{\ln(\epsilon^{-1})}$ and the numerical data for $R_0^\epsilon(0)$ shown in Figure 1.3 (the points are colored to correspond with the curves in that figure). The left-hand panel illustrates absolute accuracy, while the right-hand panel illustrates relative accuracy.

of the numerical data that we have been able to reliably compute corresponds only to the colored points in the lower right-hand corner of the plot in the left-hand panel of Figure 6.5;

although these points are apparently far from the asymptotic regime of convergence as $\epsilon \downarrow 0$, it is also clear that to the eye *they lie nearly on top of the theoretically-predicted curve*.

6.3 Exact direct scattering for $k = 0$ with $S \equiv 0$ and A being the characteristic function of a disk.

As it is formulated, Theorem 1.2.6 does not apply to compactly-supported potentials. However, the approximate formula (6.14) for $R_0^\epsilon(0)$ can be confirmed by an exact calculation in the case that $A(x, y)$ is proportional to the characteristic function of the disk of radius ρ: $A(r) = A_0\chi_{r<\rho}(r)$. Referring to (6.4), we have

$$\epsilon r \frac{\mathrm{d}w_1}{\mathrm{d}r} = A_0 w_2 \quad \text{and} \quad \epsilon r \frac{\mathrm{d}w_2}{\mathrm{d}r} = A_0 r^2 w_1, \quad 0 < r < \rho \tag{6.34}$$

while $w_j(r) = w_j(\rho)$ for $r \geq \rho$ and $j = 1, 2$. Eliminating w_2 from (6.34) gives

$$\left(r\frac{\mathrm{d}}{\mathrm{d}r}\right)^2 w_1 = \left(\frac{A_0 r}{\epsilon}\right)^2 w_1, \quad 0 < r < \rho. \tag{6.35}$$

With $A_0 r/\epsilon = Z$, this equation becomes

$$\left(Z\frac{\mathrm{d}}{\mathrm{d}Z}\right)^2 w_1 = Z^2 w_1, \quad 0 < Z < \frac{A_0\rho}{\epsilon}. \tag{6.36}$$

Thus w_1 is a solution of the modified Bessel equation of order $\nu = 0$ [11, Chapter 10]. The general solution therefore is $w_1 = c_1 I_0(Z) + c_2 K_0(Z)$. In order that w_1 be bounded at the origin $r = 0$ it is necessary to choose $c_2 = 0$ and then we may (without loss of generality, since only the ratio w_2/w_1 is important for the calculation of $R_0^\epsilon(0)$) take $c_1 = 1$. Thus we have $w_1(r) = I_0(A_0 r/\epsilon)$, and then from the first equation in (6.34) we get

$$w_1(r) = I_0(A_0 r/\epsilon) \quad \text{and} \quad w_2(r) = \frac{\epsilon r}{A_0}\frac{\mathrm{d}w_1}{\mathrm{d}r} = r I_0'(A_0 r/\epsilon), \quad 0 \leq r \leq \rho. \tag{6.37}$$

Then since $w_j(r)$ is independent of r for $r > \rho$, we obtain from (6.6) the exact formula for the reflection coefficient at $k = 0$:

$$R_0^\epsilon(0) = 2\frac{\overline{w_2(\rho)}}{\overline{w_1(\rho)}} = 2\rho\frac{I_0'(A_0\rho/\epsilon)}{I_0(A_0\rho/\epsilon)}. \tag{6.38}$$

According to [11, eqns. 10.40.1 and 10.40.3] (noting that in the notation of that reference $a_0(0) = b_0(0) = 1$), we have $I_0'(Z)/I_0(Z) \to 1$ as $Z \to +\infty$, so it follows that

$$R_0^\epsilon(0) = 2\rho + o(1), \quad \epsilon \downarrow 0, \tag{6.39}$$

which agrees with the formal asymptotic result (6.14) being as $r_{\text{Match}}(\epsilon) = \rho$ by definition in the compact support case.

Chapter 7

Numerical approaches

In this chapter we discuss various numerical approaches to the problems appearing in the semiclassical limit of the defocusing DS-II equation: the solution of the eikonal problem (1.6)–(1.7), the computation of the leading-order normalization function a_0 appearing in (4.13), and the solution of the full ϵ-dependent direct scattering problem (1.3)–(1.4). For the latter we just give a brief review of the approach for Schwartz class potentials in [22].

◁ Remark: In this chapter and the next the notation for Fourier transforms differs slightly from that defined in (5.7). Namely, here the Fourier and inverse Fourier transform operators denoted below as $\mathcal{F}$ and $\mathcal{F}^{-1}$ respectively are scaled by positive constants to be unitary on $L^2(\mathbb{R}^2)$. ▷

For the ease of representation we concentrate on the case $S \equiv 0$. Note, however, that it is straightforward to include a phase function S bounded at infinity in the approaches discussed below. With $S \equiv 0$, the relation $g = f - kz$ (cf., (5.1)) defines a function vanishing at $|z| = \infty$, which is numerically convenient. Using polar coordinates, we thus obtain from (1.6) with $S \equiv 0$ the following partial differential equation for g:

$$g_r^2 + \frac{1}{r^2} g_\phi^2 + 2k\mathrm{e}^{\mathrm{i}\phi} \left(g_r + \frac{\mathrm{i}}{r} g_\phi \right) = A^2. \tag{7.1}$$

This equation will be solved in the whole complex plane with a Fourier spectral method in ϕ and a multidomain spectral method in r. The ensuing system of nonlinear equations will be solved iteratively both with a fixed point method and a Newton iteration. The case of a radially symmetric potential A is solved in addition with a series approach similar to Section 5.1.2.

This chapter is organized as follows: in Section 7.1 we collect some facts about the spectral methods to be used in the following. In Section 7.2 we present two iterative numerical

approaches for the eikonal equation and an additional numerical approach based on Fourier series and adapted to radial potentials $A = A(r)$, and test them against the exact solution obtained in Section 5.1.2 for the case of the Lorentzian profile $A(x, y) = (1 + x^2 + y^2)^{-1}$. In Section 7.2.1, a numerical approach for computing the leading-order normalization function α_0 for a given f is presented and again checked against the corresponding exact solution for the Lorentzian profile. In Section 7.3 we briefly summarize the approach of [22] for the problem (1.3)–(1.4) with a Schwartz class potential.

7.1 Spectral methods

To compute the derivatives in (7.1), we use two different spectral techniques since spectral methods are known for their excellent approximation properties for smooth functions. In the situation that the eikonal equation is uniformly globally elliptic and the solution is regular, this should lead to a very efficient approach.

Since $g(r, \phi)$ is periodic in ϕ, a Fourier spectral method is natural in this context. We write $g(r, \phi) = \sum_{n\in\mathbb{Z}} a_n(r)\mathrm{e}^{\mathrm{i}n\phi}$ and approximate the Fourier series via a discrete Fourier transform, see for instance [39] and references therein, i.e., for even N

$$g(r, \phi) \approx \sum_{n=-N/2+1}^{N/2} a_n(r)\mathrm{e}^{\mathrm{i}n\phi}, \quad g_\phi(r, \phi) \approx \sum_{n=-N/2+1}^{N/2} \mathrm{i}n a_n(r)\mathrm{e}^{\mathrm{i}n\phi}; \tag{7.2}$$

and hence the derivative of $g(r, \phi)$ with respect to ϕ is approximated via the derivative of the sum approximating $g(r, \phi)$. Note that the *Nyquist mode* $a_{N/2}(r)$ has to be put equal to zero in the approximation of g_ϕ, see [39]. The discrete Fourier transform is computed efficiently via a Fast Fourier Transform (FFT). The numerical error in approximating the Fourier series with a truncated sum is of the order of the first neglected Fourier coefficient. Thus it decreases exponentially with N for analytic functions, indicating the *spectral convergence* of the method.

In order to obtain a spectral approach also in r, we consider two domains, I: $r \in [0, 1]$ and II: $s = 1/r \in [0, 1]$ similar to [8] and references therein. In the coordinate s equation (7.1) reads

$$s^4 g_s^2 + s^2 g_\phi^2 + 2k\mathrm{e}^{\mathrm{i}\phi}\left(-s^2 g_s + \mathrm{i}s g_\phi\right) = A^2. \tag{7.3}$$

It is assumed that A vanishes as $s \to 0$ at least as fast as s. Thus we can solve (7.3) after division by s^2. Note that equation (7.3) is singular for $s = 0$ whereas equation (7.1) is singular for $r = 0$.

In both domains I and II we approximate the functions $a_n(r)$ (respectively $a_n(s)$; in an abuse of notation, we use the same symbol in both cases), $n = -N/2 + 1, \ldots, N/2$ via a sum

of Chebychev polynomials. We only outline the approach for domain I, it is completely analogous for domain II. The idea of a *Chebychev collocation method* is to introduce the collocation points $l_j = \cos(\pi j/N_c)$, $j = 0, 1, \ldots, N_c$ and to approximate a function $F(l)$, $l \in [-1, 1]$ via the sum

$$F(l) \approx \sum_{m=0}^{N_c} b_m T_m(l), \tag{7.4}$$

where $T_m(l) = \cos(m \arccos(l))$ are the Chebychev polynomials [11, §18.3]. The *spectral coefficients* b_m, $m = 0, \ldots, N_c$ are determined by the relations following from imposing (7.4) as an equality at the collocation points,

$$F(l_j) = \sum_{m=0}^{N_c} b_m T_m(l_j) \quad j = 0, \ldots, N_c. \tag{7.5}$$

They can be determined conveniently via a *Fast Cosine Transform* (FCT) which can be computed via the FFT, see [39]. The numerical error in approximating a function via a truncated Chebychev series is as in the case of discrete Fourier series: it decreases exponentially with N_c for analytic functions making this again a spectral method.

It is well known that the derivative of a Chebychev polynomial can be expressed itself in terms of Chebychev polynomials. The basis for this is the identity

$$\frac{T'_{m+1}(l)}{m+1} - \frac{T'_{m-1}(l)}{m-1} = 2T_m(l), \quad m = 2, 3, \ldots \tag{7.6}$$

and $T'_1(l) = T_0(l)$, $T'_0(l) = 0$. The action of a derivative on a Chebychev sum (7.4) can thus be expressed in terms of the action of a differentiation matrix $\mathbf{D}$ on the vector of spectral coefficients b_m, $m = 0, \ldots, N_c$.

In a similar way the multiplication of a function with l can be expressed in terms of the action of a matrix on the vector of spectral coefficients. The approach, see for instance [8, 19], is based on the well known recurrence formula for Chebyshev polynomials,

$$T_{m+1}(l) + T_{m-1}(l) = 2lT_m(l), \quad n = 1, 2, \ldots \tag{7.7}$$

This identity allows multiplication and division in coefficient space by $l \pm 1$. We define for given Chebyshev coefficients b_m coefficients $\tilde{b}_m$ via $\sum_{m=0}^{\infty} \tilde{b}_m T_m(l) := \sum_{m=0}^{\infty} (l \pm 1) b_m T_m(l)$.

We put $r = (1 + l)/2$ in domain I. The coefficients $a_n(r)$, $n = -N/2 + 1, \ldots, N/2$ are thus approximated via the sum $a_n \approx \sum_{m=0}^{N_c} a_{nm} T_m(l)$. The action of the derivative with respect to r is therefore approximated by the action of a matrix $\mathbf{D}$ following from (7.6) on the spectral coefficients, and similarly the action of division by r becomes the action of a matrix

R following from (7.7) on the coefficients. Thus we approximate the derivatives via

$$g_r \pm \frac{\mathrm{i}}{r} g_\phi \approx \sum_{n=-N/2+1}^{N/2} \sum_{m=0}^{N_c} \left(\sum_{j=0}^{N_c} (D_{mj} \mp n R_{mj}) a_{nj} \right). \tag{7.8}$$

The same technique is used in domain II with $s = (1+l)/2$. The solutions obtained in domain I and II have to be matched for $r = s = 1$ to be continuous. As in [8], this is done with Lanczos' tau method [25]: one of the equations for each n following from using the discretization (7.8) in (7.1) is replaced by the condition that $a_n(r = 1) = a_n(s = 1)$, $n = -N/2+1, \ldots, N/2$. More concretely we replace for $n < 0$ the equations corresponding to $m = N_c$ in domain I, and for $n > 0$ the equations corresponding to $m = N_c$ in domain II. In addition the Nyquist mode is put equal to zero.

7.2 Numerical approaches for the eikonal problem

We now discuss two different numerical approaches for the eikonal problem (1.6)–(1.7), each of which produces an approximation to the function $g = f - kz$ that solves (7.1) and satisfies $g \to 0$ as $|z| \to \infty$.

Iterative methods for the discretized eikonal equation

The spectral discretization described in Section 7.1 leads to an approximation of (7.1) in terms of a $(2N_c + 2)N$-dimensional nonlinear system of equations. This system will be solved iteratively.

A first approach is based on a fixed-point iteration. We write for $|k| > 1/2$ the system corresponding to (7.1) in the form

$$\sum_{j=0}^{N_c} (D_{mj} \mp n R_{mj}) a_{nj} = G(\{a_{nm}\}), \tag{7.9}$$

where

$$\begin{aligned} G(\{a_{nm}\}) := \frac{1}{2k} \mathbb{F} \Bigg(A^2 - \sum_{n=-N/2+1}^{N/2} \sum_{m=0}^{N_c} \left(\sum_{j=0}^{N_c} (D_{mj} + n R_{mj}) a_{nj} \right) \times \\ \sum_{n=-N/2+1}^{N/2} \sum_{m=0}^{N_c} \left(\sum_{j=0}^{N_c} (D_{mj} - n R_{mj}) a_{nj} \right) \Bigg), \end{aligned} \tag{7.10}$$

where $\mathbb{F}$ denotes the combined action of the FFT and the FCT on the angular and radial

variables respectively. Since both FFT and FCT are fast, it is convenient when possible to switch between physical space and the space of spectral coefficients in order to compute products instead of convolutions in coefficient space.

We first solve (7.9) by expressing it in the form of a fixed-point iteration: $\sum_{j=0}^{N_c}(D_{mj} - nR_{mj})a_{nj}^{K+1} = G(\{a_{nm}^K\})$. Here we choose as the initial iterate the solution of the $\bar{\partial}$-problem $\sum_{j=0}^{N_c}(D_{mj} \mp nR_{mj})a_{nj}^0 = \mathbb{F}[e^{-i\phi}A^2/(2k)]$. Numerical resolution in each domain is controlled via the decrease of the spectral coefficients with N and N_c. As discussed for the examples below, numerical resolution is ideal if the coefficients decrease to the order of machine precision both in the Fourier and Chebyshev dependence. If $|k|$ is large enough, the fixed-point iteration converges linearly, i.e., $\|a_{nm}^{K+1} - a_{nm}^K\|_\infty = O(K^{-1})$, as might be expected.

Alternatively we can use a Newton iteration. To this end we write the equation following from (7.1) after the spectral discretization described in Section 7.1 in the form $F(\{a_{nm}\}) = 0$ and solve it with a standard Newton iteration:

$$a_{nm}^{K+1} = a_{nm}^K - \mathrm{Jac}(F(\{a_{nm}^K\}))^{-1}F(\{a_{nm}^K\}); \tag{7.11}$$

here the tau method is applied in the inversion of the Jacobian, the action of which is computed as a convolution in the space of coefficients. Using again the solution of the $\bar{\partial}$-problem $\sum_{j=0}^{N_c}(D_{mj} - nR_{mj})a_{nj}^0 = \mathbb{F}[e^{-i\phi}A^2/(2k)]$ for $|k| > 1/2$ as the initial iterate, we observe the expected quadratic convergence typical for Newton's method, i.e., $\|a_{nm}^{K+1} - a_{nm}^K\|_\infty = O(K^{-2})$. The disadvantage of the approach is that the Jacobian is a $(2N_c+2)N \times (2N_c+2)N$ matrix, but the quadratic convergence implies that the iteration takes roughly the same amount of time as the fixed-point iteration to reach a residual of 10^{-10} which is generally where iterations are stopped.

A Fourier series method for the radially symmetric case

In the radially symmetric case $A = A(r)$, we can proceed as in Section 5.1.2 and solve for a series in $e^{i\phi}$: writing [1]

$$g(r,\phi) = \sum_{n=0}^{\infty} \frac{c_n(r)}{(2k)^{2n+1}} e^{-i(2n+1)\phi}, \tag{7.12}$$

where $c_n = c_n(r)$, we find from (7.1) that

$$c_0' + \frac{1}{r}c_0 = A(r)^2, \tag{7.13}$$

1. The fact that only negative odd harmonics appear in (7.12) is a consequence of the form of the coefficients f_n in the series approach for radial potentials with $S(x,y) \equiv 0$ described in Section 5.1.2. Comparing with (5.36) for $\delta = \frac{1}{4}$ and (5.56) we see that in the notation of Section 5.1.2, $c_n(r) = G_{n+1}(r^2)/[2(2n+1)r^{2n+1}]$.

and for $n > 0$,

$$c_n' + \frac{2n+1}{r} c_n = \sum_{j=0}^{n-1} \left(1 - \frac{2j+1}{r}\right) \left(1 + \frac{2(n-j-1)+1}{r}\right) c_j c_{n-j-1}, \tag{7.14}$$

where the prime denotes differentiation with respect to r, and it is required that $c_n(r) \to 0$ as $r \to \infty$ for all $n \geq 0$. Equations (7.13) and (7.14) are solved again with the Chebychev collocation method described above. As noted in Section 5.1.2, the series (7.12) is a power series in odd negative powers of k and hence for given $(x, y) \in \mathbb{R}^2$ will converge if $|k|$ is large enough. For smaller $|k|$, it can only converge if the c_n decrease rapidly enough as $n \to \infty$. In applications only convergent cases are interesting where the series can be effectively truncated for some $n = N_\phi$. In this case a coupled system of N_ϕ ordinary differential equations of the form (7.13) and (7.14) has to be solved with zero initial conditions at $r = \infty$. *On the other hand, the numerical computation of the $L^\infty(\mathbb{R}_+)$-norms of $c_n(\cdot)$ and their analysis for increasing n allows one to make a good prediction of the critical radius $|k|$ above which one has a global smooth solution of the eikonal problem and below which the latter solution necessarily develops singularities analogous to turning points in the one-dimensional problem.*

Comparison with the exact solution for the Lorentzian profile

Note that the numerical approaches for the eikonal equation presented above are essentially independent and can be thus used as mutual tests. To illustrate how the codes work in practice and to establish which accuracies can be expected, we test them for the example of the exact solution (1.12) for a Lorentzian amplitude $A(x, y) = (1 + x^2 + y^2)^{-1}$. To compare with the numerics, we get $g(x, y; k)$ from (1.12) simply by omitting the term kz on the right-hand side. Since W is invariant under $z \mapsto 1/\bar{z}$, the exact solution g is symmetric with respect to reflection through the unit circle in the z-plane. As described in Section 5.1.2, g is smooth provided $|k| > 1/2$. We first plot the exact solution for $k = 1$ in Figure 7.1.

For the iterative solution of this problem, we use $N_c = 32$ Chebychev polynomials and $N = 50$ Fourier modes. It can be seen in the left-hand panel of Figure 7.2 that the coefficients a_{nm} decrease exponentially in (n, m) and that they reach machine precision well before the boundary of the spectral domain. This indicates that the solution is numerically resolved. The fixed-point iteration is stopped for this case when the difference between consecutive iterates is less than a given threshold, $\|a_{nm}^{K+1} - a_{nm}^K\|_\infty < 10^{-10}$. This is achieved in this example in 10 iterations of the fixed-point method. The difference between the numerical result and the exact solution is shown in the right-hand panel of Figure 7.2. It can be seen that the numerical error is largest near the origin and that it is of the order of 10^{-11}. Note that

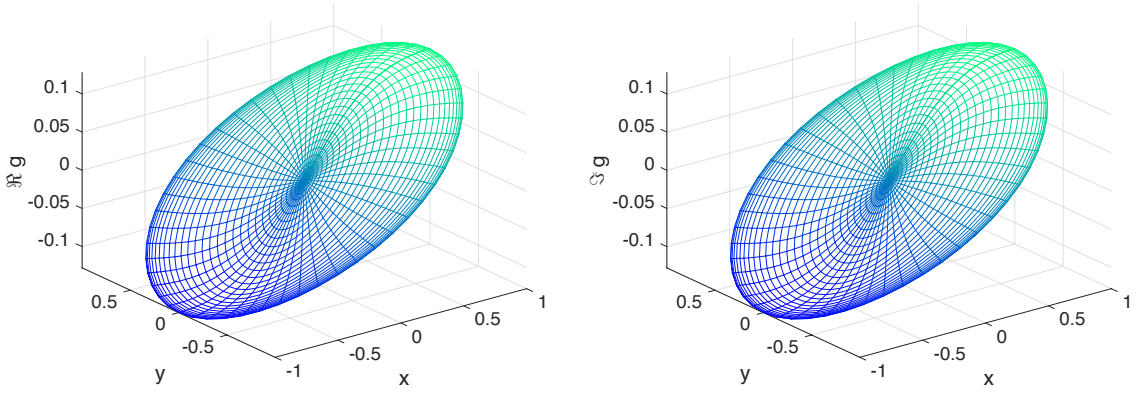

Figure 7.1 – The exact solution $g(x,y;k) = f(x,y;k) - kz$ for the Lorentzian potential $A(x,y) = (1+x^2+y^2)^{-1}$ and $S(x,y) \equiv 0$ for $k = 1$. Left: $\mathrm{Re}(g(x,y;1))$. Right: $\mathrm{Im}(g(x,y;1))$. By exact reflection symmetry through the unit circle, we only show it for $r \leq 1$.

this error is not affected if the iteration is stopped at a smaller threshold; it is due to the large condition numbers of the differentiation matrices which are for Chebychev differentiation of the order N_c^2, see e.g., the discussion in [39]. Thus the maximally achievable accuracy is of the order 10^{-11} with this approach for this example. If the problem required a higher numerical resolution (a larger N_c), the maximally achievable accuracy would be slightly lower. This problem can be addressed by introducing more than two domains in the r variable, but this will not be needed for the examples studied here.

Note that the fixed-point code finds the symmetry of the solution with respect to $r \to 1/r$ with the same accuracy, i.e., the same difference between numerical and exact solution will be found for $r > 1$. Therefore we do not show the solution for $r > 1$ in this case though it is obtained with a precision of the order of 10^{-11} in the whole complex plane.

The Newton iteration converges in this case after 3 iterations to the same precision. In practice it takes longer than the fixed-point iteration since the computation of the convolutions and the inversion of the Jacobian are computationally expensive. Krylov subspace techniques might be helpful in this context, but have not been explored so far.

As the Lorentzian $A(x,y) = (1+x^2+y^2)^{-1}$ is radially symmetric, the numerical series approach described in Section 7.2 also applies, and we use the same discretization resolution parameters as in the iterative approaches, namely $N_c = 32$ and $N = 50$ (recall that only odd powers of $\mathrm{e}^{-\mathrm{i}\phi}$ appear in this approach). The difference between numerical and exact solution in this case is of the order of 10^{-14}, mainly near the origin as can be seen in the left-hand panel of Figure 7.3. The reason for a smaller error in this case is that only ordinary differential

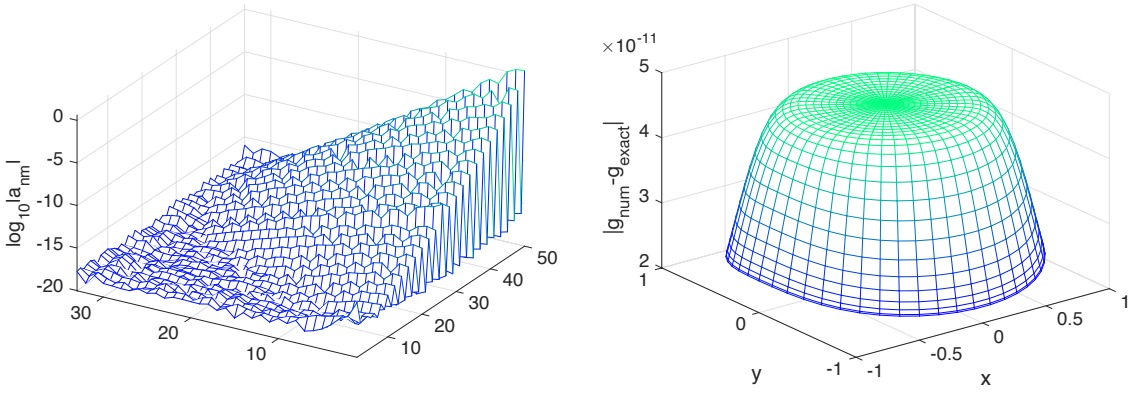

Figure 7.2 – Chebychev and Fourier coefficients of the fixed-point approximation of the solution in Figure 7.1 plotted over the (n, m)-grid on the left, and the difference of the numerical solution and the exact solution on the right.

equations have to be solved as the effect of the Fourier discretization of ϕ is essentially decoupled. Since there is no iteration, this method is also the fastest of the three discussed here. The L^∞ norm of the functions c_n decreases as $n^{-5/2}$ as expected by the formulae (5.67) and (5.68) (also noting that $|z|/(1+|z|^2) \leq \frac{1}{2}$). Note that the finite precision employed delimits the number of coefficients c_n which can be used in practice.

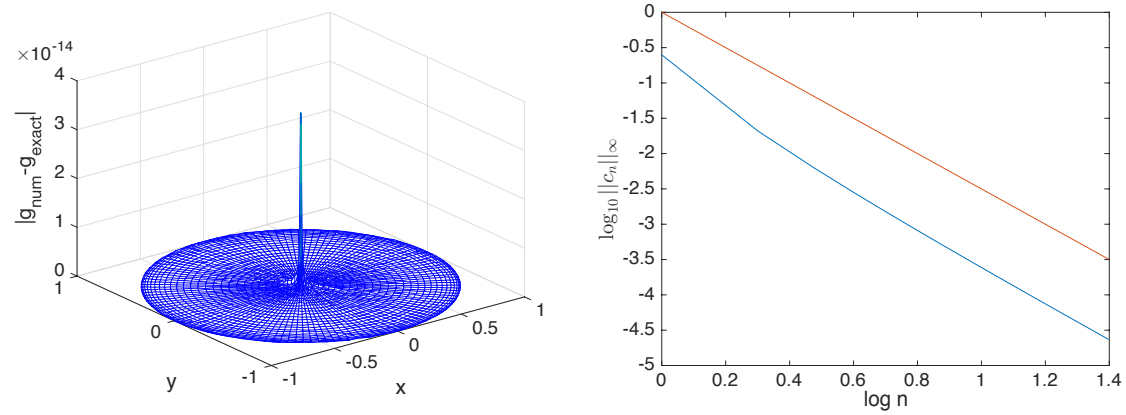

Figure 7.3 – Left: the difference between the exact solution $g(x, y; k)$ for the case of the Lorentzian amplitude $A(x, y) = (1 + x^2 + y^2)^{-1}$ with $S(x, y) \equiv 0$ and the numerical solution constructed with the series approach described in Section 7.2 for $k = 1$. Right: the L^∞ norm of the coefficients $c_n(\cdot)$ in a log-log plot in blue (for reference the red line has slope $-5/2$).

The series approach also makes clear which problems are to be expected for smaller k.

As k decreases toward the critical value of $1/2$, more and more terms in the series (7.12) will be needed to obtain the same accuracy, and for even smaller values of k the series fails to converge (the continuation of the exact solution, however, will be bounded with jump discontinuities along some branch cuts as shown in Figure 1.2). For $k = 0.6$, we thus need a considerably higher resolution in ϕ as can be seen in Figure 7.4 where we use $N_c = 40$ and $N = 140$. The decrease of the Fourier modes is visibly much slower than before. The fixed-point iteration converges after 22 iterations, and the difference to the exact solution is of the order of 10^{-10} (this time it is largest near the rim of the disk). The Newton iteration converges in just 4 iterations, but becomes too slow at these parameters in comparison to the fixed-point iteration. Using the same parameters for the series approach based on (7.12), we get as before a difference of the order of 10^{-14} between the numerical and exact solutions.

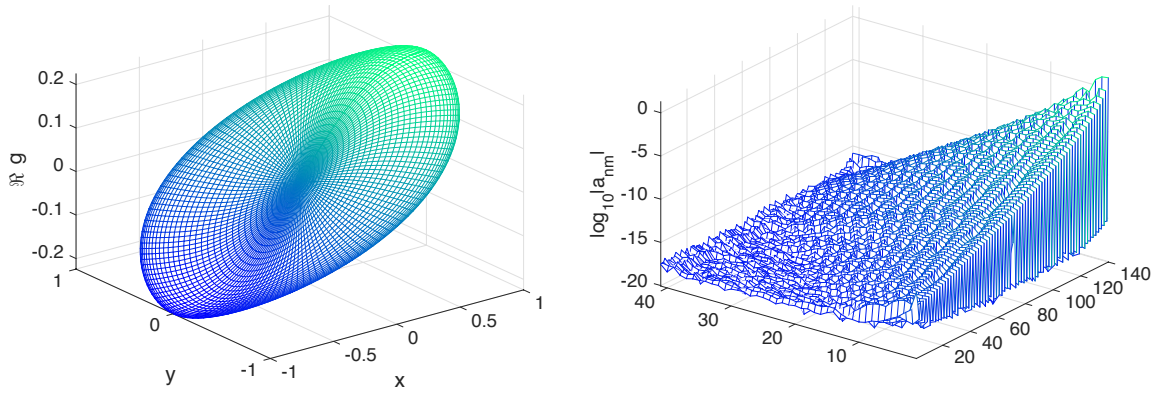

Figure 7.4 – Left: $\mathrm{Re}(g(x,y;k))$ at $k = 0.6$ for the case of the exact solution corresponding to the Lorentzian amplitude $A(x,y) = (1+x^2+y^2)^{-1}$ and $S(x,y) \equiv 0$. Right: the corresponding numerically-computed Fourier and Chebychev coefficients plotted over the (n,m)-grid.

◁ Remark: Since the equations (7.10) and (7.11) are nonlinear, *aliasing errors*, see e.g., [39], can play a role in this context due to the use of truncated series in the computation of products. To address this we use a filtering in coefficient space: if the iteration is stopped at a given level `tol` (typically 10^{-10}), all spectral coefficients with $|a_{nm} < \texttt{tol}|$ are put equal to zero. ▷

Summing up, for radially symmetric potentials A, the series approach described in Section 7.2 is the most efficient of the ones presented here. If sufficient numerical resolution is provided, which can be controlled via the decrease of the $c_n(r)$ in n and of their Chebychev coefficients, an accuracy of the order of 10^{-14} can be reached. We note that for potentials without radial symmetry, the series method is inapplicable but the fixed-point iteration method remains as an efficient option.

7.2.1 Numerical computation of the leading-order normalization function α_0

Once the eikonal problem is solved for $f(x, y; k)$, the corresponding function α_0 has to be determined in order to complete the construction of the leading term in the WKB expansion of the solution of the direct scattering problem. In the case $S \equiv 0$, α_0 is the solution of the linear equation (5.74) that satisfies $\alpha_0 \to 1$ as $|z| \to \infty$. In polar coordinates, this equation reads

$$\begin{aligned} &2\left((\mathrm{e}^{-\mathrm{i}\phi}g_r + k)\alpha_{0r} + \frac{1}{r}\left(\mathrm{e}^{-\mathrm{i}\phi}\frac{g_\phi}{r} + \mathrm{i}k\right)\alpha_{0\phi}\right) \\ &+ \left[\left(g_{rr} + \frac{1}{r}g_r + \frac{1}{r^2}g_{\phi\phi}\right) + \left(g_r + \frac{\mathrm{i}}{r}g_\phi\right)\left((\ln A)_r - \frac{\mathrm{i}}{r}(\ln A)_\phi\right)\right]\mathrm{e}^{-\mathrm{i}\phi}\alpha_0 = 0. \end{aligned} \tag{7.15}$$

This equation is treated numerically in a similar way as was the eikonal problem in Section 7.2 which allows the use of the same numerical grid. The derivatives of both the potential A and the function g are computed as described in Section 7.1 with spectral methods in the two radial domains that meet at the unit circle.

◁ Remark: The derivatives of the solution f in (7.15) contain divisions by r. As can be checked for the exact solution (1.12) in the case of the Lorentzian potential A the terms divided by r appearing in the action of the Laplacian on f do not all vanish for $r = 0$. This implies that analytically unbounded terms cancel which is numerically challenging even for a spectral method to resolve. Thus a loss in accuracy near $r = 0$ is to be expected in the computation of α_0 via (7.15). ▷

The numerical solution of (7.15) with $\alpha_0 \to 1$ as $|z| \to \infty$ in the case $A(x, y) = 1/(1 + x^2 + y^2)$ and $S \equiv 0$ is shown for $r < 1$ in the left-hand panel of Figure 7.5 (note that the corresponding exact solution (1.13) is symmetric under the reflection mapping $r \mapsto 1/r$). The right-hand panel of the same figure shows a plot of the corresponding spectral coefficients. It can be seen that the solution is well resolved for $N_r = N_\phi = 64$. The divisions by r in the expressions in (7.15) lead, however, to a saturation level for the coefficients of the order of 10^{-10}. Loosely speaking this is the level of the numerical error.

The expected accuracy is thus of the order of 10^{-10}, and that this is indeed the case can be seen in Figure 7.6 where the difference between the numerical and the exact solution (1.13) is shown for $r < 1$ on the left and for $r > 1$ on the right. It appears that the largest errors occur for $r = 0$. For other values of the radius, the numerical error is of the order 10^{-11}. This shows that the solution of (7.15) can be obtained with high accuracy on the whole complex plane.

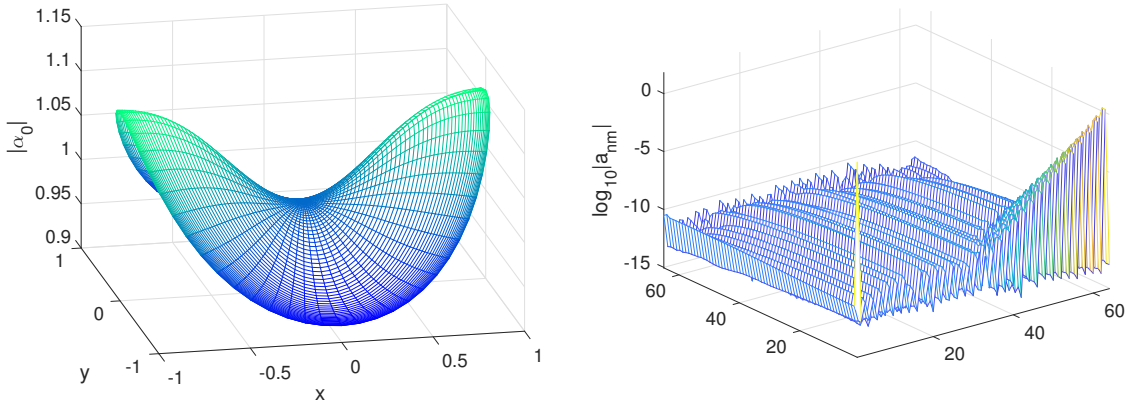

Figure 7.5 – Left: the numerical solution to the equation (7.15) with $\alpha_0 \to 1$ as $|z| \to \infty$ for the Lorentzian potential $A(r) = 1/(1+r^2)$ at $k = 1$. Right: the modulus of the spectral coefficients in a logarithmic plot over the (n, m)-grid.

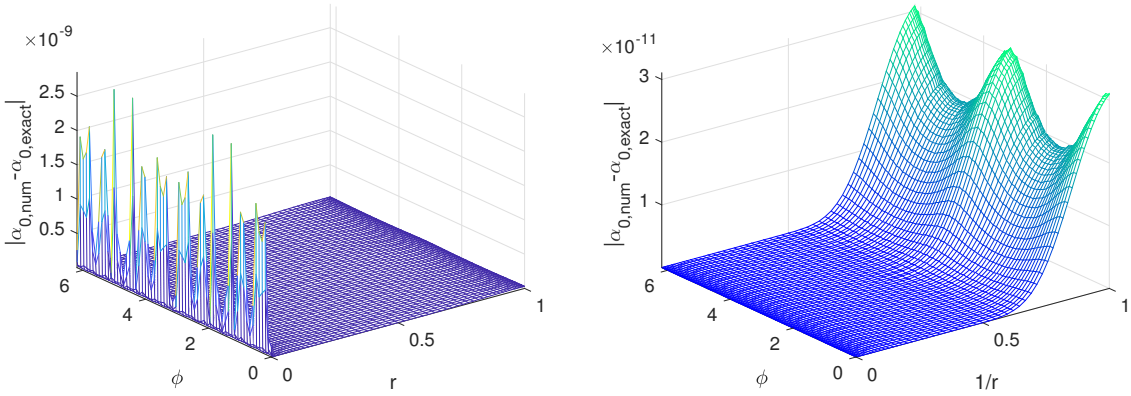

Figure 7.6 – Difference between the numerical solution to the equation (7.15) for the Lorentzian potential $A = 1/(1+r^2)$ and the exact solution (1.13) on the numerical grid. Left: $r < 1$. Right: $r > 1$.

7.3 A spectral method for the ϵ-dependent direct scattering problem for Schwartz class potentials

A spectral approach to solve the $\bar{\partial}$-problem for potentials in the Schwartz class was developed by Klein and McLaughlin in [22]. We briefly summarize the approach here; the reader is referred to [22] for details.

The idea is to introduce the functions

$$m^{\pm}(z;k) = \mathrm{e}^{-kz/\epsilon}\left(\psi_1(z;k) \pm \overline{\psi_2(z;k)}\right) - 1, \tag{7.16}$$

satisfying the boundary conditions $\lim_{z\to\infty} m^{\pm}(z;k) = 0$. In these variables, the system (1.3) becomes diagonal and takes the form

$$\bar{\partial} m^{\pm} = \pm\frac{q}{2\epsilon}\mathrm{e}^{(\overline{kz}-kz)/\epsilon}\cdot(\overline{m^{\pm}}+1). \tag{7.17}$$

We write both of these equations in the common form

$$\bar{\partial} m = \frac{Q}{2\epsilon}\mathrm{e}^{(\overline{kz}-kz)/\epsilon}\cdot(\overline{m}+1) \tag{7.18}$$

where $m = m^{\pm}$ and $Q = \pm q$. Since under the Fourier transform $\mathcal{F}$ (cf., (5.7), here scaled to be $L^2(\mathbb{R}^2)$-unitary) we have $\mathcal{F}\{\bar{\partial} m\} = \frac{1}{2}\mathrm{i}(\xi_x + \mathrm{i}\xi_y)\mathcal{F}\{m\} = \frac{1}{2}\mathrm{i}\xi\mathcal{F}\{m\}$ for $\xi = \xi_x + \mathrm{i}\xi_y$ the dual Fourier variable to $z = x + \mathrm{i}y$, in the Fourier domain the system (7.18) becomes

$$S(\xi) = -\mathrm{i}\mathcal{F}\left\{\frac{Q}{\epsilon}\mathrm{e}^{(\overline{kz}-kz)/\epsilon}\cdot\overline{\mathcal{F}^{-1}\left\{\frac{1}{\bar{\xi}}S(\xi)\right\}}\right\} - \mathrm{i}\mathcal{F}\left\{\frac{Q}{\epsilon}\mathrm{e}^{(\overline{kz}-kz)/\epsilon}\right\} \tag{7.19}$$

where $S := \xi\mathcal{F}\{m\} = -2\mathrm{i}\mathcal{F}\{\bar{\partial} m\}$.

In the numerical approach [22] the Fourier transforms in (7.19) are approximated by discrete Fourier transforms computed by a two-dimensional FFT. The integrand in (7.19) is regularized in the form

$$\mathcal{F}^{-1}\left\{\frac{1}{\bar{\xi}}S(\xi)\right\} = \mathcal{F}^{-1}\left\{\frac{1}{\bar{\xi}}\left(S(\xi) - G(\xi)\right)\right\} + \mathcal{F}^{-1}\left\{\frac{1}{\bar{\xi}}G(\xi)\right\}, \tag{7.20}$$

where $G(\xi)$ is chosen such that $(S(\xi) - G(\xi))/\xi$ is regular to machine precision (as indicated by the fact that the Fourier coefficients decrease exponentially to the order of the roundoff error), and also such that $\mathcal{F}^{-1}\{G(\xi)/\xi\}$ can be computed explicitly. A useful choice for G is

$$G(\xi) = \mathrm{e}^{-|\xi|^2}\sum_{n=0}^{M}\frac{\bar{\partial}_{\xi}^{n}S(0)}{n!}\bar{\xi}^{n}, \quad \bar{\partial}_{\xi} := \frac{1}{2}\left(\frac{\partial}{\partial\xi_x} + \mathrm{i}\frac{\partial}{\partial\xi_y}\right), \tag{7.21}$$

since it cancels the most offending terms in S near the origin, while $\mathcal{F}^{-1}\{G(\xi)/\xi\}$ can be

calculated with the help of the identity

$$\mathcal{F}^{-1}\left\{\frac{\overline{\xi}^n}{\xi}\mathrm{e}^{-|\xi|^2}\right\} = \mathrm{i}(2\mathrm{i})^n\frac{n!}{z^{n+1}}\left[1-\mathrm{e}^{-|z|^2/4}\sum_{k=0}^{n}\frac{1}{k!}\left(\frac{|z|^2}{4}\right)^k\right]. \tag{7.22}$$

The factor $e^{(\overline{k}z-k\overline{z})/\epsilon}$ appearing in (7.19) leads to a shift in Fourier space of the Fourier transform of a function multiplied by it. Indeed, if we introduce the shift operator $\mathcal{S}_{k/\epsilon}$ whose action on a function f of ξ is given by $\mathcal{S}_{k/\epsilon}f(\xi) := f(\xi + 2\mathrm{i}\overline{k}/\epsilon)$, then (7.19) can be recast in the form

$$S(\xi) = \mathcal{S}_{k/\epsilon}\circ\mathcal{K}_0 S(\xi) + \mathcal{S}_{k/\epsilon}F(\xi), \tag{7.23}$$

where the operator $\mathcal{K}_0$ and forcing function F are independent of k:

$$\mathcal{K}_0 S(\xi) := -\mathrm{i}\mathcal{F}\left\{\frac{Q}{\epsilon}\cdot\overline{\mathcal{F}^{-1}\left\{\frac{1}{\xi}S(\xi)\right\}}\right\} \quad \text{and} \quad F(\xi) := -\mathrm{i}\mathcal{F}\left\{\frac{Q}{\epsilon}\right\}. \tag{7.24}$$

As discussed in detail in [22], for larger values of $|k|/\epsilon$ the effect of the shift is that the benefit of the regularization procedure (7.20) is diminished because it is effectively removing a singularity that is not present at all since the shifted transform is large near the boundary of the (spectral) computational domain but vanishes to machine precision near the origin $\xi = 0$.

To address this problem, the equation (7.23) may be replaced by a system of equations for two functions, f and h:

$$\begin{aligned} h &= \mathcal{K}_0 f + F \\ f &= \mathcal{S}_{k/\epsilon}\circ\mathcal{K}_0\circ\mathcal{S}_{k/\epsilon}h. \end{aligned} \tag{7.25}$$

It is a direct matter to check that if (f, h) solves (7.25), then $S = f + \mathcal{S}_{k/\epsilon}h$ solves (7.23). However, since it turns out that for large $|k|/\epsilon$ both functions f and h are small near the boundary of the spectral computational domain, the system (7.25) is better suited to regularization via (7.20) than is (7.23) itself. Moreover, to recover the reflection coefficient, the function f is not needed, and it can therefore be explicitly eliminated from the first equation of (7.25) using the second equation, leading to a closed equation for a single function h. See [22, Section 5.2] for details.

Numerically this integral equation is solved by standard discretization amenable to the two-dimensional FFT. The resulting system of algebraic equations is not complex linear in h due to the complex conjugation present in the operator $\mathcal{K}_0$, but rather real linear in its real and imaginary parts. This linear system is solved with GMRES [35], a Krylov subspace

approach that is especially useful in our setting because it avoids the necessity of storage of the coefficient matrix. As discussed in [22], the numerical error in the solution is of the order of the Fourier coefficients of the largest values of ξ carried in the computation.

Recall that $S = -2i\mathcal{F}\{\bar{\partial}m\}$, so that once S is found, $\bar{\partial}m$ is available via the (spectrally-accurate) FFT. As discussed in [22], knowledge of $\bar{\partial}m^{\pm}$ is sufficient to compute the reflection coefficient. In order to obtain $m^{\pm}$, as will be needed to compare numerical solutions with the WKB approximations introduced in Section 8.2, we invert $\bar{\partial}$ in the Fourier domain for $S = f + \mathcal{S}_{k/\epsilon}h$ via division by ξ and using again the regularization procedure (7.20) with a shift in the Fourier domain for the second term in the expression for S for $k \neq 0$. It is important to realize that the quantities $m^{\pm}$ decrease only as $1/|z|$ for $z \to \infty$ and are thus not themselves suitable for a Fourier spectral approach (the periodically continued functions would not be differentiable at the computational boundary), but that the function $(S(\xi) - G(\xi))/\xi$ is in the Schwartz class. For the latter term, Fourier spectral methods on a sufficiently large computational domain are very efficient and show spectral convergence, which is controlled as always by the decay of the modulus of the Fourier coefficients at the boundaries of the computational domain in Fourier space.

As an example of the result of a computation using this numerical approach, we show the solutions to the Dirac system (1.3) obtained with a Gaussian potential $A(x,y) = \mathrm{e}^{-(x^2+y^2)}$ and $S(x,y) \equiv 0$ for $k = 0$ and $\epsilon = 1$ in Figure 7.7. The function ψ_1 has minimal modulus at the origin and tends to 1 at infinity, whereas the function ψ_2 vanishes at the origin and decreases slowly to 0 as $z \to \infty$.

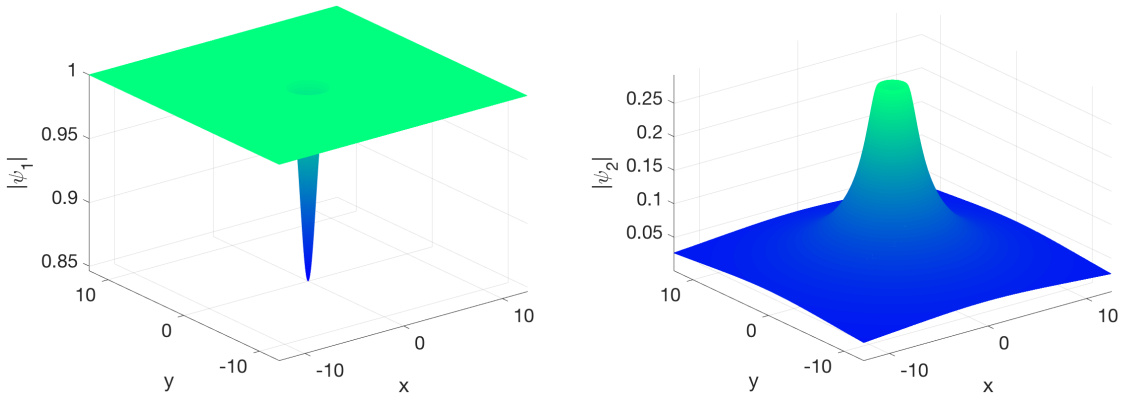

Figure 7.7 – Numerical solution to the Dirac system (1.3)–(1.4) with a Gaussian potential for $k = 0$ and $\epsilon = 1$. Left: modulus of ψ_1. Right: modulus of ψ_2.

Chapter 8

Numerical examples

In this chapter we test the conjectures formulated in the previous chapters for several examples with and without radial symmetry. We first address the case of a Gaussian potential for various values of ϵ and compare the solution to the Dirac system (1.3) for sufficiently large k to the leading order semiclassical solution built from the solution to the eikonal problem. A similar study is presented for a non-radially symmetric potential in the Schwartz class.

8.1 Gaussian potential

As a first computational example outside the realm of potentials $A(x, y)$ for which the eikonal problem (1.6)–(1.7) has a known solution, we consider here the Gaussian

$$A(x, y) = A(r) = \mathrm{e}^{-r^2} \tag{8.1}$$

as a canonical example of a smooth, rapidly decaying, and radially-symmetric potential. Since the reflection coefficient is a function of $|k|$ only for radial potentials such as (8.1), we will here restrict attention to real positive k.

Firstly, we numerically solve the eikonal problem for this potential using the series approach of Section 7.2 with discretization parameter $N_r = 40$ and 200 terms in the series (7.12). The coefficients $\{c_n(r)\}$ as computed via (7.12) have $L^\infty(\mathbb{R}_+)$ norms exhibiting algebraic decay as $n \to \infty$ as suggested by Figure 8.1, where a log-log plot of $\|c_n(\cdot)\|_\infty$ is shown on the left. The essentially linear behavior of the plot for larger values of n indicates algebraic (predominantly power-law) decay as $n \to \infty$. We can fit the norms $\{\|c_n(\cdot)\|_\infty\}$ with a least squares method to $\ln \|c_n(\cdot)\|_\infty \sim -\alpha n - \beta \ln n - \gamma$ and find $\alpha = 10^{-4}$, $\beta = 1.0951$ and $\gamma = 1.1122$ for values of $n > 20$ (the results do not change much if the fitting is done for

$n > 50$). The results of the fitting can be seen in the right-hand panel of Figure 8.1 in the form of the quantity $\Delta := \ln \|c_n(\cdot)\|_\infty - (-\alpha n - \beta \ln n - \gamma)$. The fact that α is essentially zero while β is finite is strong numerical evidence that the series (7.12) converges for $|k| > \frac{1}{2}$ and diverges for $|k| < \frac{1}{2}$. Of course this threshold value of $|k| = \frac{1}{2}$ is the known exact value for the Lorentzian potential, but for the Gaussian $A(x,y) = \mathrm{e}^{-(x^2+y^2)}$ the best analytical estimate we have is, as explained in Section 5.1.2, that the $\bar{\partial}$ derivative of (7.12) converges in $\mathrm{W}(\mathbb{R}^2)$ if $|k| \geq 1$. In general, there is obviously nothing special about the value $|k| = \frac{1}{2}$; indeed if $\{c_n(r)\}_{n=0}^\infty$ are the coefficients for the potential $A(r)$, then from (7.13)–(7.14) we see that $\{M^{2n+2}c_n(r)\}_{n=0}^\infty$ are the coefficients for the rescaled potential $MA(r)$ for any $M > 0$, and it follows that if $|k| = \frac{1}{2}$ is the threshold value for $A(r)$, then $|k| = \frac{1}{2}M$ is the threshold value for $MA(r)$. The coincidence of threshold values for the Gaussian and Lorentzian potentials is perhaps related to the fact that for both potentials $\|A^2\| = 1$ in $\mathrm{W}(\mathbb{R}^2)$ as well as in $L^\infty(\mathbb{R}^2)$, as explained in Sections 5.1.2 and 5.1.2 respectively. In any case, since it is known from the explictly-solvable Lorentzian case that upon decreasing $|k|$ through the convergence threshold singularities appear in the solution $f(x,y;k)$ of the eikonal problem (1.6)–(1.7) at certain points in the (x,y)-plane, we may reasonably conjecture that some kind of singularity formation for a critical value of $|k|$ is a generic feature at least for radial potentials.

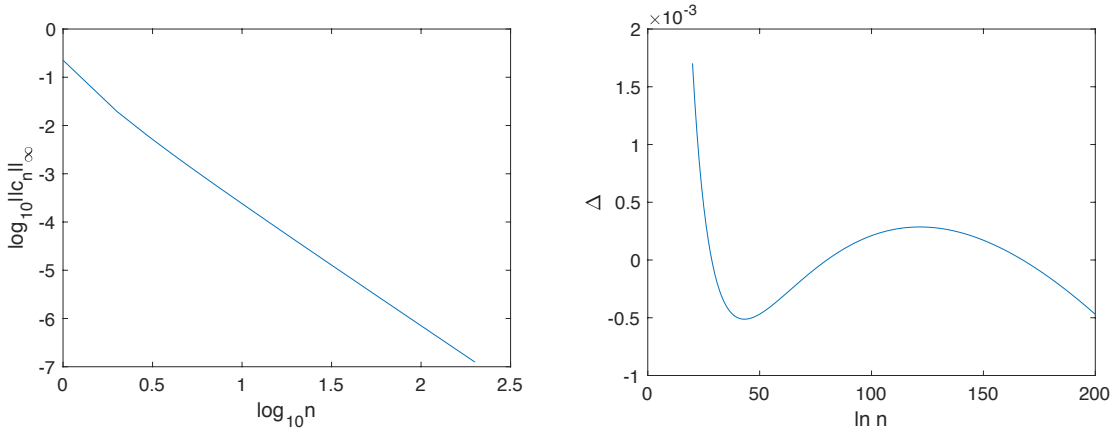

Figure 8.1 – Left: a log-log plot of the $L^\infty(\mathbb{R}_+)$ norms of the coefficients $\{c_n(r)\}$ appearing in the series solution (7.12) of the eikonal problem (1.6)–(1.7) for a Gaussian potential on the left. Right: the quantity $\Delta := \ln \|c_n(\cdot)\|_\infty - (-\alpha n - \beta \ln n - \gamma)$ obtained after a linear least-squares regression.

To solve the Dirac system (1.3) with given normalization for the Gaussian potential for various values of ϵ, we use the approach of Section 7.3 with $N_x = N_y = 2^{12}$ Fourier modes for $(x,y) \in 4[-\pi,\pi] \times 4[-\pi,\pi]$. The first row of Figure 1.1 shows plots of the modulus (scaled by $\mathrm{e}^{-kz/\epsilon}$) of the components of the solution obtained for $k = 1$ and $\epsilon = 1/16$.

In order to compare solutions to the eikonal problem (1.6)–(1.7) for a given potential as well as the corresponding leading-order normalization function α_0 to a solution to the ϵ-dependent direct scattering problem (1.3)–(1.4), we have to interpolate from the mixed Chebychev-Fourier (polar coordinate) grid used for g and α_0 to the two-dimensional Fourier (Cartesian) grid used for the computation of ψ_1 and ψ_2. There are efficient ways to do this. For simplicity we use here simply the definition of the spectral approximations of g and α_0. A function f is approximated in each of the radial domains under consideration as

$$f(r,\phi) \approx \sum_{n=0}^{N_r} \sum_{m=-N/2+1}^{N/2} c_{nm} T_n(l) e^{im\phi}. \tag{8.2}$$

Thus for given spectral coefficients c_{nm}, the corresponding function can be computed for arbitrary values of r and ϕ. For the Gaussian potential, the solution to the eikonal problem (1.6)–(1.7) can be seen after interpolation to a Cartesian grid in Figure 8.2. The correspond-

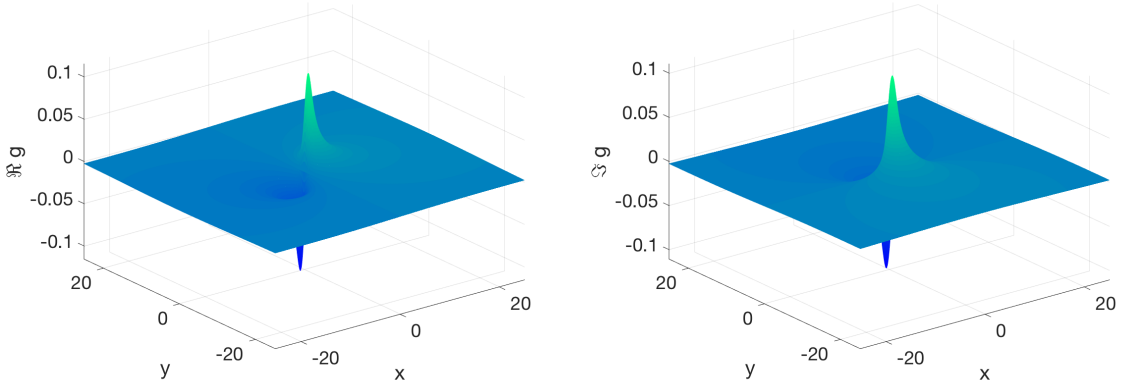

Figure 8.2 – Solution to the eikonal problem (1.6)–(1.7) for the Gaussian potential with $k = 1$. Left: real part of $g = f - kz$, right: imaginary part of $g = f - kz$.

ing Cartesian interpolation of the leading order normalization function α_0 can be seen in Figure 8.3.

With the numerical computations of f and α_0 complete, we may construct the leading term of the formal WKB approximation described in Section 8.2 for the solution of the direct scattering problem (1.3)–(1.4). We now are in a position to compare this approximation with numerically-computed solutions to the direct scattering problem obtained as described in Section 7.3. To quantify the comparison, we use (1.11) for $S(x,y) \equiv 0$ to define the quantities

$$\Delta_1 := \left| \psi_1 \mathrm{e}^{-f/\epsilon} - \frac{\alpha_0}{k} \partial f \right| \tag{8.3}$$

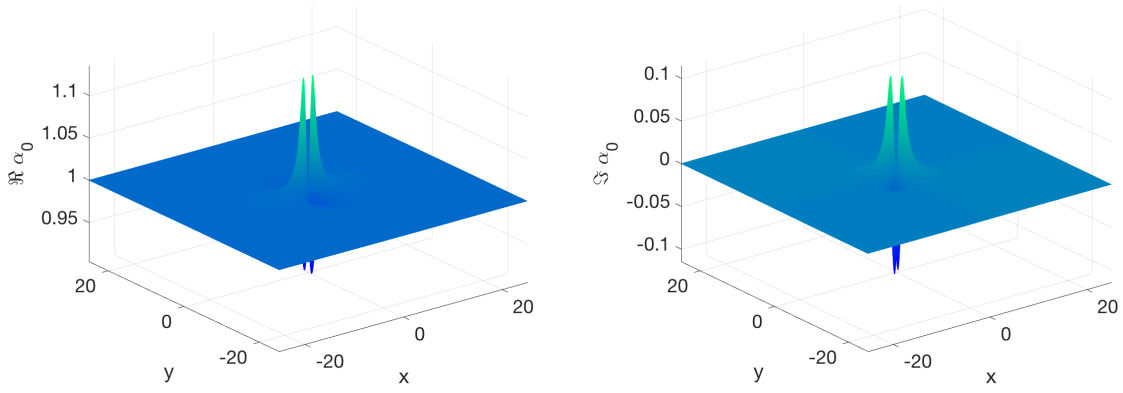

Figure 8.3 – Leading order normalization function α_0 for the Gaussian potential with $k = 1$. Left: real part, right: imaginary part.

and

$$\Delta_2 := \left| \psi_2 \mathrm{e}^{-f/\epsilon} - \frac{\alpha_0 A}{2k} \right|. \tag{8.4}$$

Conjecture 1.2.3 asserts that both of these quantities should be proportional to ϵ as $\epsilon \downarrow 0$. For the Gaussian potential at $k = 1$ we plot Δ_1 and Δ_2 for four values of ϵ in Figures 8.4 and 8.5 respectively.

The expected scaling in ϵ can indeed be seen from these plots, but it is even more obvious from the results of a linear regression to determine the best fit to the logarithms of the L^∞ norms of Δ_1 and Δ_2 as functions of $\ln(\epsilon)$ as is shown in Figure 8.6. The data for the regression is calculated for the values $\epsilon = 2^0, 2^{-1}, \ldots, 2^{-5}$, although we should keep in mind that for the larger values of ϵ, accuracy of the WKB approximation might not be expected. On the serial computers we used for our numerical simulations, we cannot go much lower than $\epsilon = 0.04$ for lack of resolution. The precise results of the linear regression are as follows. In the left panel of Figure 8.6, it can be seen that $\log_{10} \|\Delta_1\|_\infty \sim \alpha \log_{10} \epsilon + \beta$ with $\alpha = 0.99$ and $\beta = -1.24$. In the same way we get for Δ_2 the values $\alpha = 0.99$ and $\beta = -0.46$ as can be seen in the right panel of Figure 8.6. *Thus in both cases the expected linear dependence in ϵ predicted by Conjecture 1.2.3 is numerically confirmed.*

To show that the good agreement between numerics and conjecture is not due to a special choice of the spectral parameter k, we make similar plots as shown in Figure 8.6 for two more values of k. The upper and lower rows of Figure 8.7 correspond to $k = 0.75$ and $k = 1.25$ respectively. (Note that the solution of the eikonal problem is expected to become singular for sufficiently small k.) Even though for ϵ as large as $\epsilon = 1$, Δ_1 might not be expected to be small, still the regression line taking the corresponding data into account has the slope 0.97.

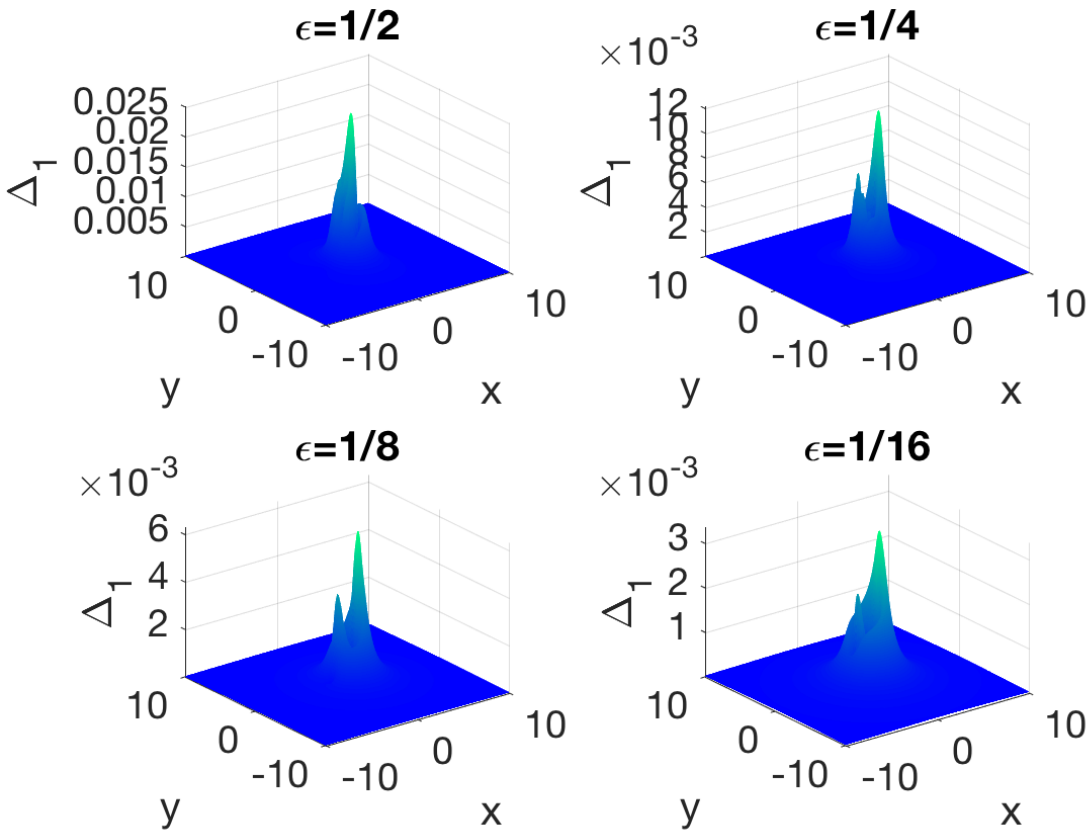

Figure 8.4 – The quantity Δ_1 of (8.3) for the Gaussian potential with $k = 1$ for $\epsilon = 1/2, 1/4, 1/8, 1/16$.

For Δ_2 the slope of the regression line is 0.99. For $k = 1.25$ we find that the slope of the line for Δ_1 is 0.88, and for Δ_2 it is 1.03. Thus in all cases the results are compatible with the expected $O(\epsilon)$ scaling. The slopes (exponents) obtained from regression would be expected to be even closer to 1 if numerical simulations for smaller values of ϵ were performed; however such experiments are out of reach for the serial computer we used for our simulations.

◁ Remark: A comparison between the WKB approximation and the numerical solution of the direct scattering problem can be made only if the eikonal problem has a global solution, hence allowing the construction of the WKB approximation globally in the (x, y)-plane. According to Theorem 1.2.1, this is guaranteed for $|k|$ sufficiently large. The lower bound on $|k|$ sufficient to guarantee a global solution is given in (1.8). In Section 5.1 it is shown that for phase-free potentials ($S(x, y) \equiv 0$) the lower bound (1.8) can be optimized by choice of the constant B to $|k| > \sqrt{\|A^2\|_W}$, and in Section 5.1.2 the lower bound is calculated for the Gaus-

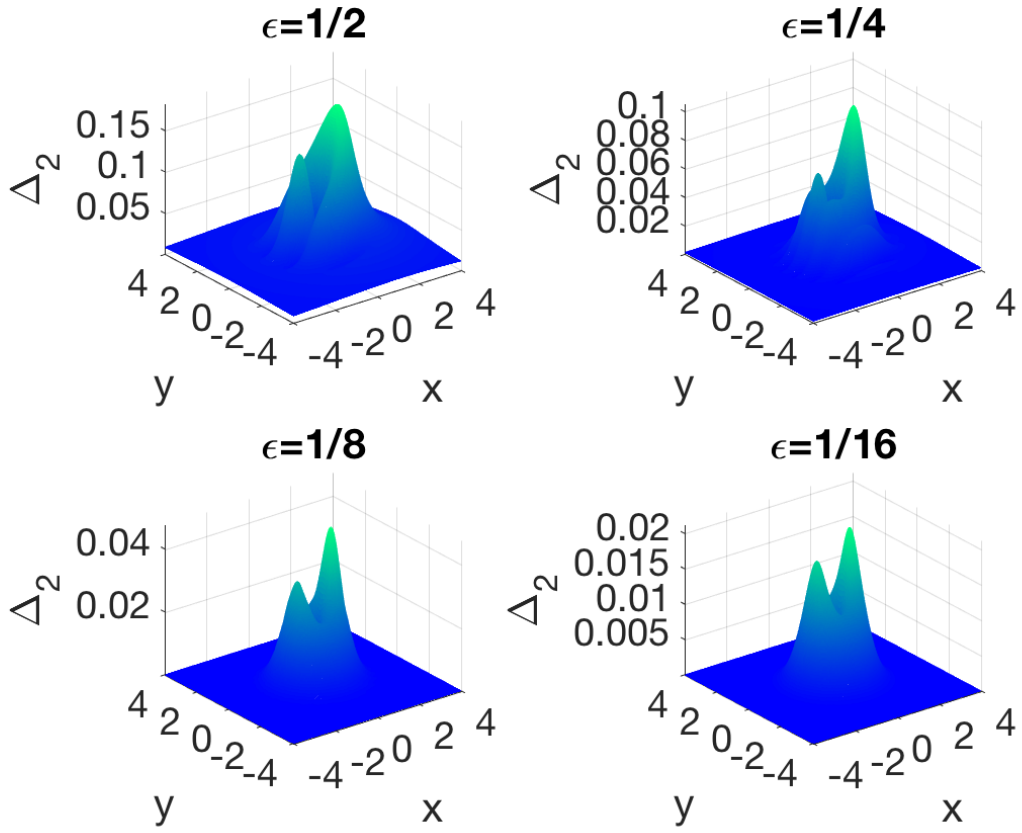

Figure 8.5 – The quantity Δ_2 of (8.4) for the Gaussian potential with $k = 1$ for $\epsilon = 1/2, 1/4, 1/8, 1/16$.

sian potential to be $|k| > 1$. However, even the optimized lower bound is only a sufficient condition for the global solvability of the eikonal problem (1.6)–(1.7). Since the hypotheses of Conjecture 1.2.3 only refer to the existence of a global solution of (1.6)–(1.7), we chose in our study to deal with values of k for which the eikonal problem can be solved numerically (which as pointed out above appears to be possible for $|k|$ larger than $\frac{1}{2}$), even if those values lie on or within the optimal radius $|k| = 1$ for Theorem 1.2.1 to make a theoretical prediction about the eikonal problem. ▷

8.2 Potential without radial symmetry

Next we consider the numerical solution of the eikonal problem (1.6)–(1.7) and coincident construction of the leading-order WKB approximation together with the numerical solution

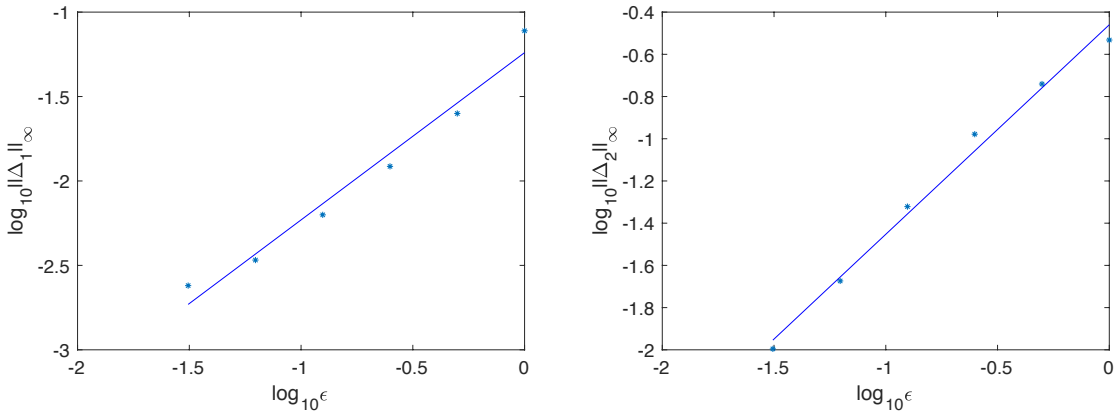

Figure 8.6 – Dependence of $\|\Delta_1\|_\infty$ (left panel) and $\|\Delta_2\|_\infty$ (right panel) on ϵ for $k = 1$, together with the result of linear least-squares regression for the logarithms.

of the ϵ-dependent direct scattering problem (1.3)–(1.4) in the case of a phase-free potential ($S \equiv 0$) and an amplitude $A(x, y)$ in the class of rapidly decaying smooth functions, but now *without radial symmetry even asymptotically for large* $|z|$. Concretely, we consider the potential

$$A(x, y) = \mathrm{e}^{-(x^2+5y^2+3xy)}. \tag{8.5}$$

To solve the Dirac system (1.3)–(1.4) for the potential (8.5) for various values of ϵ, we once more use the approach of Section 7.3 with $N_x = N_y = 2^{12}$ Fourier modes for $(x, y) \in 4[-\pi, \pi] \times 4[-\pi, \pi]$. The modulus of the solutions obtained for $k = 1$ and $\epsilon = 1/32$ can be seen in Figure 8.8.

Since the potential (8.5) is not radially symmetric, the numerical series-based approach described in Section 7.2 does not apply, so we must use instead an iterative approach to the eikonal problem as described in Section 7.2, and it turns out that we will also need higher resolution in ϕ than for radially-symmetric potentials to effectively solve for $g = f - kz$. We use $N_r = 64$ Chebychev polynomials and $N_\phi = 128$ Fourier modes for the case $k = 1$. The real and imaginary part of the function $g(x, y; k) = f(x, y; k) - kz$ are plotted in the left and right panels of Figure 8.9 respectively. The corresponding spectral coefficients $r \leq 1$ and $r \geq 1$ are shown in Figure 8.10, indicating that the solution is well resolved.

Next, we solve for the leading-order normalization function $a_0(x, y; k)$ also for $k = 1$ as described in Section 7.2.1. The real and imaginary parts of the the numerically-computed $a_0(x, y; 1)$ can be seen in Figure 8.11.

Given f and a_0, we may again compare the numerical solution to the Dirac system (1.3)–(1.4) to the leading term of the formal WKB approximation described in Section 8.2. For

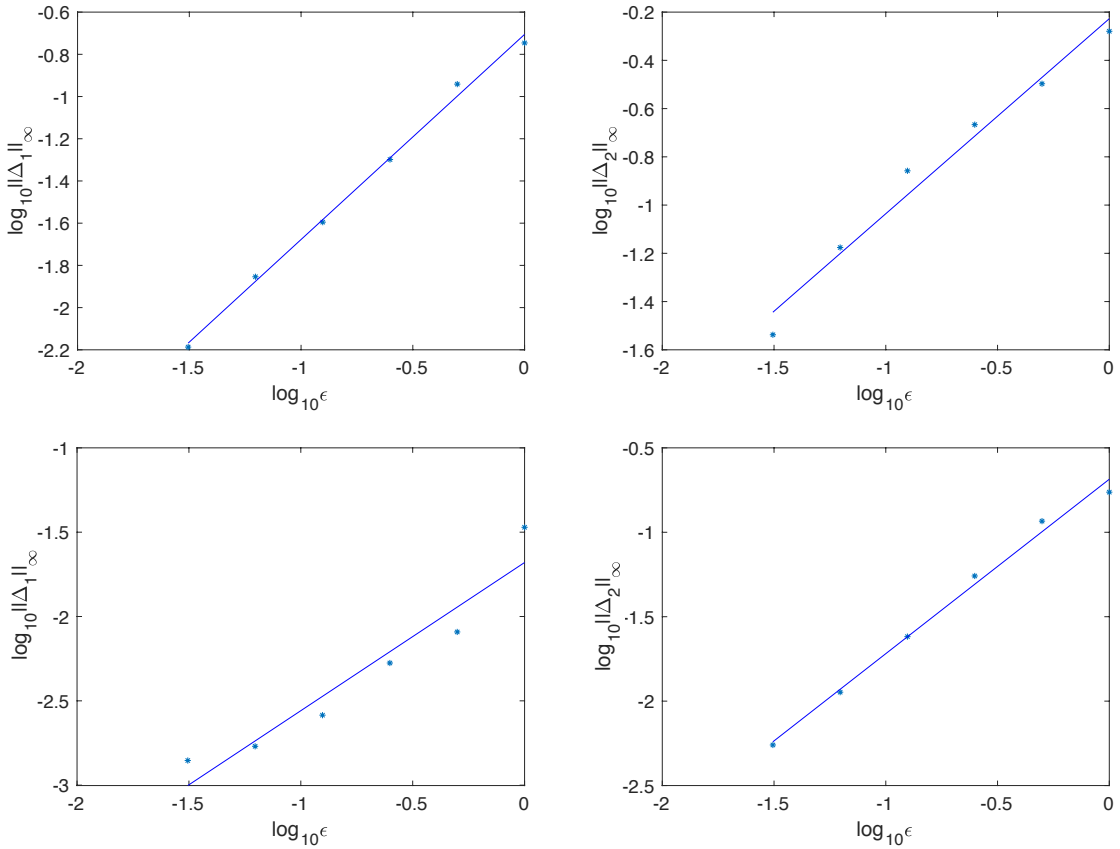

Figure 8.7 – Dependence of $\|\Delta_1\|_\infty$ (left column) and $\|\Delta_2\|_\infty$ (right column) on ϵ together with the results of linear least-squares regression for the logarithms; upper row for $k = 0.75$, lower row for $k = 1.25$.

the potential (8.5) at $k = 1$ we plot Δ_1 and Δ_2 defined by (8.3)–(8.4) for four values of ϵ in Figures 8.12 and 8.12 respectively.

It is clear that the numerical treatment of potentials lacking radial symmetry is considerably more challenging than for radially symmetric potentials such as the Gaussian considered in Section 8.1. Thus the numerical errors for small values of ϵ are larger, and we would need access to parallel computers in order to get the same accuracy as in the Gaussian case for a given small ϵ. Nonetheless we computed the quantities Δ_1 and Δ_2 of (8.3) and (8.4) respectively for the same values of ϵ as in the Gaussian case. In Figure 8.14 we plot the $L^\infty(\mathbb{R}^2)$-norms of these quantities for the potential (8.5) for various values of ϵ and compare the data in a log-log plot with lines of slope 1, which would correspond to the $O(\epsilon)$ relative error predicted by Conjecture 1.2.3. Obviously the somewhat surprising good agreement for values of $\epsilon \approx 1$ observed in the Gaussian case is not present here, and for small values of

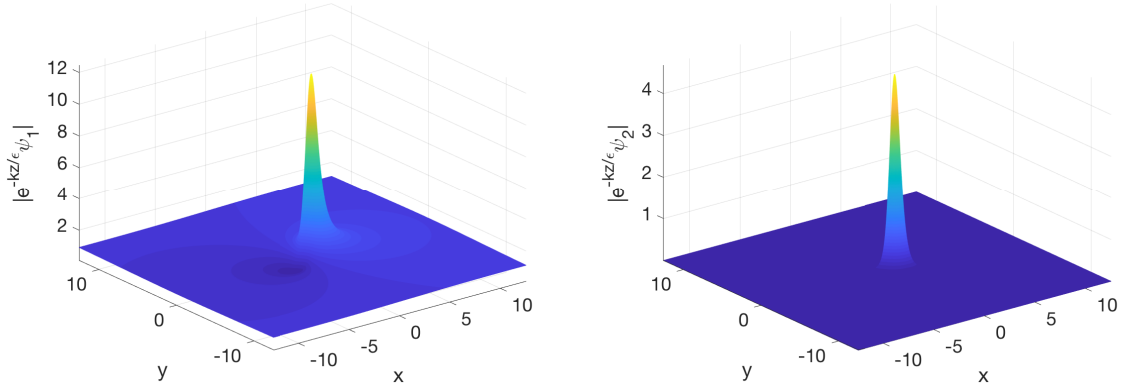

Figure 8.8 – Numerical solutions to the Dirac system (1.3)–(1.4) with potential (8.5) for $k = 1$ and $\epsilon = 1/32$. Left: the modulus of $e^{-kz/\epsilon}\psi_1$. Right: the modulus of $e^{-kz/\epsilon}\psi_2$.

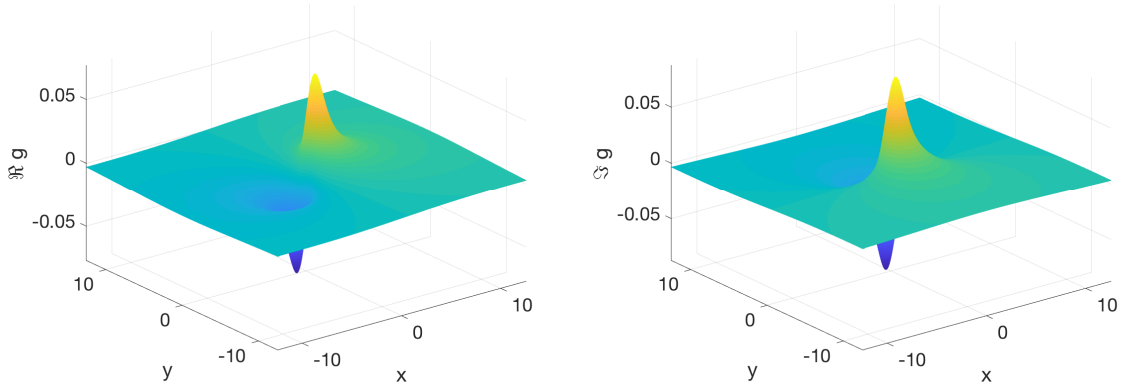

Figure 8.9 – Numerical solution $g = f - kz$ to the eikonal problem (1.6)–(1.7) with $k = 1$ for the potential (8.5) with $S \equiv 0$. Left: real part. Right: imaginary part.

ϵ the above mentioned resolution problems in the solution of the Dirac system (1.3)–(1.4) are visible. Nonetheless compatibility with the conjectured scaling proportional to ϵ can be recognized. *Thus, our numerical computations also confirm Conjecture 1.2.3 for certain potentials outside the class of radially-symmetric functions.* We leave the numerical study of potentials $A(x,y)e^{iS(x,y)/\epsilon}$ for which $S(x,y) \not\equiv 0$ and the investigation of Conjecture 1.2.3 in such cases for the future.

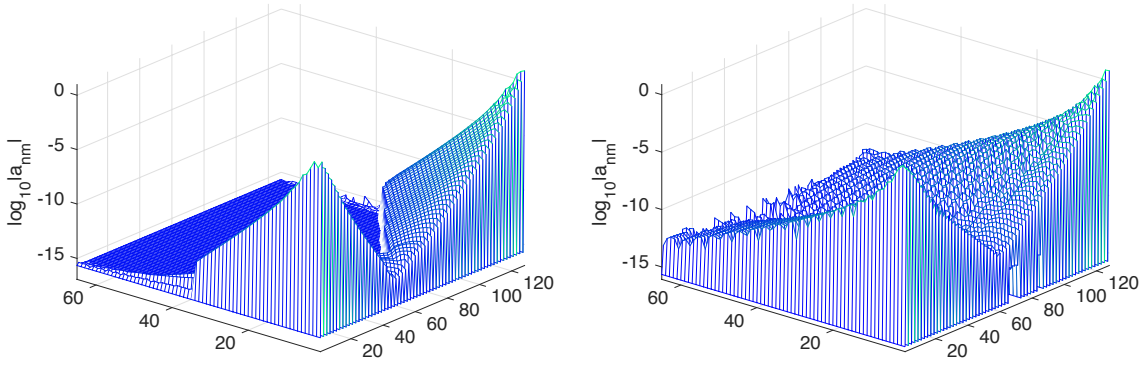

Figure 8.10 – Chebychev and Fourier spectral coefficients plotted over the (n, m)-grid for the solution shown in Figure 8.9. Left: the coefficients for $r \leq 1$. Right: the coefficients for $r \geq 1$.

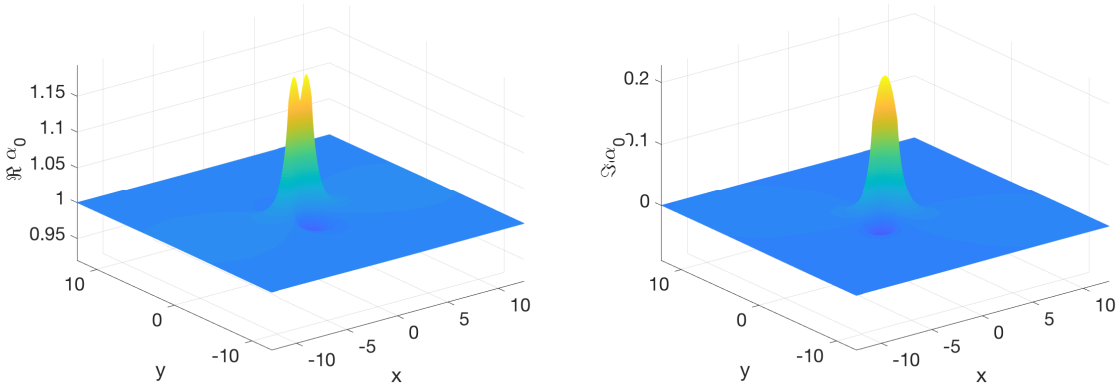

Figure 8.11 – The numerically-computed leading-order normalization function α_0 for the potential (8.5) without radial symmetry at $k = 1$. Left: real part, right: imaginary part.

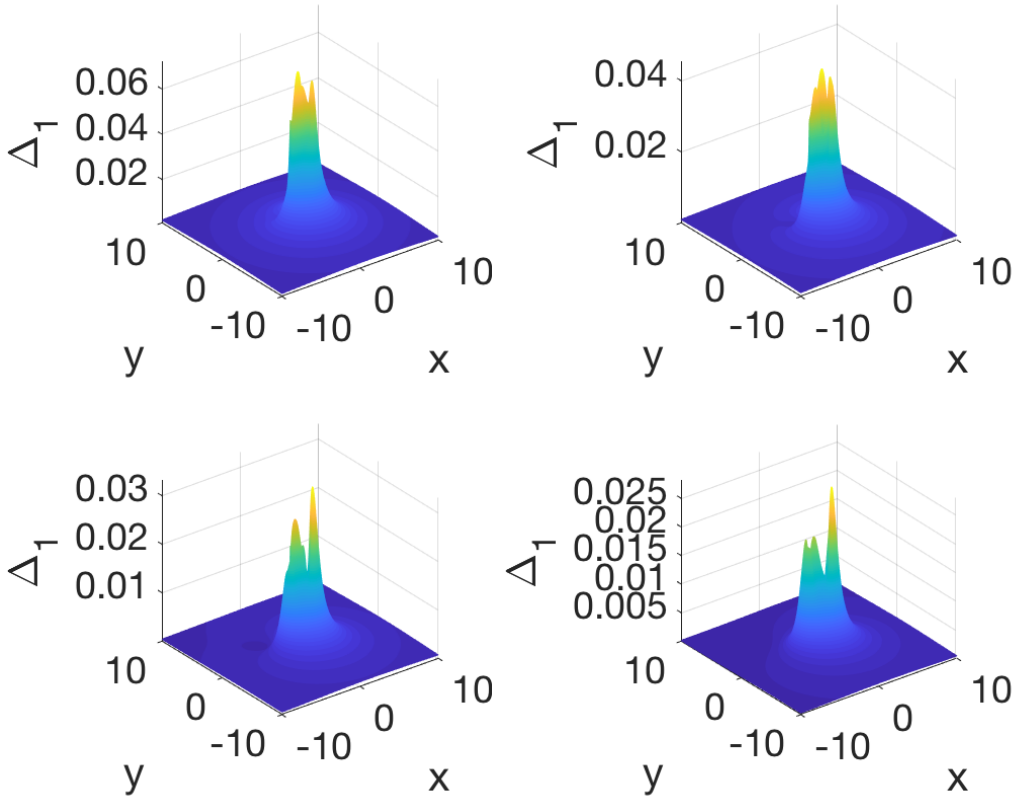

Figure 8.12 – The quantity Δ_1 of (8.3) for the potential (8.5) with $k = 1$ for $\epsilon = 1/2$ (upper left), $1/4$ (upper right), $1/8$ (lower left), $1/16$ (lower right).

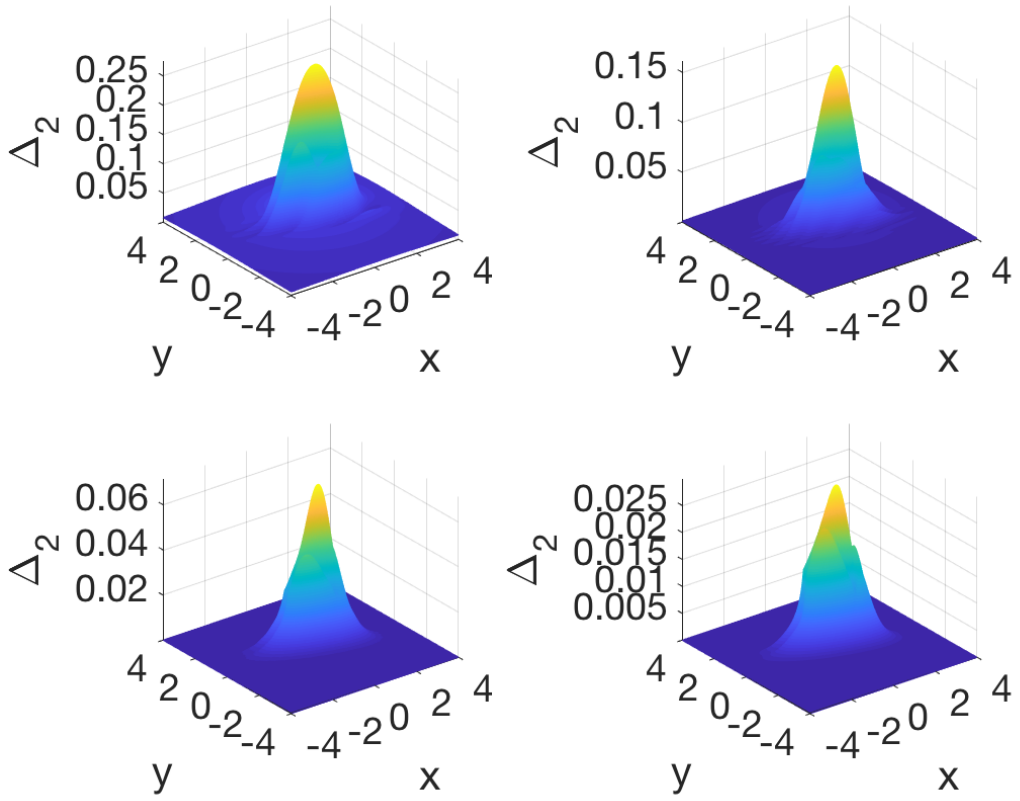

Figure 8.13 – The quantity Δ_2 of (8.4) for the potential (8.5) with $k = 1$ for $\epsilon = 1/2$ (upper left), $1/4$ (upper right), $1/8$ (lower left), $1/16$ (lower right).

Figure 8.14 – Dependence of $\|\Delta_1\|_\infty$ (left panel) and $\|\Delta_2\|_\infty$ (right panel) on ϵ, together with lines with slope 1.

Bibliography

[1] A. Davey and K. Stewartson. On three dimensional packets of surface waves. Proc. Roy. London Soc. A, 338:101–110, 1974.

[2] W. Craig, U. Schanz, and C. Sulem. The moldulational regime of three-dimensional water waves and the Davey-Stewartson System. Ann. Inst. Henri Poincare, 14(5):131–175, 1999.

[3] Ablowitz, M. J.; Clarkson, P. A. *Solitons, Nonlinear Evolution Equations and Inverse Scattering*, London Mathematical Society Lecture Note Series, 149, Cambridge University Press, Cambridge, 1991.

[4] K. Astala K,M. Lassas, and L. Päivärinta. The borderlines of the invisibility and visibility for Calderón's inverse problem. Analysis and PDE, 9:43–98, 2016.

[5] Astala, K.; Iwaniec, T.; Martin, G. *Elliptic partial differential equations and quasiconformal mappings in the plane*. Princeton Mathematical Series, 48. Princeton University Press, Princeton, NJ, 2009.

[6] Beals, R.; Coifman, R. R. Multidimensional inverse scatterings and nonlinear partial differential equations. *Pseudodifferential Operators and Applications (Notre Dame, Ind., 1984)*, 45–70, *Proc. Sympos. Pure Math.*, 43, Amer. Math. Soc., Providence, RI, 1985.

[7] Beals, R.; Coifman, R. R. Linear spectral problems, nonlinear equations and the $\bar{\partial}$-method. *Inverse Problems* **5** (1989), no. 2, 87–130.

[8] Birem, M.; Klein, C. Multidomain spectral method for Schrödinger equations. *Adv. Comput. Math.* **42** (2016), no. 2, 395–423.

[9] Brown, R. M. Estimates for the scattering map associated with a two-dimensional first-order system. *J. Nonlinear Sci.* **11** (2001), no. 6, 459–471.

[10] Deift, P.; Venakides, S.; Zhou, X. New results in small dispersion KdV by an extension of the steepest descent method for Riemann-Hilbert problems. *Internat. Math. Res. Notices* **1997**, no. 6, 286–299.

[11] NIST Digital Library of Mathematical Functions. `http://dlmf.nist.gov/`, Release 1.0.6 of 2013-05-06. Online companion to [33].

[12] Dubrovin, B. A.; Novikov, S. P. Hydrodynamics of weakly deformed soliton lattices. Differential geometry and Hamiltonian theory. *Russian Math. Surveys* **44** (1989), no. 6, 35–124.

[13] Dym, H.; McKean, H. P. *Fourier series and integrals*. Probability and Mathematical Statistics, 14. Academic Press, New York, 1972.

[14] Ferapontov, E. V.; Khusnutdinova, K. R. On the integrability of $(2+1)$-dimensional quasilinear systems. *Comm. Math. Phys.* **248** (2004), no. 1, 187–206.

[15] Fokas, A. S. Inverse scattering of first-order systems in the plane related to nonlinear multidimensional equations. *Phys. Rev. Lett.* **51** (1983), no. 1, 3–6.

[16] Fokas, A. S.; Ablowitz, M. J. The inverse scattering problem for multidimensional $(2+1)$ problems. *Nonlinear phenomena (Oaxtepec, 1982)*, 137–183, *Lecture Notes in Phys.* **189**, Springer, Berlin, 1983.

[17] Fokas, A. S.; Ablowitz, M. J. Method of solution for a class of multidimensional nonlinear evolution equations. *Phys. Rev. Lett.* **51** (1983), no. 1, 7–10.

[18] Fokas, A. S.; Ablowitz, M. J. On the inverse scattering transform of multidimensional nonlinear equations related to first-order systems in the plane. *J. Math. Phys.* **25** (1984), no. 8, 2494–2505.

[19] Frauendiener, J. Calculating initial data for the conformal Einstein equations by pseudospectral methods. Computational astrophysics. *J. Comput. Appl. Math.* **109** (1999), no. 1–2, 475–491.

[20] Grenier, E. Semiclassical limit of the nonlinear Schrödinger equation in small time. *Proc. Amer. Math. Soc.* **126** (1998), no. 2, 523–530.

[21] Jin, S; Levermore, C. D.; McLaughlin, D. W. The semiclassical limit of the defocusing NLS hierarchy. *Comm. Pure Appl. Math.* **52** (1999), no. 5, 613–654.

[22] Klein, C.; McLaughlin, K. D. T.-R. Spectral approach to D-bar problems. *Comm. Pure Appl. Math.* **70** (2017), no. 6, 1052–1083.

[23] Klein, C.; Roidot, K. Numerical study of the semiclassical limit of the Davey-Stewartson II equations. *Nonlinearity* **27** (2014), no. 9, 2177–2214.

[24] Konopelchenko, B. G. Quasiclassical generalized Weierstrass representation and dispersionless DS equation *J. Phys. A* **40** (2007), no. 46, F995–F1004.

[25] Lanczos, C. Trigonometric interpolation of empirical and analytic functions. *J. Math. and Phys.* **17** (1938), 123–199.

[26] Lieb, E. H.; Loss, M. *Analysis*. Second edition. Graduate Studies in Mathematics, 14. Amer. Math. Soc., Providence, RI, 2001.

[27] Madelung, E. Quantum theory in hydrodynamic form. *Zeitschr. Phys.* **40** (1926), no., 3–4, 322–326.

[28] Manakov, S. V.; Santini, P. M. Inverse scattering problem for vector fields and the Cauchy problem for the heavenly equation. *Phys. Lett. A* **359** (2006), no. 6, 613–619.

[29] Miller, P. D. *Applied asymptotic analysis*. Graduate Studies in Mathematics, 75. Amer. Math. Soc., Providence, RI, 2006.

[30] Miller, P. D. On the generation of dispersive shock waves. *Phys. D* **333** (2016), 66–83.

[31] Miller, P. D.; Qin, Z.-Y. Initial-boundary value problems for the defocusing nonlinear Schrödinger equation in the semiclassical limit. *Stud. Appl. Math.* **134** (2015), no. 3, 276–362.

[32] Nachman, A. I.; Regev, I.; Tataru, D. I. A nonlinear Plancherel theorem with applications to global well-posedness for the defocusing Davey-Stewartson equation and to the inverse boundary value problem of Calderon. `arXiv:1708.04759`, 2017.

[33] *NIST handbook of mathematical functions*. Edited by F. W. J. Olver, D. W. Lozier, R. F. Boisvert, and C. W. Clark. U.S. Department of Commerce, National Institute of Standards and Technology, Washington, DC; Cambridge University Press, Cambridge, 2010. Print companion to [11].

[34] Perry, P. A. Global well-posedness and long-time asymptotics for the defocussing Davey-Stewartson II equation in $H^{1,1}(\mathbb{C})$. With an appendix by Michael Christ. *J. Spectr. Theory* **6** (2016), no. 3, 429–481.

[35] Saad, Y.; Schultz, M. H. GMRES: a generalized minimal residual algorithm for solving nonsymmetric linear systems. *SIAM J. Sci. Statist. Comput.* **7** (1986), no. 3, 856–869.

[36] Satsuma, J.; Yajima, N. Initial value problem of one-dimensional self-modulation of nonlinear waves in dispersive media. *Progr. Theoret. Phys. Suppl. No.* 55 (1974), 284–306.

[37] Sung, L.-Y. An inverse scattering transform for the Davey-Stewartson II equations. *J. Math. Anal. Appl.* **183** (1994), no. 1, 121–154 (part I), no. 2, 289–325 (part II), no. 3, 477–494 (part III).

[38] Tovbis, A.; Venakides, S. The eigenvalue problem for the focusing nonlinear Schrödinger equation: new solvable cases. *Phys. D* **146** (2000), no. 1–4, 150–164.

[39] Trefethen, L. N. *Spectral methods in MATLAB*. Software, Environments, and Tools, 10. Society for Industrial and Applied Mathematics (SIAM), Philadelphia, PA, 2000.

[40] Whitham, G. B. Non-linear dispersive waves. *Proc. Roy. Soc. Ser. A* **283** (1965), 238–261.

[41] Wolfram Research, Inc. *Mathematica*, Version 10.1. Champaign, IL, 2015.

[42] Yi, G. Investigation of Integrable Dynamical Systems and Evolution Partial Differential Equations. Doctoral dissertation, University of Roma "La Sapienza," 2014.

[43] Zakharov, V. E.; Shabat, A. B. Interaction between solitons in a stable medium. *Zhurnal Experimentalnoi Teoreticheskoi Fiziki* **64** (1973), no. 5, 1627–1639. *Sov. Phys. JETP* **37** (1973), 823–828.

[44] , Gripenberg, G. and Londen, S. O. and Staffans, O. Volterra Integral and Functional Equations *Cambridge, Encyclopedia of Mathematics and its Applications, Cambridge University Press*, 1990

[45] Assainova, O.; Klein C.; McLaughlin, K.; Miller P.D. A Study of the Direct Spectral Transform for the Defocusing Davey-Stewartson II Equation in the Semiclassical Limit, *to appear in Comm. Pure Appl. Math.*